THERMAL AND ELECTRICAL PERFORMANCE INVESTIGATION OF SOLAR PHOTOVOLTAIC MODULE WITH AND WITHOUT COOLING SYSTEM

Chaltu Nagesh Megersa

A Thesis Submitted to

The Department of Thermal and Aerospace Engineering
School of Mechanical, Chemical and Materials Engineering

Presented in partial fulfillment of the requirement of the degree of Master's in Thermal Engineering

Office of Graduate Studies
Adama Science and Technology University

August, 2021

Adama, Ethiopia

THERMAL AND ELECTRICAL PERFORMANCE INVESTIGATION OF SOLAR PHOTOVOLTAIC MODULE WITH AND WITHOUT COOLING SYSTEM

Chaltu Nagesh Megersa

Advisor: Dr. Gezahegn Habtamu

A Thesis Submitted to

The Department of Thermal and Aerospace Engineering

School of Mechanical, Chemical and Material Engineering

Presented in partial fulfillment of the requirement of the degree of Master's in Thermal Engineering

Office of Graduate Studies

Adama Science and Technology University

August, 2021

Adama, Ethiopia

DECLARATION

I hereby declare that this Master Thesis entitled "Thermal and Electrical Performance Investigation of Solar Photovoltaic Module with and without Cooling System" is my original work. That is, it has not been submitted for the award of any academic degree, diploma or certificate in any other university. All sources of materials that are used for this thesis are duly acknowledged through citation.

Chaltu Nagesh Megersa	__________________	__________________
Name of student	Signature	Date

RECOMMENDATION

I, the advisor of this thesis, hereby certify that I have read the revised version of the thesis entitled" Thermal and Electrical Performance Investigation of Solar Photovoltaic Module with and without Cooling System" prepared under my guidance by Chaltu Nagesh Megersa submitted in partial fulfillment of the requirements for the degree of Mater's of Science in Thermal Engineering. Therefore, I recommend the submission of the revised version of the thesis to the department following the applicable procedures.

Dr. Gezahegn Habtamu	________________	________________
Advisor	Signature	Date

APPROVAL SHEET

I, the advisors of the thesis entitled "Thermal and Electrical Performance Investigation of Solar Photovoltaic Module with and without Cooling System" and developed by Chaltu Nagesh Megersa; hereby certify that the recommendation and suggestions made by the board of examiners are appropriately incorporated into the final version of the thesis.

Dr. Gezahegn Habtamu	________________	________________
Advisor	Signature	Date

We, the undersigned, members of the Board of Examiners of the thesis by Chaltu Nagesh Megersa have read and evaluated the thesis entitled "Thermal and Electrical Performance Investigation of Solar Photovoltaic Module with and without Cooling System" and examined the candidate during the open defense. This is, therefore, to certify that the thesis is accepted for partial fulfillment of the requirement of the degree of Master of Science in Thermal Engineering.

________________	________________	________________
Chairperson	Signature	Date
________________	________________	________________
Internal Examiner	Signature	Date
________________	________________	________________
Eternal Examiner	Signature	Date

Finally, approval and acceptance of the thesis is contingent upon submission of its final copy to the Office of Postgraduate Studies (OPGS) through the Department Graduate Council (DGC) and School Graduate Committee (SGC).

________________	________________	________________
Department Head	Signature	Date
________________	________________	________________
School Dean	Signature	Date
________________	________________	________________
Office of Postgraduate Studies, Dean	Signature	Date

ACKNOWLEDGEMENT

First and foremost my deepest and utmost gratitude to Almighty God, for his overwhelming love, strength and protection throughout and by his power I become successful after enormous challenges and also gives me patient, courage and wisdom to finish my study. Then, I am greatly grateful to my thesis advisor Dr. Gezahegn Habtamu (Assistant professor of Thermal Engineering), who is a charity for me to complete this thesis work. His genuine advice; diligent follow up; his precious & boundless support, patience and the instruction he has given me a great motivation to have a deep interest in every state of thesis work and has been a source of constant encouragement. I would like to acknowledge Dr. Addisu Bekele for lending me his digital thermocouple detector.

I would like to express my sincere thanks to Mr. Addis Alemayyo Mechanical System and Vehicle Engineering staff, for his unpaid suggestions and continuous support throughout my study period. I would also like to thanks to my best friend Shimelis Tsegga for his encouragement, suggestion, and gave a worthy comment on my work and through the process of researching

I must express deepest thankfulness to my families (especially my mam Zawditu Gurmu) for providing me with consistent support and continuous encouragement throughout my years of study. Without mam, I would have not ever been able to reach my dream and thanks for her support, in always having my back.

Finally, special thanks to Adama Science and Technology University for their financial support to pursue my study and related research activities to achieve my research objectives.

TABLE OF CONTENTS

Contents

LIST OF TABLES

LIST OF FIGURES

ABBRIVATIONS

AC	Alternative current
CFD	Computational fluid dynamics
DC	Direct Current
EES	Engineering equation solver
HIT	Higher intermediate temperature
PCM	Phase change materials
PV	Photovoltaic module
STC	Standard test condition

NOMENCLATURE

M	Air mass modifier
n	Day of the year
H_0	Daily total extraterrestrial solar radiation (J/m^2)
H_t	Monthly average daily global radiation (J/m^2)
$\bar{n}_s$	Monthly average daily hours of bright sunshine
$\bar{N}_s$	Monthly average of the maximum daily hours of bright sunshine
H_b	Monthly average daily beam solar radiation (J/m^2)
H_d	Monthly average daily diffuse solar radiation (J/m^2)
I_d	Hourly average diffused solar radiation (W/m^2)
I_T	Total hourly irradiance on a tilted surface (W/m^2)
I_b	Hourly beam irradiance (W/m^2)
R_b	The ratio of beam radiation on the tilted surface to that on a horizontal surface
T_{max}	Mean daily maximum temperature (℃)
T_{min}	Mean daily minimum temperature (℃)
t	Time of the day (hr.)
P_{out}	Photovoltaic module power output (W)
P_{in}	Input power (W)

I_{sc}	Short circuit current (A)
V_{OC}	Open circuit voltage (V)
FF	Fill factor
A_a	Area of the PV module (m^2)
Q_u	Useful heat removal from PV (W)
G	Solar radiation ($W/_{m^2}$)
Q_r	*Radiation loss*(W)
Q_e	Convection loss (W)
m_w	Mass flowrate $\left(kg/_s\right)$
C_P	Specific heat of water
T_{fo}	Outlet water temperature (°C)
T_{fi}	Inlet water temperature (°C)
L_{st}	Standard meridian for the local time zone
L_{loc}	Longitude of the location in question and longitudes are
E	Equation of time
S_{PV}	Absorbed solar radiation by PV module ($W/_{m^2}$)
m	Air mass
U_L	Overall heat loss coefficient ($W/_{m^2\ K}$)
N_u	Nusselt number
$h_{r_{c-a}}$	Radiative heat transfer coefficient ($W/_{m^2\ K}$)
G_r	Grash of number
B	Volumetric thermal expansion coefficient $\left(\frac{1}{K}\right)$
v	Kinematic viscosity ($m^2/_s$)
a	Thermal diffusivity ($m^2/_s$)
l	Length of the panel (m)

GREEK LETTERS

η_e	Electrical efficiency (%)
η_{th}	Thermal efficiency (%)

ω	Hour angle (°)
β	Tilt angle (°)
ω_s	Sunset hour angle (°)
φ	Latitude angle (°)
δ	Declination angle (°)
γ_s	Solar azimuth angle (°)
θ_z	Zenith angle (°)
θ	Incidence angle (°)
ρ	Ground reflectivity
τ	Transmittance
$\boldsymbol{\alpha}$	Absorptivity
$\theta_{e,d}$	Effective incidence angle for diffuse radiation from the sky (°)
$\theta_{e,g}$	Effective incidence angle for ground reflected radiation (°)

SUBSCRIPTS

a	Ambient
avg	Average
in	Inner
out	Outer
ref	Reference
b	Beam
d	Diffuse
g	Ground
sc	Solar constant
U	Useful
SC	Short circuit
W	Water
st	Standard time
loc	Local

ABSTRACT

Electricity generated by commercial solar photovoltaic module is inversely proportional to module surface temperature and directly proportional to solar radiation intensity. Manufacturer test photovoltaic module power output at constant temperature. Actually, as surface temperature, increase the power output and its efficiency decrease. This is due to a rise in intrinsic carrier concentrations at higher temperatures, which tend to increase the dark saturation current of the P–N junction, causes the open-circuit voltage to decreases. To decrease this effect cooling PV module surface is one of the solutions of this problem. The main aim of this study is to develop and experimentally test the thermal and electrical characteristics of solar photovoltaic module with and without cooling system. The study set up consisted of two polycrystalline PV modules of solar area 0.945 m × 0.55 m with power output of 60 W integrated with either air or water-cooling system. Theoretically, the tilted surface solar radiation and solar radiation absorbed by photovoltaic module were estimated to compute the thermal and electrical efficiencies of the PV modules. Experimental test was done on bar) and cooled photovoltaic modules exposed to sun towards East, West, and South axes of earth for four cases of cooling arrangement: continuous film water cooling versus bare module; continuous air cooling versus bare module, intermittent water-cooling versus bare module, and continuous film water-cooling versus continuous air cooling. Typical day experimental results show that the maximum uncooled average surface module temperature was 50.4, 58.64 and 55.4℃ for South, West and East facing PV modules, respectively. The result illustrated that the photovoltaic module film water-cooling, intermittent water and air-cooling were decrease in temperature 20.45, 15.5, and 9.35℃, respectively. The maximum average current and voltage output of the module for film water, intermittent water, and air cooling cases were 3.38, 3.26, and 3.4 A and 19.54, 19.53 and 19 V, respectively. For south facing module, 23.15% increases in electric power output and efficiency was observed for continuous film water-cooled PV module when compared with uncooled PV module. The maximum electrical efficiency observed was 11.11% for continuous film water-cooled module and 9% for uncooled PV module. The maximum thermal efficiency was for cooled 50% and 82.7% for uncooled PV module. Therefore, the study recommends that integrating the cooling system to the photovoltaic module grids for small society or hospitals purpose as it enhances its electrical performances compared to operating it bare. Among the cooling technique studied, top overflow PV module water-cooling is better than the others are.

***Keywords**: Solar electricity, experimental performance of photovoltaic module, active cooling of PV cells, passive cooling of PV cells, thermal performance of PV system, electrical performance of PV systems*

CHAPTER ONE

INTRODUCTION

1.1 Background of the Study

Solar energy is the most abundant renewable energy resource on earth and could therefore be the solution for the growing demand for global energy consumption. In general, utilization of solar energy can be broadly classified into two systems: thermal energy system, which converts solar energy into thermal energy, and photovoltaic energy system that converts solar energy into electrical energy.

Photovoltaic (PV) module utilizes photoelectric conversion semiconductors, called solar cells, which directly convert absorbed sunlight into electric power(Arifin et al., 2020). During this energy conversion process, these cells only convert part of the incoming solar radiation into useful power output while the remaining is lost as waste heat. Consequently, this waste heat raises the cell temperature. With an increase in the photovoltaic module temperature, the open-circuit voltage and short circuit current are reduced, which decreases the conversion efficiency of the PV system (Baloch et al., 2015). The efficiency of Photovoltaic (PV) modules is highly dependent on parameters, which are surface temperature, dusting, radiation intensity, and climatic conditions. The most important of these parameters is undoubtedly the panel surface temperature (Wongwuttanasatian et al., 2020).

Non-uniform panel surface temperature across the photovoltaic (PV) string has been found to affect the module efficiency and overall system performance in a negative manner. Non-uniformity in temperature distribution affects the PV system performance in two ways:

(i) Cells experience efficiency loss due to loss in power output.

(ii) Temperature difference induces thermal fatigue because of the large number of thermal cycles and stresses.

Module temperature greatly influences the efficiency and yield of the system by decreasing the open-circuit voltage. The module voltage linearly decreases with increase in cell temperature by approximately 2.2 mV per every 1 °C rise in temperature and the electrical efficiency decreases approximately by 0.5 %/°C (Yesilyurt et al., 2018).

Photovoltaic modules based on silicon material can convert 8-20% of solar radiation into electrical energy but the rest of the solar radiation is reflected in the surrounding environment and upsurge the temperature of the photovoltaic device and as a result decrease the total power output (Sato and Yamada, 2019).

Hence, a cooling technique is requires to maintain the module at the operating temperature and should be such that it keeps the average module temperature at its lowest. In addition to this, there is a uniform distribution in temperature and to increase the electrical efficiency of the photovoltaic system. There are two types of cooling techniques. These are active and passive cooling systems. Active cooling systems operate by a mechanical or electrical device such as fans or pumps that require external power input, while passive cooling does not require additional power to operate.

In this, study the thermal and electrical performance of two the photovoltaic modules were experimentally investigated by integrating passive and active cooling systems under Adama weather conditions. The two photovoltaic modules were made of polycrystalline cells with solar collecting area 0.945 m x 0.55 m. The thermal and electrical efficiency of the two photovoltaic modules has been studied for active and passive cooling systems using water and air as cooling fluids. One of the two PV modules was cooled by water or air and the other was simply exposed to solar radiation in parallel during the experimentation. Water-cooled PV module performance was studied by flowing water under gravity flow over the surface of the PV model. The air-cooled PV module performance was studied by blowing air using a fan. The performance of the photovoltaic module with and without cooling (bare) was investigated experimentally in terms of the current, voltage, power, electrical efficiency, and reduction of the surface temperature and thermal efficiency of the solar module due to cooling. Then, performances of the two modules were investigated for South faced, East faced and West faced solar PV module without and with the cooling system in parallel. In addition to this the performance comparison of the water and air cooled photovoltaic module were investigated.

1.2 Problem Statement

The solar photovoltaic system is promising technology that generates electricity free from pollution. However, the standard of living of human being depends on energy consumption. Energy is needed for numerous applications such as cooking, lighting, industrial developments, and agriculture applications. Before industrial growth, fossil fuels were used for power generation.

The increasing consumption of fossil fuels increased greenhouse gas emissions. To reduce the problem of the greenhouse effect, using sustainable energy is one of the basic solutions. From sustainable energy, using photovoltaic energy is the essential way to solve the problem.

However, the electric generation performance of the photovoltaic system decreases with an increase in surface temperature of the photovoltaic system when the module is working from morning up to evening. This decline is determined first by the droplet of open-circuit cell voltage. The reason behind this is due to a rise in intrinsic carrier concentrations at higher temperatures, which tend to increase the dark saturation current of the P‑N junction. To maintain a more or less constant temperature and electric generation performance, the photovoltaic system, must be cooled. Thermal control means such as passive cooling and active cooling systems can be integrated into the photovoltaic system to control the surface temperature of the photovoltaic system, which is a key factor to no reduction in its efficiency. Thus, this research investigates the thermal and electrical performance of photovoltaic cooling systems experimentally.

1.3 Objectives

1.3.1 General Objective

The general objective of this thesis is to investigate the thermal and electrical performance of the photovoltaic system when the photovoltaic system is working under Adama weather conditions by integrating passive and active cooling systems.

1.3. 2 Specific Objectives

- ❖ Estimate solar radiation absorbed for South Facing, East facing and West facing tilted solar PV models in Adama
- ❖ Develop a prototype of passive cooling and active cooling system for the photovoltaic system using air and water as cooling fluids
- ❖ Integrate the passive and active cooling systems with the photovoltaic module
- ❖ Investigate the thermal and electrical performance of solar photovoltaic systems experimentally and analyze the data in terms of current, voltage, power, temperature and efficiencies

1.4 Significance of the Study

The majority of people in our country, Ethiopia depend on biomass energy sources like firewood and electricity to prepare food and use these as source of light.

- ❖ Examine the suitable cooling system for the photovoltaic (PV) module
- ❖ Provide a way to boost the electric and thermal performance of the PV module by minimizing cell temperature
- ❖ Surviving efficient photovoltaic (PV), reduce dependence on electricity and biomass energy consumption for human beings, and provide eco-friendly areas by reducing, pollution that affects human health

1.5 Scope and Limitation of the Study

1.5.1 Scope of the Study

This thesis study mainly focuses on the performance analysis of solar a photovoltaic module. The analysis of this thesis covers the thermal and electrical performance of the solar photovoltaic module with and without a cooling system. The scope can be summarized in the following points.

- ❖ Estimate solar insolation of Adama and solar energy absorbed by tilted photovoltaic module
- ❖ Developing prototype and testing the experiment for the photovoltaic without and with water (passive) and fan blower (active) cooling system.
- ❖ Conduct experimentation to collect thermal and electrical characteristics of photovoltaic module with and without a cooling system in parallel setup.
- ❖ Analyze the thermal and electrical efficiency of the photovoltaic (PV) with and without a cooling system.
- ❖ Finally comparison the performance of the module without and with the cooling system.

1.5.2 Limitation of the Study

The major limitation of this thesis study is lack of the instruments such as pyrometer, anemometer, and data logger that could collect the experimental data continuously. Due to the lack of instruments, the experimental efficiencies were determined for estimated solar radiation intensity and wind speed data obtained from meteorology station. In addition, the study considered the electric energy used for the active cooling as parasitic power used to drive the fan and focuses only on the enhancement in PV module output power because of cooling by air.

1.6 Research Questions

Numerous questions arise concerning the solar photovoltaic module cooling system. Even though, for this thesis study the list specific research question raised is-

- How to assess the solar energy of the study area and absorbed solar energy by a photovoltaic module?
- How does the photovoltaic module temperature rise?
- How the performances of the photovoltaic module decrease as the surfaces module temperature rise?
- How the photovoltaic module cooling, improve the performance of the photovoltaic module?
- What is/are the factor affecting the performance of the photovoltaic module system?

CHAPTER TWO
LITERATURE REVIEW

2.1 Introduction

Under this chapter, a detailed review of the previous works related to the electrical and thermal performance of solar photovoltaic modules with or without a cooling system is summarized. Brief description on the various techniques of solar photovoltaic module the cooling systems and the different parameters that affect the performance of the photovoltaic module are discussed. Lastly, the summary of the reviewed previous studies are provided, and the research gaps identified for the present study are explained.

2.2. Classification of Solar Photovoltaic Module Cooling Systems

Solar Photovoltaic Module Cooling Systems are external attached systems that are needed to reduce the surface temperature of the PV module so that electric power loss due to rise in surface temperature could be minimized. The classifications of the commonly used cooling systems of solar PV module are indicated in Figure 2.1.

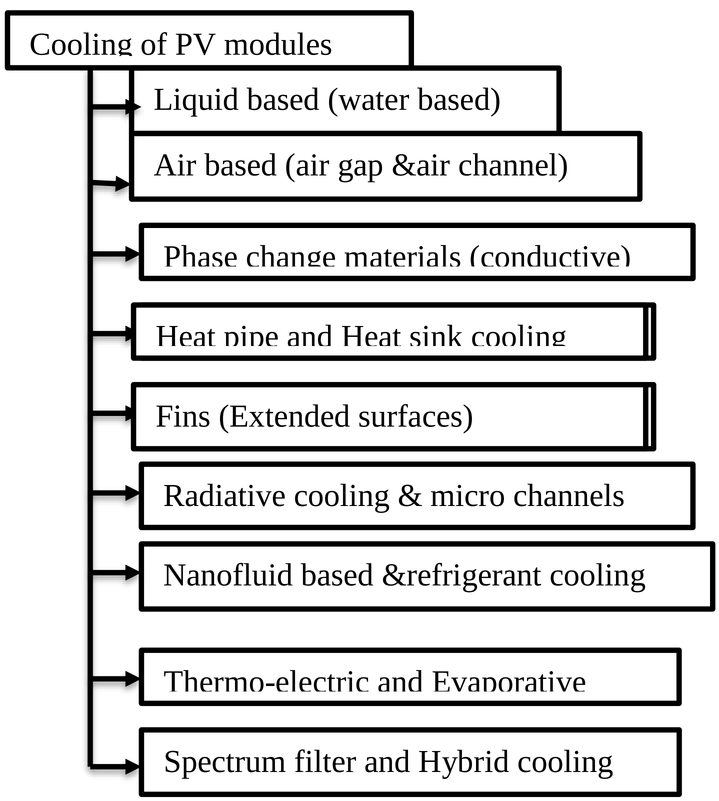

Figure: 2. 1 Classification of cooling techniques (Dwivedi et al., 2020).

Photovoltaic module cooling systems are mainly classified as active and passive cooling systems (Yesilyurt et al., 2018).

2.2.1 Active Cooling Methods

Active cooling methods can be considered as those methods that continuously consume power to cool the photovoltaic module. Most of the methods used were based on air and water as a cooling fluid. Hence, the main consumption system is a pump or fan needed for maintaining fluid circulation (Grubisic et al., 2016).

2.2.2 Passive Cooling Methods

A passive cooling system does not require power to operate. The passive cooling system is carried out naturally without any mechanical technique. Due to its simplicity, it is perhaps the most popular method for photovoltaic Module cooling, no additional materials are required, and the cost is relatively small.

The photovoltaic front and back surface cooling techniques are given in figure 2.2.These cooling are also classified under passive and active cooling methods.

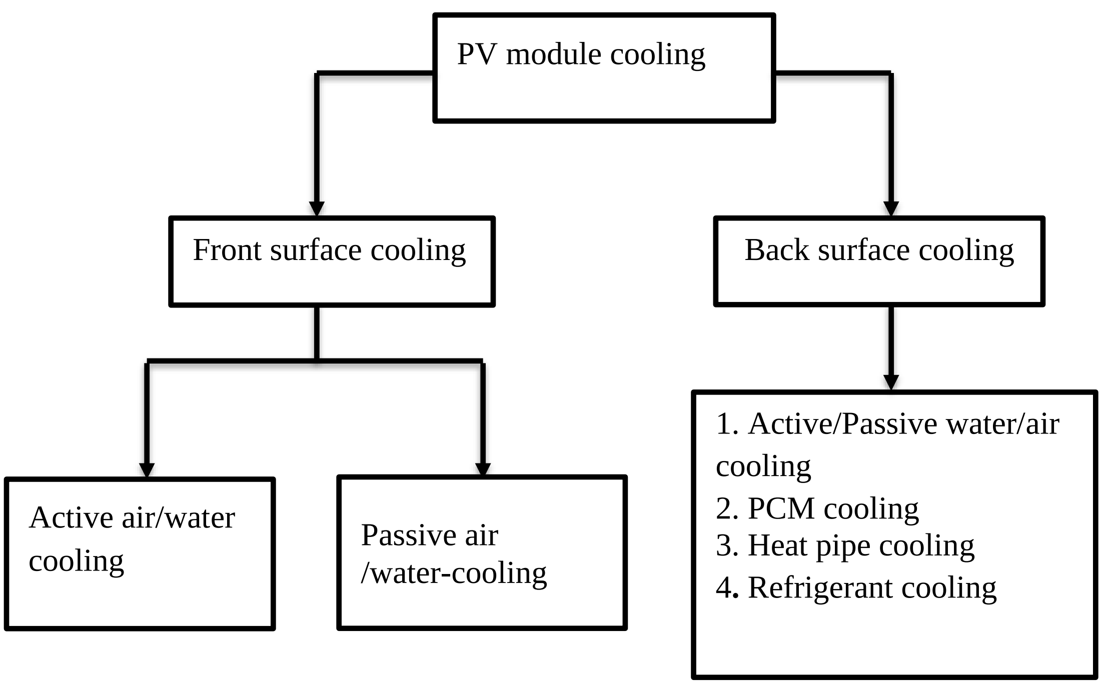

Figure: 2. 2 Cooling techniques of the photovoltaic module front and back surface (Bhakre et al., 2021).

2.3 Review of Related Works on the Photovoltaic Modules Cooling System

Under this portion, a detailed review of the previous works related to the electrical and thermal performance of solar photovoltaic modules with or without a cooling system is summarized. Brief of water-cooled, air-cooled, PCM cooled and fin (extended surface) cooled solar photovoltaic module systems last works are reviewed.

2.3.1 Fin Cooled Photovoltaic Module

El Mays et al., (2017) experimentally studied to enhance the performance of (Poly crystalline Silicon) photovoltaic module (70 cm x 35 cm) with capacity 30 W using an Aluminum finned plate, and cooling under natural convection. Experiments were done by placing the finned plate of aluminum on the backside of the photovoltaic panels to obtain maximum cooling. The lowest surface temperature of the PV panel is around 49.9 ℃ obtained when using a finned plate of aluminum, while it reaches the maximum value of 56 ℃ in the standard PV module. The results showed that of two panels the average efficiency is around 17.7 % that was obtained when using the photovoltaic panel with a finned plate while the efficiency is dropped to 15.9 % in the standard PV panel. A finned plate can gently improve electrical efficiency by around 1.77%. Firoozzadeh et al., (2019) experimentally investigated two identical multi-crystalline photovoltaic modules with the maximum power of 60 W. Conventional photovoltaic modules and photovoltaic module mounted with fins. In the case of PV with fins, 10 numbers of aluminum fins with 1 mm thickness, 50 mm spaces, were mounted at the back surface PV module. Experiments were done under two different irradiations of 420 W/m^2 and 630 W/m^2. The results showed that in steady-state conditions, the temperature differences of about 7.5 and 4 °C have been established for mentioned irradiation, respectively. In addition to temperature, the results showed that of 2.34 and 2.68 % additional in efficiencies for mentioned irradiation, respectively.

Hasan et al., (2015) experimentally evaluated three 65 W polycrystalline panels with 771 mm to 665 mm dimensions were used. Ethyl vinyl acetate (EVA) was used as the encapsulated material. The experiment done under stable solar radiation intensity ranging from 400 to 950 W m^{-2}. One photovoltaic module without phase change material and the other two photovoltaic modules were each attached at the back with rectangular metallic containers having internal fins to contain phase change materials. The metallic containers were fabricated from a 5 mm thick sheet of aluminum having internal dimensions 600 mm × 700 mm × 40 mm. The containers were internally fitted with straight vertical back-to-back fins of the same alloy with 75 mm horizontal spacing between fins as shown in Figure 2.3. The reference photovoltaic module and the two photovoltaic integrated phase change materials were deploying outdoors facing south at the latitude angles. The system has been evaluated outdoors with two-phase change materials (PCMs); a, hydrate calcium chloride ($CaCl_2$_$6H_2O$), and a eutectic mixture of fatty acids, cupric acid, palmitic acid in two different climates of Dublin, Ireland (53.33 N, 6.25 W) and Vehari, Pakistan (30.03N, 72.25E). In the best case, $CaCl_2$_$6H_2O$ achieved a 3–4 ℃ higher photovoltaic temperature drop and resulted in 3% more power saving than cupric palmitic acid in Vehari, Pakistan. Comparing the two climates, it was observed that both the phase change materials (PCM) achieved higher photovoltaic module temperature drop in Vehari than in Dublin, reaching up to 21℃ and resulting in associated power saving of 13 % in Vehari.

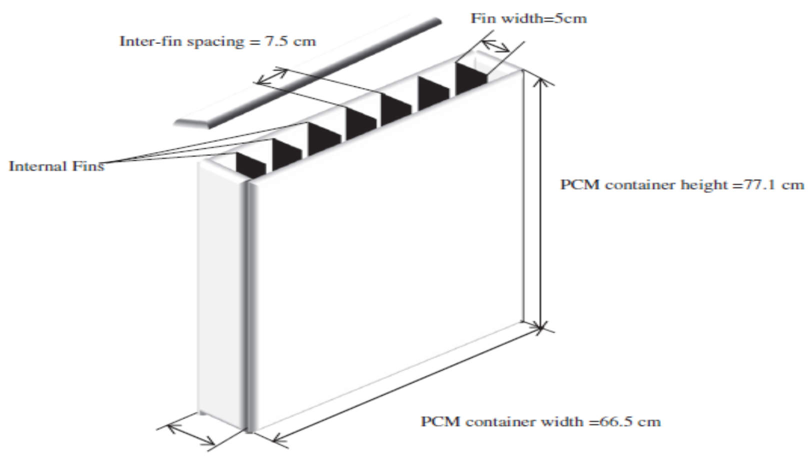

Figure: 2. 3 A phase change material container with vertically installed back-to-back fins (Hasan et al., 2015).

Johnston et al., (2021) investigated the performance of fin heat sink mounted on the rear of a Photovoltaic module by simulation and experimentation. The orientation and fin height influence the heat sink's capacity to reduce cell temperature. With a heat sink fin height of 20 mm, the temperatures of the front and rear surfaces of the module reached 62 and 51℃, respectively. When the fins were extended to 300 mm, these temperatures were reduced to 45 and 30℃, respectively. It is showed that the heat sink's performance in eliminating heat when the direction is rotated through 180^o (from appearance upwards to appearance downwards). The accompanying effect on the power output was also investigated. When the 20 mm heat sink was applied to a solar module, the power output increased by 11.3 % (relative), compared to the power generated from a bare solar module. Increasing the fin height further to 100 mm means the power output is further increases to 15.27 % compared to the bare solar module. Elbreki et al., (2020) investigated the effect of lapping fins and planner reflector on the cooling of a photovoltaic module of size 670 mm x 530 mm experimentally and using computational fluid dynamics. They studied the effect of lapping fin height, the number of fins, fin spacing, and solar irradiance intensity on the photovoltaic module performance using computational fluid dynamics. The result conveyed that, photovoltaic module without cooling surface temperature was numerically modeled and solved by engineering equation solver (EES), and its efficiency decreased from 11.1 to 9.81% as solar irradiance and module temperature increases. Nehari et al., (2016) simulated using a two-dimensional heat conduction model the performance of a PV module integrated with PCM and extended surfaces (fins) to improve conductive heat transfer and reinforce the thermal homogeneity. They investigated several inner fins of different length, 5, 10, 15, 20,25,30,35 and 40 mm. The results showed that furthermore, the fins length of 25, 30, and 35 mm provide a preferable PV cell cooling. Suresh and Shanmadhi,(2020) experimentally tested the performance of the photovoltaic module without incorporating evaporative cooling technique and with incorporating evaporative cooling technique on the performance of the photovoltaic module. The results showed the improved power generation of solar photovoltaic modules up to 10 % increasing in the morning or evening time, up to 16 % increase in the afternoon time. In addition, they concluded that at lower relative humidity, the rate of evaporation is faster due to the presence of lesser moisture content in the air. At lower water flow rates, the interaction between air and water is better due to the availability of more time. Hence, evaporation takes place at a better rate and as discussed above, the temperature of spray water decreases faster. Iqbal et al., (2016) experiments were performed in two 12 W polycrystalline photovoltaic modules with a dimension of 32 cm × 27 cm, to observe the effect of cooling on the efficiency of the solar PV module. Very cheap water sponges can be utilized as a means to cool the solar panel. The result shows that, temperature with water-cooling reduces by 4ºC keeping the flow rate at 2 liters /hour. Averagely the temperature is decreased by 1.7ºC as compared to panel without cooling. The result showed that the power output gives away its maximum value and this value with cooling becomes 6.4 % at maximum and 4.3 % averagely. Hourly assessment of output efficiencies shows that with cooling it increases maximally at a rate of 0.39 % on average and 2.69 % at maximum at compared to reference panel 11.84 % was the maximum efficiency achieved with water cooling and 9.15 % for an ordinary panel.

Sato and Yamada, (2019) studied radiative cooling is, a passive cooling method that enhances the radiative cooling effect by modifying the emissivity spectrum of the module surface for spectrally selective thermal radiation absorption, without any additional mechanical and electrical devices. The earth's atmosphere has a transparent window in the infrared spectrum range of 8 to 14 μm. They prove radiative cooling of the terrestrial body occurs when the radiative heat flux release is greater than the incoming heat flux, including radiative, conductive, and convective heat. On the commonly used non-concentration crystalline silicon PV module and radiative cooling performance of spectrally selective surfaces on the PV module surface is revealed by using a more realistic thermal budget model. Kadam et al., (2018) designed, fabricated and experimentally investigated active cooling system for PV module. To actively cool the PV cells (flat plate collector), the fins type of heat exchanger were attached at the back of a panel for the air-cooling**.** It observed that when the temperature of the surface of the module was 51.1 and 54.9 ^{0}C, the current was found to be 2.86 and 2.61 A without and with an active cooling system, respectively. The experimental results showed active cooling system has increased efficiency by 2-3 %.

Arifin et al., (2020) investigated a PV module performance with CFD and with experimental test, used 50 W polycrystalline solar cells with an aluminum heat sink mounted at back of the PV module and with fins base that is 2 mm thickness. The results show PV module with and without heat sink at solar intensity 1000 W/m^2, the average surface temperature 72.8 and 85.3^{0}C respectively. The heat sinks increased voltage by 10% and reduce current by 1.18%. Because of the increase in voltage was higher than the decrease in current, the power from the cell was increased by 18.67% and the electric efficiency gained with heat sink reach 2.6% under the same solar irradiation.

Zubeer et al., (2017) investigated experimentally and numerically the impact of the operating temperature of the cells on the electrical and thermal performance of the PV systems by using different cooling techniques. Using ribbed wall heat sink, the maximum power produced by the panel is increased by 6.97 and 7.5 %, by DC water pump. The temperature was decreased by 5 to 23 ^{0}C and power output was increased 9 to 22%, by using a heat exchanger connected to PV operating temperature was reduced by about 20%, and electric efficiency was increased by 9 % and by using aluminum fins, cell temperature decreased and power input enhanced by 4.2 and 5.5 % respectively. Wongwuttanasatian et al., (2020) designed grooved tubes and finned containers of the same volume (3000 cm^3) filled with palm wax as PCM. It was observed that introducing PCM cooling in a finned box could enhance the module efficiency by up to 9.82 %. This approach contributes to a 5.3% improvement in electrical efficiency. However, their study reveals the electrical efficiency of the module could be significantly enhanced if the irradiance level is more than 500

W/m^2 and the use of PCM are not feasible for low irradiance location.

2.3.2 Water Cooled Photovoltaic Module

Moharram et al., (2013) experimentally studied the efficiency of water-cooled polycrystalline photovoltaic modules through cooling of its surface by spraying water. They also developed a mathematical model to determine when to start cooling of the photovoltaic panels as the temperature of the panels reaches the maximum allowable temperature. An active cooling system model has been developed to determine how long it takes to cool down the photovoltaic (PV) panels to their normal operating temperature, which is 35 ℃ based on the proposed cooling system. It is found that arise in the solar module temperature by 10℃, which is from 35 to 45 ℃ result in decreases the efficiency of the cells from 12 to 10.5%. In this study, it was reported that operating the water spray cooling system for 5 min resulted in a decrease in the solar module temperature by 10℃ and an increase in the solar cell electrical efficiency by 12.5%.Dorobantu et al., (2013) experimentally explored the electrical performance of a laboratory-scale polycrystalline photovoltaic module when operated outdoors under natural light luminance. Water-cooling is implemented using a perforated tube disposed of on the top of the panel. To produce film water over the photovoltaic module, a tube with 25 holes of 1.5 mm diameter has been installed on the top end of the panel. The flow rate of water is two lit/min. The temperature of the front and the back surfaces of the panel were measured; the result showed that the temperature on the back of the panel is reduced from 48 to 35.5 °C. The temperature difference between the back and front-side of the panel remains the same, about 7 to 8 °C. As a whole, it was concluded that free flow front water cooling of PV panels can improve the efficiency and reliability of photovoltaic energy conversion the open circuit voltage of the panels is increases when the photovoltaic temperature decreases and due to the lower operating temperature, its life cycle could be increased. In addition, the study reported that the accidental debris spots, which could destroy the photovoltaic panel, could be eliminated by the water flow.

Govardhanan et al., (2020) experimentally investigated photovoltaic module performances with water-cooling and without a cooling system. The solar module has a capacity of 25 W with dimensions 54 cm × 47 cm. Three different mass flow rates (5.3, 3.8, and 2.3 kg/min) of cooling water flowing on the top of the solar module were used. The result conveyed that the power output accelerated to a maximum of 21 W when cooling with a mass flow rate of 2.3 kg/min, 22 W when the flow rate is set to 3.8 kg/min, and 23 W at the highest flow rate of 5.3 kg/min whereas without cooling yields a maximum power of 19 W only. The cooled PV module has a maximum of 15% higher output power than the conventional modules (uncooled PV) while flowing water is at a mass flow rate of 5.3 kg/min. The cooling of the PV module increases efficiency and yields a minimum rise of 4 % at the cooling rate of 2.3 kg/min and a maximum of 14.3 % at the flow rate of 5.3 kg/min. It shows good results in both thermal and electrical performances. Ale and Rotipin, (2019) experimentally studied 150 W power rated monocrystalline Photovoltaic module of size 1480 mm by 670 mm cooled by water. The result conveyed that the temperature of the photovoltaic module with water-cooling decreases maximally by 24.1 ℃ and averagely by 11.76 ℃ as shown in Figure 2.4. It was observed that the open-circuit voltage of the module with water-cooling increases maximally by 10.06 % and averagely by 5.2 %. It was observed that the Output Power of the module with water-cooling increases maximally by 9.83 % and averagely by 5.2%.

Figure: 2. 4 Photovoltaic modules cooled with water cooling system (Ale and Rotipin, 2019)

Milind et al., (2017) investigated experimentally a polycrystalline solar panel with area 60 cm × 60 cm by using free front flow water cooling system. The water was made to flow over the surface of the panel as shown Figure 2.5. The cooling system consists of a ¾-inch polyvinylchloride (PVC) pipe of length 27 inches, a ball valve of ¾ inch, a hose nipple for connecting the garden hose to the ball valve, for collecting water in a 4-inch pipe of length 27 inches, and a stopper. The flow of the water is controlled using the ball valve. The result showed that by free front water-cooling the power generated increased from 5% to 19.05%.

Figure: 2. 5 Photovoltaic modules with free front water flow cooling (Milind et al., 2017)

Mehrotra et al., (2014) cooled experimentally 2 W polycrystalline silicon solar panel having area of 0.033 m^2 by water immersion, as shown in Figure 2.6. Which is placed inside a plastic box filled with water to a depth of 10.8 cm. The experiment was done under an ambient temperature that varies slightly from 33.5 to 38.4 ^{0}C and the solar intensity varies from 1170 to 670 W/m^2 during the day. Without water, the average output voltage, power output, and electrical efficiency of the whole day were obtained as 8.011 V, 1.346 W, and 4.04 %, respectively. Their results conveyed that the maximum increase in output voltage with water immersion is observed at a depth 4 cm with the average value of the day as 8.811 V and power output and electrical efficiency were observed at depth of 1cm and the average values of the whole day were 1.418 W and 4.76 %, respectively. Therefore, an increase of 9.98 % in output voltage, 5.34 % in power output, and 17.8 % in electrical efficiency were achieved by water immersion techniques.

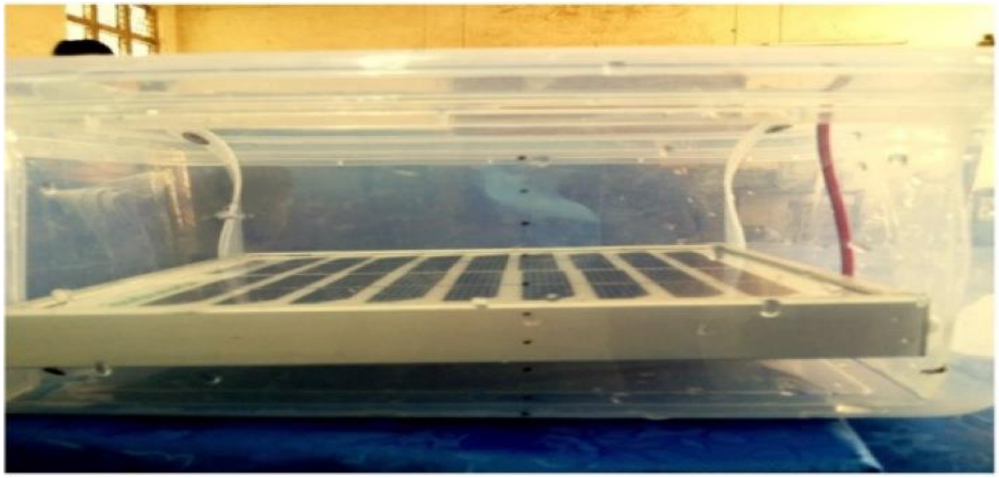

Figure: 2. 6 Photovoltaic immersed in water (Mehrotra et al., 2014)

Rahimi et al., (2014) designed and fabricated a jet impingement laboratory scale-cooling device based on a conic wind tunnel to cool photovoltaic cells and an experimental system was developed. The average temperature of photovoltaic cells decreased from 15 to 20 ^{o}C depending up on the solar intensity applied. At a constant flow rate of air 100 m^3/ hr. When the solar intensity increases from 570 to 1100 W/m^2, the photovoltaic cell achieves a maximum power output from 0.86 to 2.39 W. This corresponds to about a 3 and 15 % increase in output power compared to the reference photovoltaic module. Arcuri et al., (2014) studied the performance of photovoltaic cooling systems with water for different construction aspects such as use of metal sheet and plastic material on the photovoltaic cooling system. In regards to the water system, the analyzed plastic material for the cooling ducts offers low thermal performance, therefore metallic ducts with higher thermal conductibility. The low-temperature difference between the ducts, the maximum variation of 3 K has been achieved with a duct pitch of 159 mm. corresponding to an overall heat loss coefficient of the photovoltaic water system of 45.09 W/m^2k concerning the air system; the use of the metal sheet produces an almost flat cell temperature profile. Du et al., (2012) developed an active water cooling system for photovoltaic cells performance test. This has been used for testing the PV module's performance for different parameters such as operating temperature, power output, and efficiency it has been found that the output electricity of the concentration solar cell is 4.7 to 5.2 times higher than the fixed cell. During the test day, the maximum produced electricity at solar noon from the concentration solar cell was 71.13 W, and from the fixed cell was 16.55 W. The concentration of solar cells is around 4.9 times more than the fixed cell during the test day. It has been concluded that with the higher water flow rate, the more heat is extracted from the solar cell, and therefore the cell temperature decrease and electrical efficiency increases. Alobaid et al., (2018) experimentally investigated the effect of the outlet water temperature and cell temperature on both electrical and thermal efficiency of photovoltaic cells, by considering factors that influence PV module performance like solar radiation, ambient temperature, inlet fluid temperature, cell temperature. The result showed that for cell temperature decrease from 29.1^0C to 18.5^0C, the electrical and thermal efficiency increased from 14.72 to 15.44% and 72 to 83%, respectively. Bahaidarah et al., (2013) investigated through experiment and simulation for the active water-cooling effect of the cooling panel, which was attached to the PV module back surface and uses circulating water. As a result, cells temperature was decreased to 36 °C (ΔT cell =10 °C) when solar irradiance was of cell 979 W/m^2, ambient temperature 20 °C, wind velocity 2 m/s, and cooling water flow rate of 1 L/min (0.81 L/min). Abdelrahman et al., (2013) experimentally investigated a 40 W Mono crystalline solar module for the three cooling systems. These cooling are front film water-cooling, back 22 L duck finned cooling, and the combination of back and front cooling's. The results show that due to decrease the module temperature from 57 to 41.5°C, thus increase the maximum output power from 20.3 to 25.4 W. The module surface temperature is decrement due to the three cooling related to the non-cooling module with maximum temperatures changes of 16, 18, and 25 ºC for film, back, and joined cooling, respectively. In addition to this, the daily output power of the PV cooling module increased up to 22, 29.8, and 35% for film, back, and joined cooling modules, respectively compared to the non-cooling module.

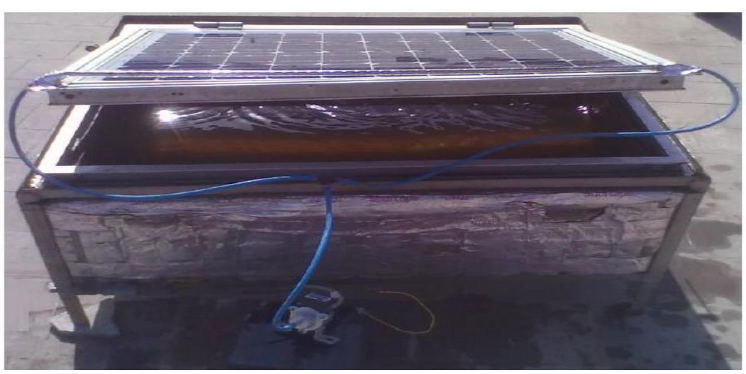

Figure: 2. 7 Photovoltaic module with water film cooling (Abdelrahman et al., 2013).

Rasham et al., (2015) experimentally and numerically, the photovoltaic Module cooling has been investigated on continuous and intermittent water cooling techniques. Two monocrystalline modules were used. One with cooling and the other without cooling of an area of 0.4600525 m^2.

The average values of the cooling rate for continuous and intermittent were (3.4804 ℃⁄min) and (3.1617 ℃⁄min) respectively. The output power and efficiency enhancement of and intermittent were (7.349 %) and (5.587 %), (8.389 %) and (6.826 %) respectively, then for non-cooling.

2.3.3 Air Cooled Photovoltaic Module

Amelia et al.,(2016) experimentally investigated the effect of air-cooling on the performance of a PV module with a maximum power output rating of 100 W. A DC motor drove the fan. Experiment was conducted on the photovoltaic panels with no cooling system attached to it for 8 hours from 9.00 am to 5.00 pm at 10-minute intervals. The average ambient temperature for this test day was 36.50 °C. The maximum module temperature was found to be about 59.88 °C when the ambient temperature was 39.21 °C. However, for the same condition, the module temperature could be reduced to 53.64 °C with one unit DC fan. The result showed that using four units of DC fans, the average module temperature was reduced by about 22.22 %. About 14.5% of percentage increments in voltage output was observed by attaching four units, DC fan at the backside PV panel. By further increasing the DC fan from two, three and four, the power output increased to 67.7, 72.43, and 76.54 W respectively. This corresponds to 37.17, 41.28, and 44.34 % increase power output of a photovoltaic module respectively. Ibrahim, (2018) experimentally tested performance the of a photovoltaic module that has a maximum power rating of 200 W and maximum power current and open-circuit voltage rating of 7.61 A, and 32.9 V, respectively. The aim of the study was to test the influence of cooling and cleaning processes by using fans, sprinklers, and wipers on the operational performance of the photovoltaic module energy system. The result conveyed that the module temperature without and with cooling have increased up to 50 and 38℃, respectively. They concluded that a cooling and cleaning PV module could achieve a power gain of about 34.55 %.

The photovoltaic module cooling system is studied experimentally by using a DC brushless fan and DC water pump. The experiment has been done using two polycrystalline solar modules. The result showed that PV module with DC water pump cooling system increases by 3.52, 36.27, and 38.98 % in terms of output voltage, current, and power respectively. The DC brushless fan cooling system increases to 3.47, 29.55, and 32.23 % in terms of output voltage, current, and power respectively. It was concluded that, the cell temperature decreased by 6.1 ℃ compared to PV modules without DC brushless fan cooling system (Amelia et al., 2016). Chandrashekar et al.,

(2020) designed and investigated experimentally the effect of water circulation and phase change material (paraffin wax 70% and bee wax 30%) on PV efficiency enhancement. It was found that the PV module with PCM integrated the efficiency was 7.31% greater than the bare. Sajjad et al., (2019) experimentally investigated the photovoltaic modules (Monocrystalline Silicon) cooling in open-air conditions. Two modules were used. One module was installed on the duct of cooled air of air-conditioners and the other was the bare photovoltaic module for the sake of the comparison. The result shows that the power output efficiency of the cooled module was increased by 2.3%.

2.3.4 Phase Change Materials Cooled Photovoltaic Module

Chandrashekar et al., (2020) evaluated experimentally the photovoltaic module integrated with a smart cooling system, to increase electrical efficiency. The experiment used photovoltaic module polycrystalline silicon with a maximum power of 40 W and has an area of 2866.1499 cm^2. Tested was carried out on this setup to determine the effect of water circulation and use of phase change material (PCM) as cooling medium on the performance of the photovoltaic module. Paraffin wax and bee wax were used as phase change, material (PCM). The experimental results conveyed that the photovoltaic module, integrated PCM was 7.31 % more efficient than the normal system. Prajapati et al., (2017) investigated experimentally 12.75 W and 18.023 V maximum voltage Monocrystalline solar PV module. A 12 V rating DC fan was used to cool the module. Experiments were performed at two levels of radiation, namely 500 W/m^2 and 1000 W/m^2. The improvement in the open-circuit voltage is however marginal in all these cases, when the temperature is lowered with cooling. The results showed that the lowering of the temperature by a simple cooling fan arrangement can result in a decrease in temperature by 5 to 6 ºC, depending on the radiation levels on the PV module. Khanna et al., (2018) studied the performances of three photovoltaic modules: the first system consists of a photovoltaic panel. The second system consists of a photovoltaic panel equipped with a phase change material. In the third system, aluminum fins are introduced inside the PCM container. Based on the proposed methodology, the thermal response of the finned-PV-PCM system in terms of temperature variations with time has been studied and analyzed for the range of spacing between fins, fin length, fin thickness, and depth of the PCM box. The most suitable dimensions of fins and depths of the container for various daily solar radiation values optimally cool the PV have been calculated. Thus, 2.8 cm can be considered as the most suitable depth for the total solar radiation of 3 $kWh/m^2/day$. The results show that for a system having spacing as 100 cm, the suitable depth of the container is 3.9 cm for the total solar radiation of 5 kWh/m^2/day. It means that the photovoltaic module temperature starts increasing again for the total solar radiation of greater than 5 kWh/m^2/day. If spacing decreases to 25 cm, the suitable depth increases to 4.6 cm. It is because, for smaller spacing, the number of fins in the system is larger and the heat extraction rate of phase change material is higher and, thus, it melts in shorter. It is observed that for a system having fin thickness of 0.5 mm, the suitable depth of the container is 4.1 cm for the total solar radiation 5 kWh/m^2/day. It conveys that the photovoltaic temperature starts to increase again for total solar radiation greater than 5 kWh/m^2/day. If fin thickness increases to 2 mm, the suitable depth increases to 4.5 cm. The results showed that as spacing decreases, the temperature of the PV decreases. Since, decrease in spacing, the number of fins in the system increases the rate of heat extraction from photovoltaic leading to a decrease in module temperature. The results also showed that a decrease in spacing beyond 25 cm does not lead to a significant decrease in photovoltaic module temperature. Thus, the best spacing between fins is 25 cm. The results show that the photovoltaic temperature decreases with an increase in fin length. Thus, the best length of the fin is equal to the depth of the container. The results also show that an increase in thickness beyond 2 mm does not lead to a significant decrease in photovoltaic temperature. Therefore, the best thickness of fins is 2 mm. Khanna et al., (2018) investigated experimentally three 4000 W photovoltaic array arrangements slanted each at 45°.These are convectional photovoltaic, phase change material equipped photovoltaic and fins embedded phase change material for photovoltaic are compared for Southeast united kingdom. The result conveyed that the photovoltaic module was cooled from 45 to 29 and 27℃ using phase change material and fins embedded phase change material, respectively. Power improvements are 220 W and 260 W using phase change material and fins equipped phase change material respectively around solar noon. Daily power improvements are 1200 W and 1400 W using phase change material and fins equipped phase change material respectively. Firoozzadeh et al., (2019) introduced the major cooling methods of photovoltaic modules and review different methods of cooling photovoltaic modules by using phase change materials. They summarized the result as follows: using the PCM, thermal, and electrical performance of photovoltaic increased more than 10%. They concluded that both integrating impurity and metal fins to phase change materials, can greatly enhance the photovoltaic performance and materials which used as phase change materials, a good melting point of about 25 to 35℃, which is the best thermal operating condition for photovoltaic modules. Mahamudul et al., (2016) numerically and experimentally investigated the effect of the PCM layer of width 0.02 m of RT 35 in cooling the PV module. The results showed that at constant radiation of 1000 W/m^2, photovoltaic module temperature without PCM raises to 70 ℃ and when a PCM layer of Rubitherm (RT) 35 is integrated with a module, the temperature was reduced to 35 ℃ carried out for 8000 seconds. For photovoltaic module without or with PCM rises in temperature was 60 ℃ and 35 ℃ at constant radiation value of 750 W/m^2, respectively. Bayrak et al., (2020) experimentally investigated the performances of a polycrystalline PV module using different cooling methods. These are phase change materials, thermoelectric and aluminum fins were chosen as the cooling methods. The result showed that with fins and thermoelectric the reference temperature difference is 2.4 and 2.8 ℃, respectively. The power output for the finned and thermoelectric cooled was increased by 2.14 and 7.72 %, respectively. Stropnik and Stritih, (2016) studied experimentally and through simulation the cooling effect on the performance of a PV module by using a phase change materials with melting point of 28 ℃ enclosed with an acrylic glass. The photovoltaic temperature on October 17 for conventional photovoltaic module reached a maximum of 75.5 ℃ at 13.30S, which was 57.7 ℃ above the ambient temperature. The average temperature of the PV module integrated with PCM panel during the experiment was 35.9 ℃. The results show that the maximum increase of the PV with PCM electrical power under the given conditions was 23.2 % and on October 17, the electrical efficiency was 9.2 %. According to the simulation, the performance improvement of the PV-PCM module results, show that electrical power output increased by 4.3 to 8.7 %. Nizetic et al., (2017) reviewed the performance gain of passive cooling techniques for the photovoltaic modules. Regarding performance analysis for passive cooling techniques, the efficiency gain of cooled PV module compared to bare where, respectively from 2 to 6% for PCM cooled systems, from 10 to 15% for liquid cooled systems, from 3 to 5% for air cooled systems, and from 0.5 to 1% for average radiative cooling techniques. Kiwan et al., (2020) theoretically analyzed based on mathematical formulation and experimental test to PV system cooled by phase change material (PCM). The investigation was done for two PV panels, experimentally to find the effect of using paraffin graphite (PCM 47) on efficiency and power output. This study found that the phase change material would give positive results only when the temperature of the panel exceeds the phase change material melting point.

2.4 Factor Affecting Photovoltaic Module Performances

Various environmental parameters affect the solar panel. For example, sunlight, ambient, and module surface temperature, wind speed, humidity, shading, dust, installation height, etc. Among several variables, key role-players are indeed solar irradiance and temperature (Dwivedi et al., 2020).

2.4.1 Effect of Solar Irradiance and Effect of Ambient Temperature

The fraction of the phone energy of the solar irradiance absorbed by the PV module cell is responsible for generating electric power. The higher the energy fraction the higher will be the electric power generated. However, when higher solar energy is absorbed, the cell temperature will also be higher that reduces the electric power to be generated.

The short circuit (I_{SC}) current was affected by the number of photons absorbed by the semiconductor material and is related to the light intensity. The conversion efficiency is therefore constant in such a way that the power output is usually associated with the irradiance, but the efficiency is reduced for the cell temperature rises. The open-circuit voltage decreases so much with the rise in temperature of the module above 25℃. Nevertheless, short circuit current (I_{sc}), increases only marginally. The temperature effect on PV performance is identified as the temperature coefficient. The net result is a reduction in power output with temperature rise (Dwivedi et al., 2020).

2.4.2 Effect of Turbidity and Effect of Water Vapors

As the turbidity increases the short circuit current decreases but this decrement is different for different PV cells depending upon its spectral response. The percentage of this decrement is as follows 4.4% for a monocrystalline PV module, 4.8% for a multi-crystalline PV module, and 7.33% for the amorphous PV module. Increasing water vapors only affect monocrystalline and multi-crystalline PV cells as it would decrease solar irradiance at large wavelengths but its effect on amorphous PV cells is negligible (Amjad et al., 2019).

2.4.3. Effect of Dust on Photovoltaic Module

Accumulation of dust on the surface of a PV module decreases the amount of energy to be absorbed by the PV cell. Thus, blow air or flowing water over the PV surface can remove dust in addition to cooling the PV surface temperature. Aldihani et al., (2014) studied the effect of cooling fluids in reducing the impact of dust on the PV power output. Experimentally investigated the performance of solar PV panels under Kuwait environment and numerically simulates the effect of cooling in reducing the impact of dust on the PV power output. The solar panel used is made of HIT solar cells and has overall dimensions of 1580 mm x 798 mm. Experimental measurements for the higher intermediate temperature (HIT) PV panel have shown that the accumulated dust over 12 months can lead to a maximum loss in power output of 16% at noon for the July month. Numerical simulation results have shown that the use of cooling can partially compensate for this power loss. A water-cooled panel with a temperature reduction of 20 k can improve the power output from 150 to 171 W at midday.

2.5 Summary from Literature Review

The electrical power generation performance of a solar PV module for different size and power rating like from 2, 25, 30, 100 W etc, were studied with and without integration of cooling system by previous researches as discussed above. The reviewed literature covered the effect of surface module temperature and another parameter on the thermal and electrical performance of the photovoltaic module through applying different cooling techniques. The passive cooling system and active cooling system that can be applied for the reduction of PV module cell temperature are summarized as follows:

Table 2.1 Literature summary

Authors	Year	Methods	Results
Mays et al.,	2017	Experimental	efficiency is around 1.77 % enhanced
Firoozzadeh et al.,	2019	Experimental	2.34 and 2.68 % enhanced efficiencies for irradiations of 420 W/m^2 and 630 W/m^2 respectively.
Johnston et al.,	2021	simulation and experimental	When 20 mm heat sink was applied power increased by 11.3 % Increasing the fin height further to 100 mm the power is increases to 15.27 % compared to the bare solar module
Elbreki et al.,	2020	Experimentally and simulation	efficiency increases from 9.81 to 11.1 % as solar irradiance and module temperature decreases
Nehari et al.,	2016	Simulation	fins length of 25, 30, and 35 mm provide a preferable PV cell cooling
Iqbal et al.,	2016	Experimental	The power output gives value with cooling becomes 6.4 % at maximum and 4.3 % averagely
Kadam et al.,	2018	Experimental	With an active cooling, has increased efficiency by 2-3 %.
Moharram et al.,	2013	Experimental	10^0C reduction in temperature and electrical efficiency was increased by 12.5%.
Dorobanțu et al.,	2013	Experimental	The temperature on the back of the panel is reduced from 48 to 35.5 °C.
Govardhanan et al.,	2020	Experimental	Cooled PV module has a maximum of 15% higher output power than bare
Milind et al.,	2017	Experimental	Power generated increased from 5% to 19.05%.
Mehrotra et al.,	2014	Experimental	An increase of 9.98 % in output voltage, 5.34 % in power output, and 17.8 % in electrical efficiency were achieved by water immersion techniques
Amelia et al.	2016	Experimental	About 14.5% of increments in voltage output was observed by attaching four units, DC fan.
Ale and Rotipin	2019	Experimental	The temperature decreases maximally by 24.1 ℃ and averagely by 11.76 ℃ and Voc increase maximally by10%
Rasham et al.,	2015	Experimental	8.389 % increase in efficiency for continues and (6.826 %) for intermittent water
Bayrak et al.,	2020	Experimental	The result showed that with fins and thermoelectric the reference temperature difference is 2.4 and 2.8 ℃, respectively.
Stropnik and Stritih		Experimental	PV-PCM module results, show that electrical power output increased by 4.3 to 8.7 %

2.6 Research gaps

Based on the information acquired from the literature reviewed above the following gaps are identified to be researched in the present study.

- ❖ As more literature is reviewed, more research is required to integrate the active and passive cooling systems into photovoltaic modules for different location.
- ❖ Most of the previous works on solar PV module cooling for facing to the South. East and West facing PV modules performances were not studied.
- ❖ In terms of the photovoltaic air, cooling most of the previous work used DC fan cooling system and the experimental test with cooling and without cooling, was done on different days in the previous work not simultaneously in the same day.

Therefore, this study focuses on doing experimental work for the PV with cooling and without cooling by exposing it to the sun on the same day.

CHAPTER THREE

PERFORMANCE ANALYSIS METHODS OF THE SOLAR PHOTOVOLTAIC MODULE

3.1. Introduction

This thesis focus to investigate the thermal and electrical performance of solar photovoltaic module while operating under Adama weather condition experimentally. The electrical performance analysis method involves measuring the voltage and current generated by the photon absorbed by the PV module to determine the electrical power and electrical efficiency of the PV module using measuring instruments such as a multimeter. The thermal performances analysis method requires measurement of PV module surface temperature to evaluate the heat absorbed and thermal efficiency of the module using thermocouples wires. However, no solar radiation-measuring instrument is available in ASTU lab and Adama meteorological station has discontinued measuring global solar radiation falling on a horizontal surface. In addition, solar electricity can be generated using solar PV module using any available surface orientation in building; offices, cafeteria, hospital etc. and solar radiation data for these surfaces are needed. Even though the orientation of the buildings towards the sun are complicated and affects the maximum possible solar energy that can be harnessed by a solar PV systems, the most common building orientation relative to the sun are East facing building, West facing building, and South facing building. The same collector facing East , West or South axis will receive a different amount of solar energy and the surface temperatures of the solar PV system is also different for these different surfaces. The amount of electricity that can be generated by a solar PV system is inversely proportional to temperature and directly proportional to global solar radiation that excites the charge particles in the semiconductor cell of the PV. The amount of solar energy falling on East, West, and South facing solar PV system in Adama are needed to be estimated theoretically to determine the experimental performance of the PV module for these orientations.

Thus, this chapter discusses mainly the theoretical data generation and analysis methods used to find performances of the solar PV system such as solar radiation, the average ambient temperature and average wind velocities. Chapter four discusses the experimental procedure and the experimental performance analysis methodology used in this study in detail.

3.2 Materials and Methods

3.2.1 Methodology of Estimating Solar Radiation Falling on Photovoltaic Module

The experimental performance of the solar PV model is to be evaluated for the three possible orientations towards the sun: East facing, West facing, and south facing. The methodologies of estimation of solar radiation falling on the solar PV system used in this thesis are:

- ❖ Collecting sunshine hour duration data and wind speed
- ❖ Estimating beam and diffused radiation on horizontal surface using correlations for East, West, and South facing
- ❖ Estimating global solar radiation for the PV module East, West and South facing
- ❖ Estimating global solar radiation on tilted solar PV system, for the PV module East, West, and South facing
- ❖ Estimation of the Photovoltaic Module Absorptance on the Inclined surface PV system, for the PV module East, West, and South facing
- ❖ Estimation of average ambient temperature

3.2.2 Methodology of Measuring Experimental Performance of Photovoltaic Module

The methodologies used for estimating the experimental thermal and electrical performance of the solar PV system in this thesis are

- ❖ Purchasing of two PV models from market
- ❖ Fabrication of supporting structure for the solar PV system
- ❖ Assembling the experimental setup
- ❖ Measuring surface temperature of the PV system
- ❖ Measuring short circuit current
- ❖ Measuring open circuit voltage
- ❖ Estimating DC power outputs
- ❖ Estimating electrical efficiency of PV module for both cooled and uncooled case
- ❖ Estimating thermal efficiency of PV module for both cooled and uncooled case
- ❖ Writing results and discussions using figures, graphs, and charts
- ❖ Writing the conclusion
- ❖ Writing the recommendation
- ❖ Write future works

- Finally rearrange thesis paper and submitted

3.2.3 The Overall Methodology used in the Thesis Experimental Performance of Photovoltaic Module

The overall methodology used in this thesis work are summarize as indicated in Figure 3.1.

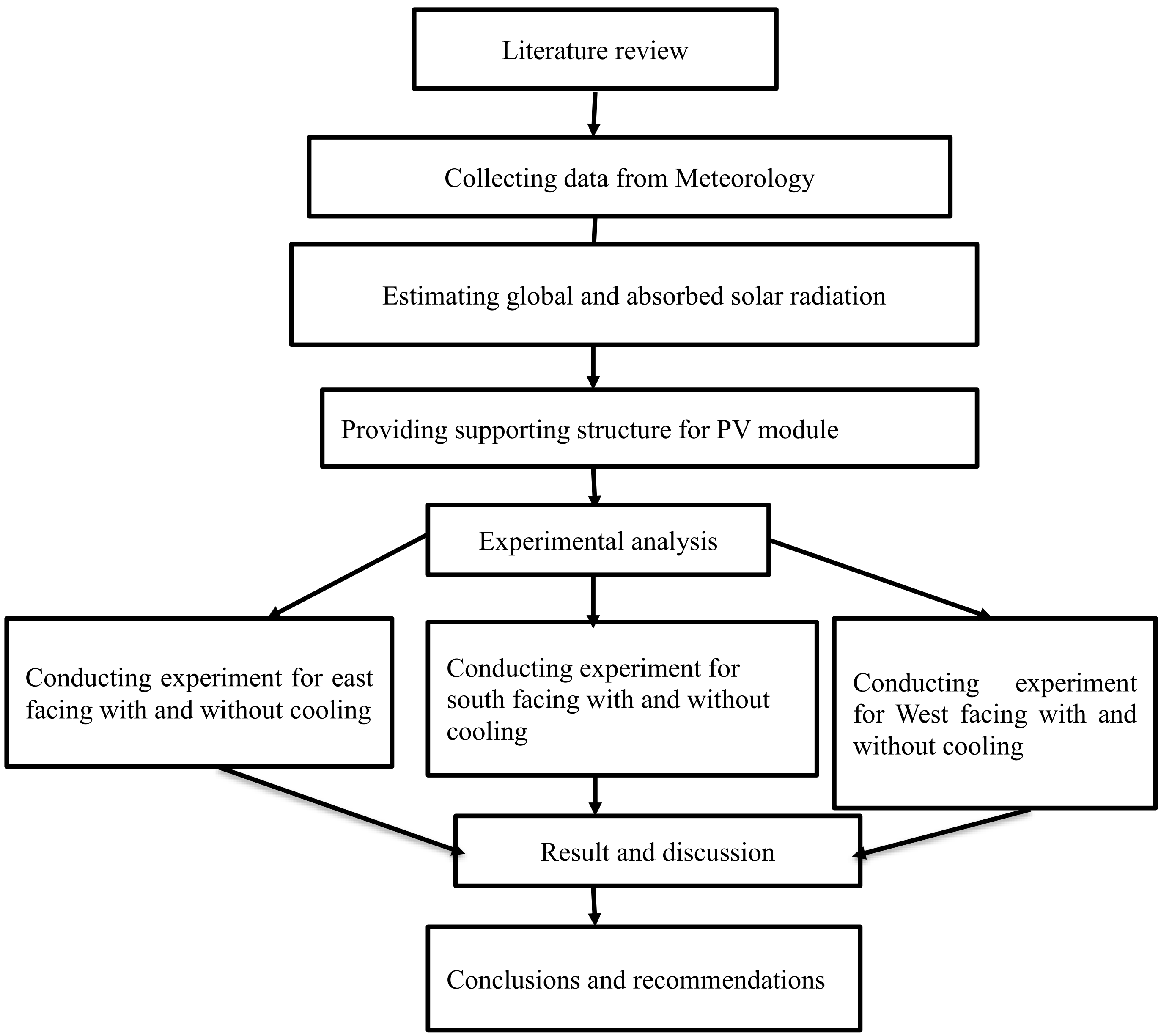

Figure: 3. 1 Research methodology flow chart

3.3 Data Collected from Meteorology

The meteorology weather data needed to analyze the theoretical solar radiation are sunshine hour duration (SSH), ambient temperature, geographical data of Adama, etc.

3.3.1 Sunshine Hour Duration

Sunshine duration is the length of time that, the ground surface is irradiated by direct solar radiation and was used to characterize the climate of sites. To estimate solar radiation the data like geographical coordinate of site, sunshine hours, and weather condition are the most important requirements. Simply, sunshine duration is the length of time that the ground surface is irradiated by direct solar radiation and used to characterize the climate of the sites. Adama mereology collects sunshine duration data every three hour over a period of 24 hour. These data collected every three hour were purchased from Adama meteorology and converted to daily average sunshine duration data and then into monthly average sunshine data for each year from 2011 to 2020. Then, the ten years average sunshine duration data were obtained that, were used to theoretically estimate the global solar radiation on the needed surfaces.

Therefore, the ten years (from 2011 to 2020) average sunshine duration data used to estimate the hourly solar radiation of Adama, are given in Table 3.1 and shown in Figure 3.2.

In addition to sunshine duration, the other data used to estimate solar radiation intensity is geographical data of Adama. Geographical coordinates of Adama station: -Latitude (ϕ) =8.5263' 23.8'' N = 8.558°; Longitude = 39 .17' 2.5'' E = 39.28°; Altitude = 1648 m above sea level (Hasen, 2019).

Table3. 1 Estimation of ten-year average sunshine duration

Months	Jan	Feb	Mar	Apr	Ma	Jun	Jul	Aug	Sep	Oct	Nov	Dec
Ava(2011-2020)	8.73	9.25	9	8.4	8.23	7.96	6.8	6.86	7.32	8.9	9.38	9.35

Figure 3.2 indicates that the sunshine hour attains maximum and minimum value on the month December and July, respectively. This is due to the behavior of the season, sunshine hour is maximum during winter in Ethiopia because most of the time it is clear sky. During the summer season, there is cloud and rain so the sunshine hour leads to the minimum value.

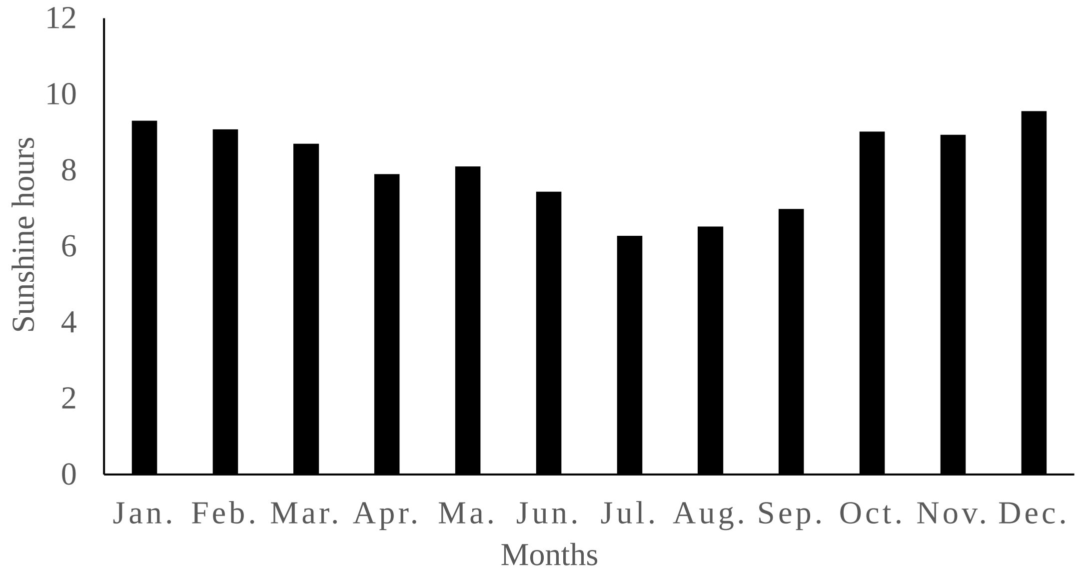

Figure: 3. 2 Sunshine hour for the representative day of each month in Adama for an average climatic condition of Ten years.

3.3.2 Preliminary Terminology and Sign Conventions for Estimation of Solar Radiation

Solar Time: Time based on the apparent angular motion of the sun across the sky with solar noon the time the sun crosses the meridian of the observer. Solar time is the time used in all of the sun-angle relationships; it does not coincide with local clock time. It is necessary to convert standard time to solar time by applying two corrections. First, there is a constant correction for the difference in longitude between the observer's meridian and the meridian on which the local standard time was based. The second correction is from the equation of time, which takes into account the perturbations in the earth's rate of rotation which affect the time the sun crosses the observer's meridian(Duffie and Beckman, 2006).

$$\text{Solar time} - \text{standard time} = 4(L_{st} - L_{loc}) + E \quad (3.1)$$

Where: L_{st} -is the standard meridian for the local time zone

L_{loc} - is the longitude of the location in question, and longitudes are in degrees west, that is, $0° < L < 360°$.

The parameter E is the equation of time (min) and sited (Iqbal, 1983)

$$E = 229.2(0.000075 + 0.001868\cos B - 0.032077\sin B - 0.014615\cos 2B - 0.04089\sin 2B) \quad (3.2)$$

$$B = \frac{360}{365}(n-1), [°] \qquad (3.2a)$$

Where, n: is the day of the year

Hour angle(ω) : is the angle between projections of the Sun's rays (solar meridian) and the line running south north through the center. The south-north line is also referred to as the "line due south." In other words, the hour angle is defined as the angular displacement of the Sun from the local meridian because of the Earth's rotation around its axis(Tiwari and Tiwari, 2016). Expression for the hour angle is given by:

$$\omega = (\text{Solar time} - 12) \times 15° \qquad (3.3)$$

Zenith angle (θ_z): the angle between the vertical and the line to the sun, that is, the angle of incidence of beam radiation on a horizontal surface (Duffie and Beckman, 2013).

Where,φ − angular location north or south of the equator; $-90 \leq \varphi \leq +90$

The angle of incidence (θ): the angle made between normal to the inclined surface and the solar beam radiation falling on the inclined surface (Tiwari and Tiwari, 2016).

$$cos\theta = (cos\varphi cos\beta + sin\varphi sin\beta cos\gamma)cos\delta cos\omega + cos\delta \sin\omega\, sin\beta sin\gamma + sin\delta(sin\varphi cos\beta - cos\varphi sin\beta cos\gamma) \qquad (3.4)$$

Latitude angle (φ): is the angular geographical location that is made in between the line joining location with a center of the earth and its projection on equatorial plane. northern is positive.$-90° \leq \varphi \leq 90°$(Tiwari and Tiwari, 2016).

Declination angle (δ): is the angular position of the sun at solar noon (that is, when the sun is on the local meridian) concerning the plane of the equator, north positive;$-23.45 \leq \delta \leq 23.45°$ (Duffie and Beckman, 2013). The declination δ found from the approximate equation of (Cooper, 1969).

$$\delta = 23.45 \sin(360\frac{284+n}{365}) \qquad (3.5)$$

Tilt angle (β):- the angle between the plane of the surface in question and the horizontal. $0° \leq \beta \leq 180°$**.** The yearly optimum slope angle of the solar collector is presented by(Duffie and Beckman, 2013)**.**

$$\beta_{opt} = \varphi + (10 \text{ to } 15)° \qquad (3.6)$$

Sunset hour, sunrise hour and day length

Sunset: - solved when the zenith angle is at 90° and sun is said to rise and set when the solar altitude angle (α) is zero. So the hour angle at sunset can be found by (Duffie and Beckman, 2013).

$$\cos\omega_s = -\frac{\sin\varphi\sin\delta}{\cos\varphi\cos\delta} = -\tan\varphi\tan\delta \tag{3.7}$$

Where: ω_s- positive for sunset

φ -Latitude angle

δ - Declination angle

The sunrise hour angle is the negative of the sunset hour angle. It also follows that the number of daylight hours is given by (Duffie and Beckman, 2013).

$$N_s = \frac{2}{15}(\omega_s) \tag{3.8}$$

Solar azimuth angle: - the angular displacement from south of the projection of beam radiation on the horizontal plane. Displacements east of south are negative and west of south are positive. The sign function in equations (3.9) is equal to +1 if ω is positive and is equal to −1 if ω is negative (Duffie and Beckman, 2013)

$$\gamma_s = \text{sign}(\omega)\left|\cos^{-1}\left(\frac{\cos\theta_z\sin\varphi - \sin\delta}{\sin\theta_z\cos\varphi}\right)\right| \tag{3.9}$$

Where: - γ_s -solar azimuth angle

ω -Hour angle

θ_z-Zenith angle

φ- Latitude of the place

δ -declination angle

3.4. Estimation of Global Solar Radiation Falling on a Horizontal Photovoltaic System

3.4.1. Estimation of the Extraterrestrial Solar Radiation on a Horizontal Surface

Solar radiation (I_o) incident on a horizontal plane in the extraterrestrial region/outside the atmosphere in W/m^2, which is equivalent to being in the absence of atmosphere, is a component of I_{ext} along the normal to a horizontal surface and can be given by (Tiwari and Tiwari, 2016):

$$I_o = I_{sc}[1.0 + 0.033\cos\left(\frac{360n}{365}\right)\cos\theta_Z \tag{3.10}$$

Where: I_{sc} - (solar constant) =1367 W/m^2

n- Day of the year

$$cos\theta_z = \cos\varphi\, cos\delta cos\omega + sin\varphi sin \quad (3.10a)$$

By integrating the equation above over the period from sunrise to sunset the daily total extraterrestrial radiation on a horizontal surface gives

$$H_0 = \frac{24\times3600}{\pi} I_{sc}\left(1 + 0.033\cos\frac{360n}{365}\right) \times (\cos\varphi\cos\delta\sin\omega_s + \frac{\pi\omega_s}{180}\sin\varphi\sin\delta) \quad (3.11)$$

Where: ω_s- is sun set hour angle

H_0 - Daily total hourly extraterrestrial solar radiation on a horizontal surface (J/m^2)

$I_{sc} = 1367$ -Solar constant ($W/_{m^2}$)

n-is the day of the year

The extraterrestrial solar radiation on a horizontal surface from sunrise to sunset hour calculated using the above relation for the representative days of each month of Adama are shown in Figure 3.3.

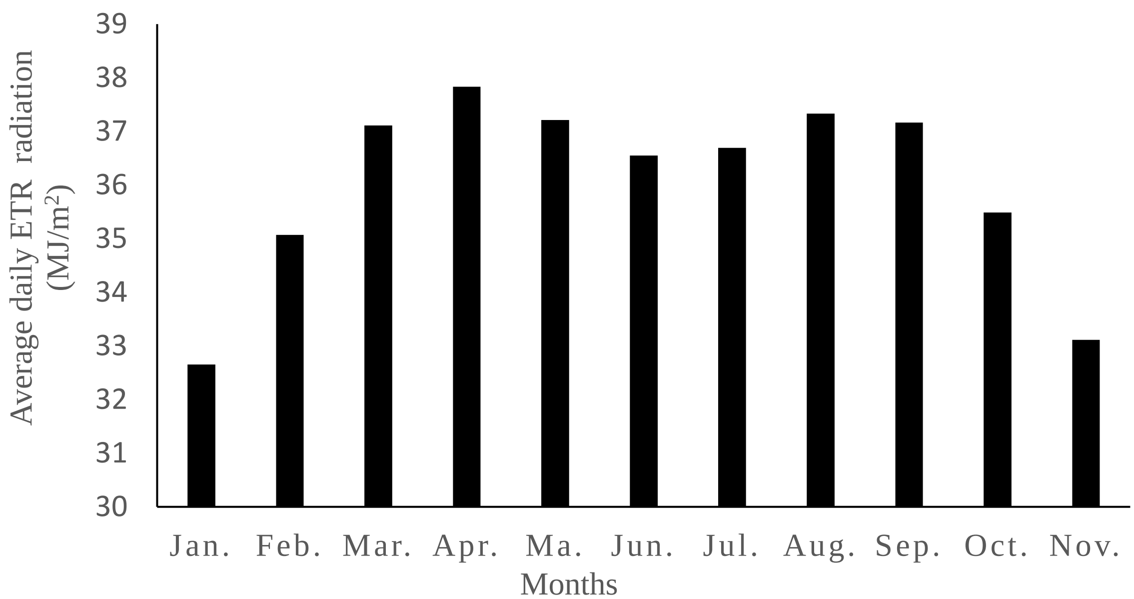

Figure: 3. 3 Graph of the daily solar radiation incident on a horizontal surface outside of the atmosphere (extraterrestrial (ETR) solar radiation

3.5 Estimation of Average Daily, Beam, and Diffuse Radiation on a Horizontal Surface

3.5.1 Estimation of the Monthly Average of Daily Global Radiation on Horizontal Surface

The first empirical correlation using the idea of employing sunshine hours for the estimation of global solar radiation was proposed by Angstrom. The Angstrom correlation was modified by

(Page, 1964). The simplest model used to estimate the monthly average daily solar radiation on a horizontal surface is the well-known Angstrom equation (Gana et al., 2014).

$$\frac{H_t}{H_o} = a + b\left(\frac{\bar{n}_s}{\bar{N}_s}\right) \quad (3.12)$$

Where: H_{t-} monthly average daily global radiation on the horizontal surface

$H_o -$ Monthly average daily radiation outside of the atmosphere on horizontal surface

$a, b -$ empirical constant, (values are obtained by regression)

$\bar{n}_s$- Monthly average daily hours of bright sunshine

$\bar{N}_s$- Monthly average of the maximum possible daily hours of bright sunshine

The (empirical constant) regression parameters a and b can be determined from-

$$a = -0.11 + 0.232cos\varphi + 0.323\left(\frac{\bar{n}_s}{\bar{N}_s}\right) \quad (3.12a)$$

$$b = 1.449 - 0.533cos\varphi - 0.694\left(\frac{\bar{n}_s}{\bar{N}_s}\right) \quad (3.12b)$$

The monthly average of daily global radiation on a horizontal surface from sunrise to sunset hour calculated using the above relation for the representative days of each month of Adama are shown in Figure 3.4.

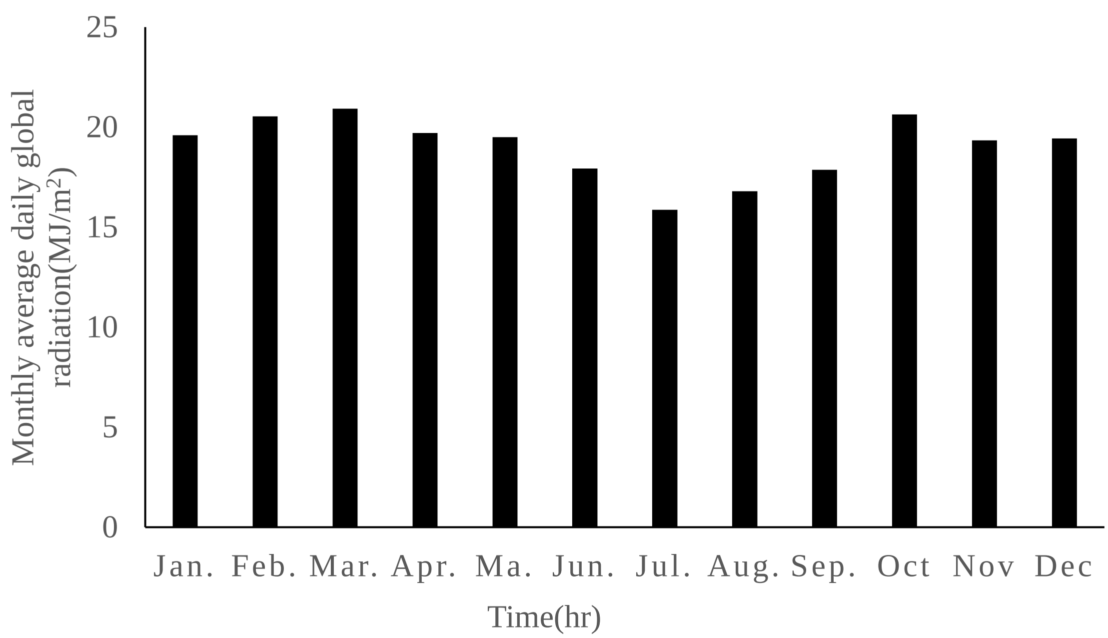

Figure: 3. 4 Graph of the monthly average of daily global radiation on a horizontal surface

3.5.2 Estimation of the Monthly Average of Daily Diffuse Radiation on a Horizontal Surface

The prediction of monthly average daily diffuse radiation based on the monthly average daily global radiation equation and the number of bright sunshine hours. Has been obtained using the following correlations (Tiwari and Tiwari, 2016).

$$\frac{\bar{H}_d}{H_t} = 0.931 - 0.814\left(\frac{\bar{n}_s}{\bar{N}_s}\right) \tag{3.13}$$

The monthly average daily diffuse radiation on a horizontal surface from sunrise to sunset hour calculated using the above relation for the representative days of each month of Adama are shown in Figure 3.5.

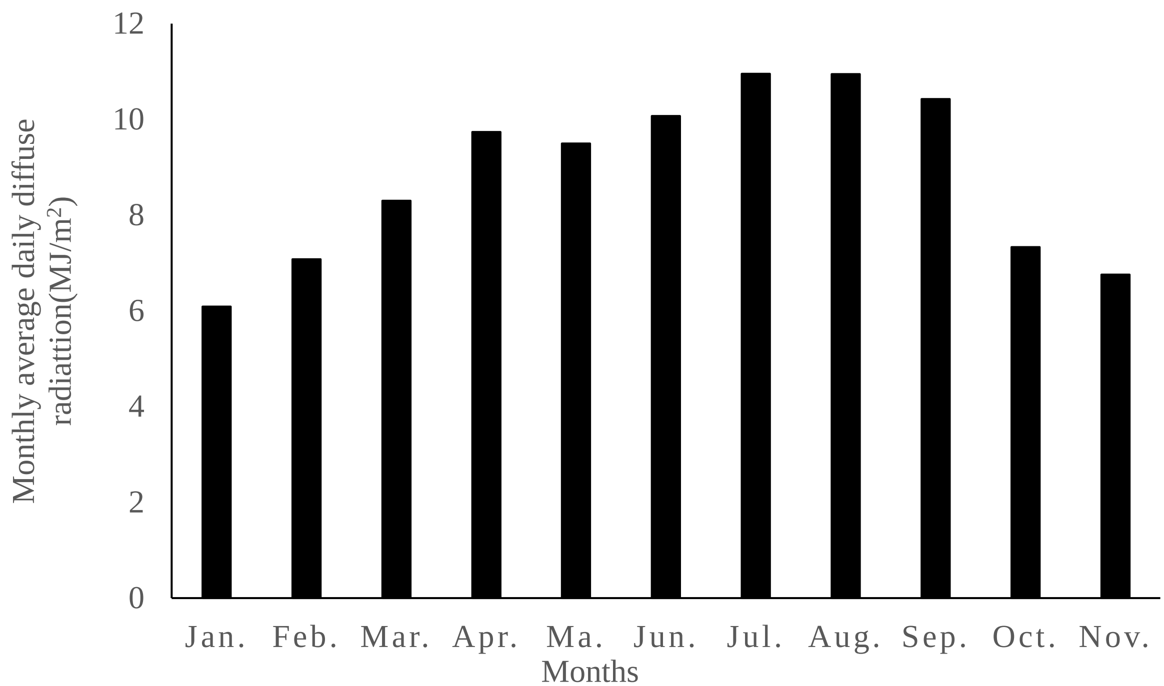

Figure: 3. 5 Graph of the monthly average of daily diffuse radiation on a horizontal surface.

3.5.3 Estimation of the Monthly Average of Daily Beam Radiation on a Horizontal Surface

Beam Radiation is solar radiation received from the sun without having been scattered by the atmosphere. Beam radiation is often referred to as direct solar radiation. Monthly average daily beam radiation on a horizontal surface (H_b) is the difference between global and diffuse monthly daily average radiation. With the monthly average daily total radiation and the monthly average daily diffuse radiation known, the monthly average beam radiation on a horizontal surface can be calculated equation (3.14) (Kalogirou, 2014).

$$H_b = H_t - \bar{H}_d \tag{3.14}$$

The monthly average of daily beam radiation on a horizontal surface from sunrise to sunset hour calculated using the above relation for the representative days of each month of Adama are shown in Figure 3.6 together with monthly average daily global, beam, and diffuse radiations.

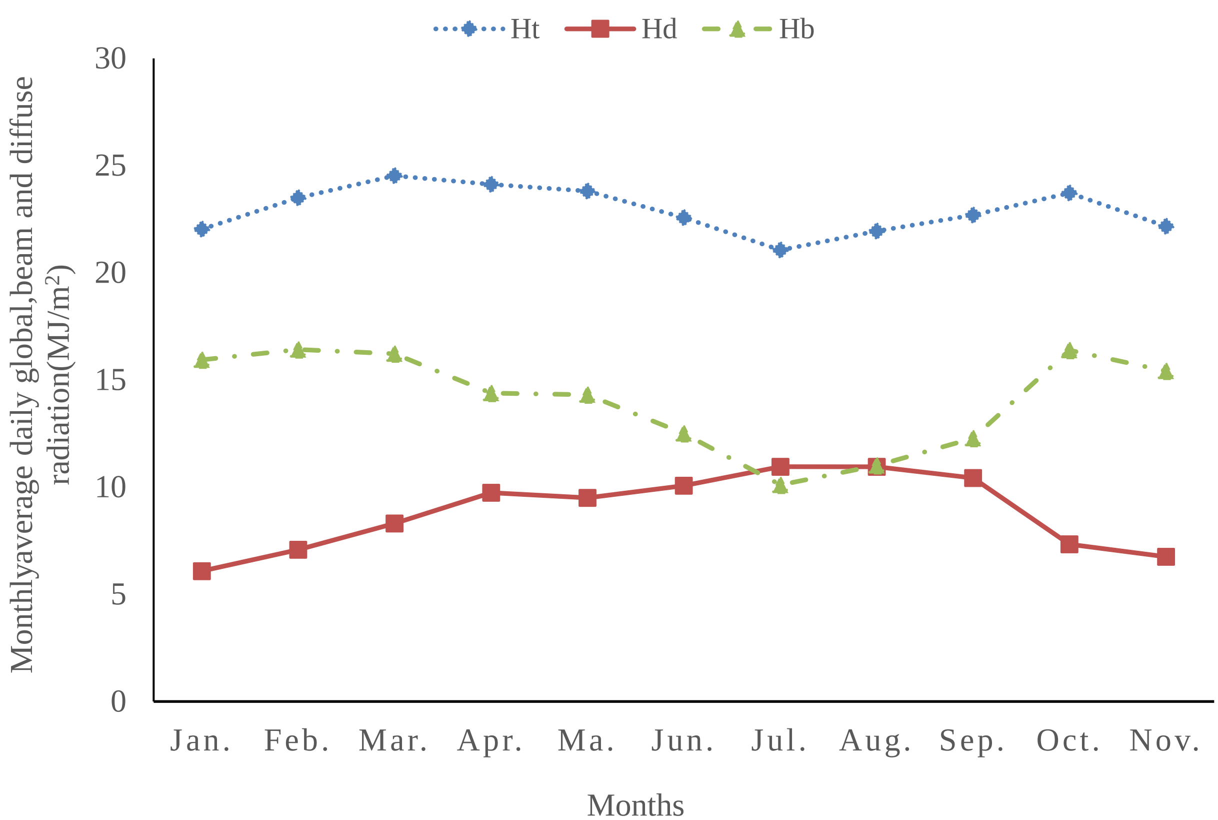

Figure: 3. 6 Graph of monthly average daily global, diffuse, and beam of solar radiation.

3.6 Estimation of the Monthly Average Hourly Global, Diffuse and Beam Radiation on a Horizontal Surface

3.6.1 Estimation of the Monthly Average Hourly Global Radiation on a Horizontal Surface

The monthly average hourly global solar radiation can be calculated from the knowledge of the monthly average daily global solar radiation on a horizontal surface.

The total hourly solar radiation falling on a horizontal surface, $\bar{I}$ (W.h/m^2, could be estimated from the daily global radiation, H_t (kJ/m^2 per day) following (Tiwari and Tiwari, 2016).

$$\frac{\bar{I}}{H_t} = \frac{\pi}{24}(a + b\cos\omega)\frac{\cos\omega - \cos\omega_s}{\sin\omega_s - \frac{\pi}{180}\omega_s\cos\omega_s} \tag{3.15}$$

Where a and b are regression constants. Given by:-

$$a = 0.409 + 0.5016\sin(\omega_s - 60) \tag{3.15a}$$

$$b = 0.6609 - 0.4767\sin(\omega_s - 60) \tag{3.15b}$$

The monthly average hourly global radiation on a horizontal surface from sunrise to sunset hour calculated using the above relation for the representative days of each month of Adama are shown in Figure 3.7.

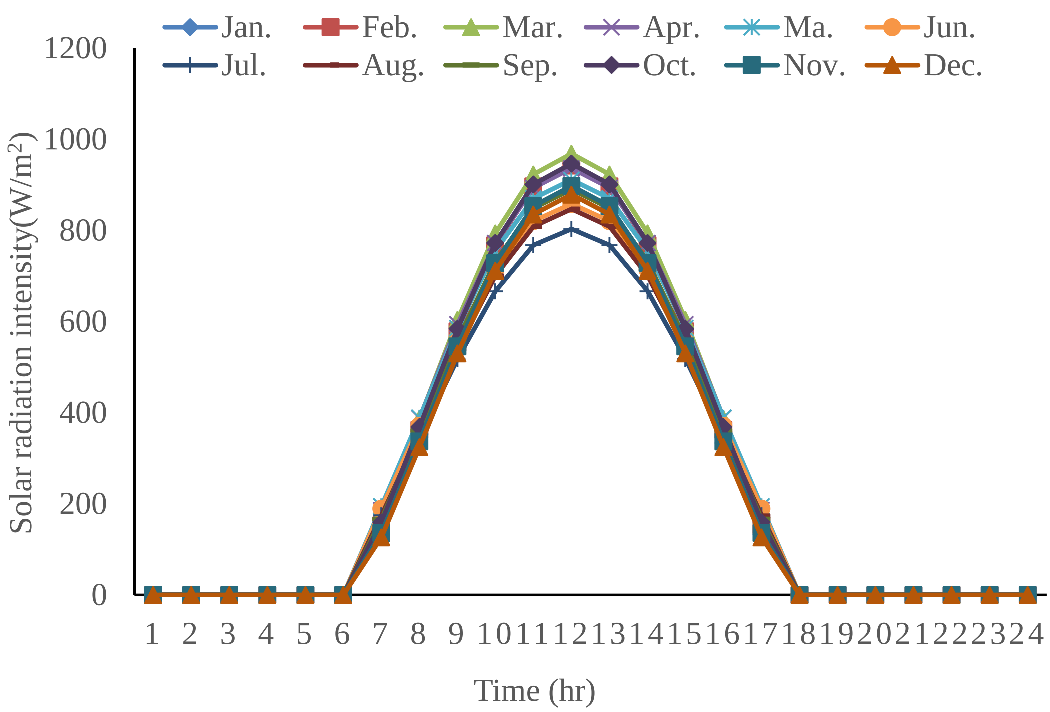

Figure: 3. 7 Graph of the monthly average hourly Global Radiation on Horizontal surfaces.

3.6.2 Estimation of the Monthly Average Hourly Diffuse Radiation on a Horizontal Surface

The monthly average hourly diffuse radiation on a horizontal surface can be calculated from the monthly average daily diffuse radiation on a horizontal surface(Duffie and Beckman, 2006).

$$\frac{I_d}{H_d} = \frac{\pi}{24} \frac{\cos\omega - \cos\omega_s}{\sin\omega_s - \frac{\pi}{180}\omega_s \cos\omega_s} \tag{3.16}$$

Where: I_d -Hourly average diffused solar radiation on the horizontal surface

H_d- Daily average diffused solar radiation on the horizontal surface

ω- Hour angle

ω_s- Sunset hour angle

The monthly average hourly beam radiation on a horizontal surface from sunrise to sunset hour calculated using the above relation for the representative days of each month of Adama are shown in Figure 3.8.

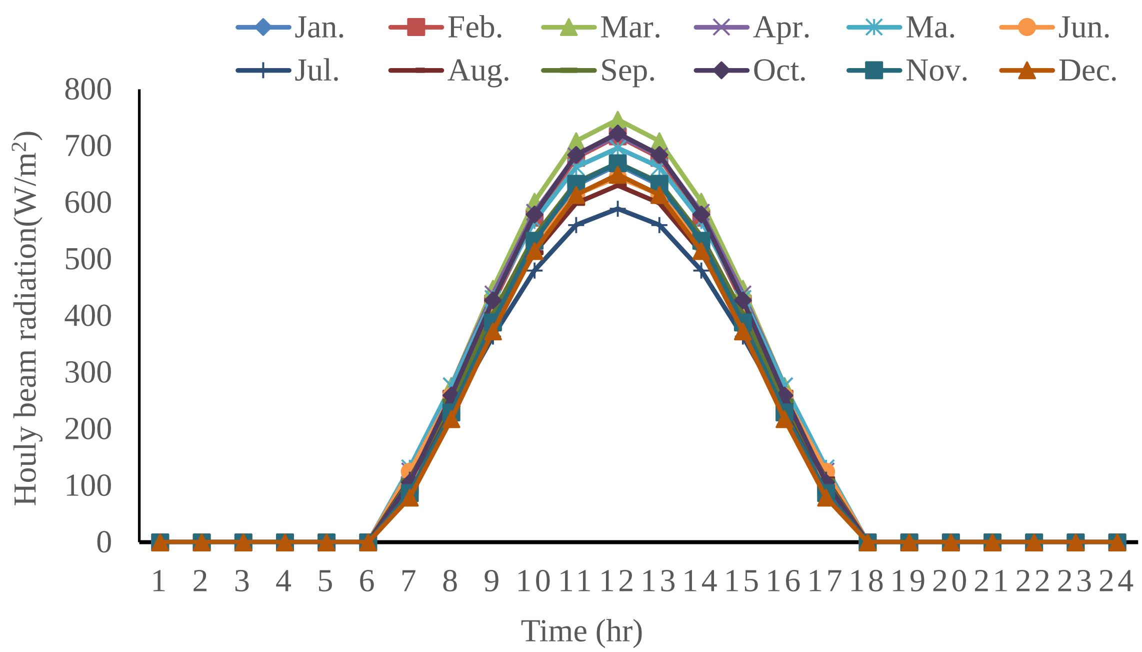

Figure: 3. 8 Graph of the monthly average hourly beam radiation on horizontal surfaces.

3.7 **Estimation of Global Solar Radiation Falling on Inclined Photovoltaic System**

3.7.1 Estimation of Solar Radiation Intensity for South Facing Tilted Solar Photovoltaic System

Frequently, the PV module is not installed horizontally but at an angle to increase the amount of radiation intercepted and reduce reflection and cosine losses. Therefore, system designers need data about solar radiation on such tilted surfaces.

The amount of insolation on the terrestrial surface at a given location for a given time depends on the orientation and slope of the surface. For the solar photovoltaic facing south, the surface azimuth angle is zero.

The general form of total hourly solar radiation energy incident on an inclined surface I_T is given by (Duffie and Beckman, 2013).

$$I_T = I_b R_b + I_d \left(\frac{1+\cos\beta}{2}\right) + (I_b + I_d)\rho\left(\frac{1-\cos\beta}{2}\right) \quad (3.17)$$

Where: I_T - Total hourly irradiance on a tilted surface (W/ m^2)

I_b -Hourly beam irradiance (W /m^2)

I_d - Hourly diffuse irradiance (W/ m^2)

R_b –The ratio of beam radiation on the tilted surface to that on a horizontal surface

$$R_b = \frac{\cos\theta}{\cos\theta_z} \quad (3.17a)$$

Where β - Surfaces slope angle,

ρ –Ground reflectivity - 0.2 for bare earth and- 0.7 for snow.

θ_z -Is the solar zenith angle

θ- is the angle of incidence

$$cos\theta = cos\varphi cos\beta cos\delta cos\omega + sin\varphi sin\beta cos\delta cos\omega + sin\delta(sin\varphi cos\beta - sin\beta cos\varphi) \quad (3.17b)$$

$$cos\theta_z = \cos\varphi\, cos\delta cos\omega + sin\varphi sin\delta \quad (3.17c)$$

The input energy in PV solar radiation on a tilted surface having a tilt angle of β from the horizontal and an azimuth angle of (assumed zero as south facing) is the sum of the beam, sky diffuse (and ground reflected solar radiation. The radiation components on the tilted surface are computed using equation (3.17), and it is shown in Figure 3.9.

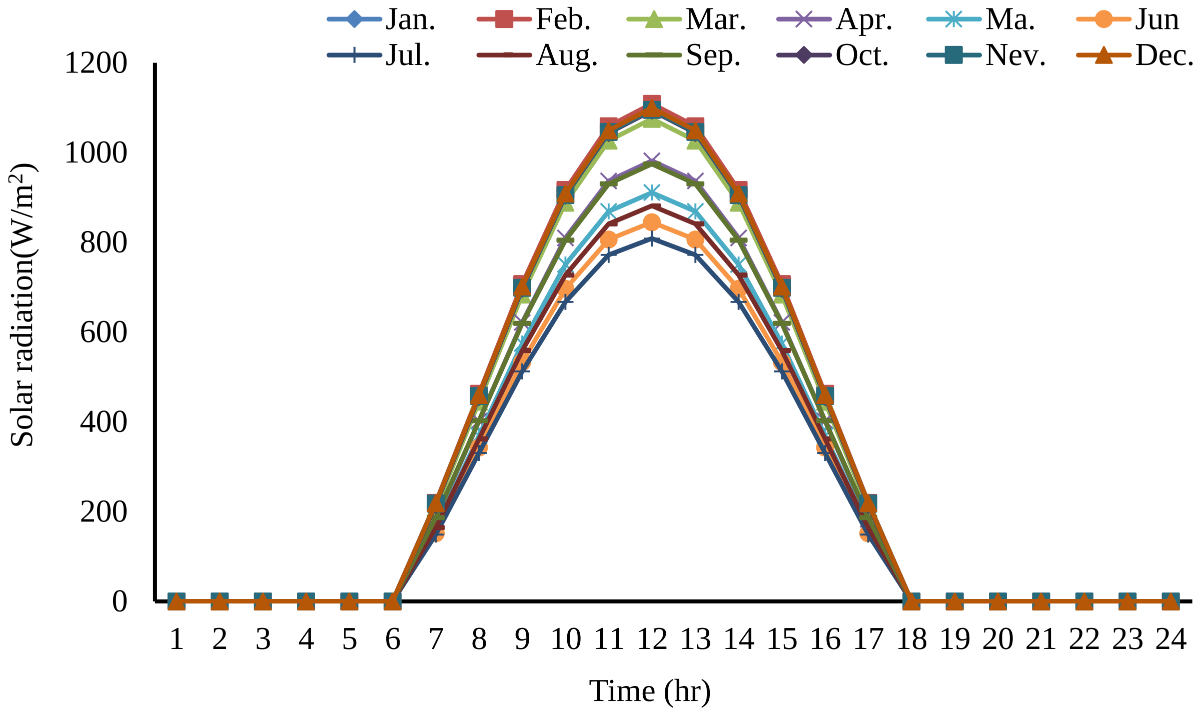

Figure: 3. 9 Global hourly solar radiation on 23.5° tilted surface (W.h/m^2) for south facing.

For a plane rotated about a horizontal east-west axis with a single daily adjustment so that the beam radiation is normal to the surface at noon each day,

$$cos\theta = sin^2\delta + cos^2\delta cos\omega \tag{3.18}$$

The radiation components on the tilted surface are computed using equation (3.17) and its diffused & beam components are shown in Figure 3.10. In this Figure, the estimation of hourly total (global), beam, and diffuse solar radiation were shown. The hourly estimated global, beam, and diffuse radiation shown as a sample were for May 15th of the tilted surface at 23.5°.

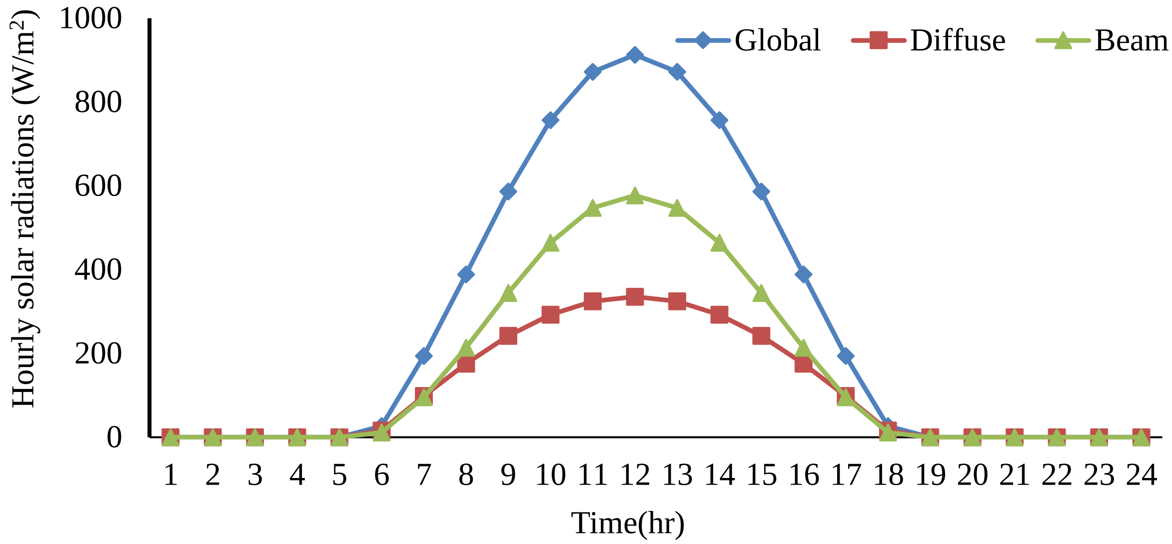

Figure: 3. 10 Graph of maximum hourly global, diffuse and beam solar radiation on inclined surfaces (23.5°) on may15th.

3.7.2 Estimation of Solar Radiation Intensity for East Facing Tilted Solar Photovoltaic System

The east and west total tilted surface average hourly solar radiation was estimated by equation (3.17) by using the appropriate azimuth angle values. In most solar PV energy-calculator tools, an azimuth value of zero is facing the equator in both northern and southern hemispheres; +90° degrees is facing due west and –90° degrees is facing due east (Dhimish and Silvestre, 2019). Figure 3.11 shows the estimated global solar radiation intensity for east facing of earth axis.

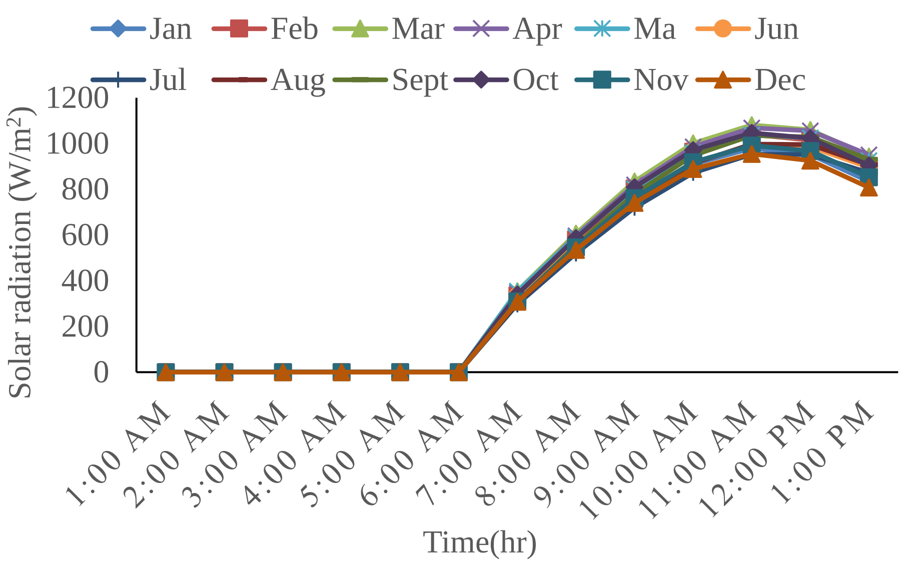

Figure: 3. 11 Global hourly solar radiation on 23.5° tilted surface (W/m^2) for East facing

3.7.3 Estimation of Solar Radiation Intensity for West Facing Tilted Solar Photovoltaic System

The west total tilted surface average hourly solar radiation was estimated by equation (3.17).In most solar PV energy-calculator tools, an azimuth value of zero is facing the equator in both northern and southern hemispheres; +90° degrees is facing due west (Dhimish and Silvestre, 2019).Figure 3.12 shows the west facing estimated total solar radiation.

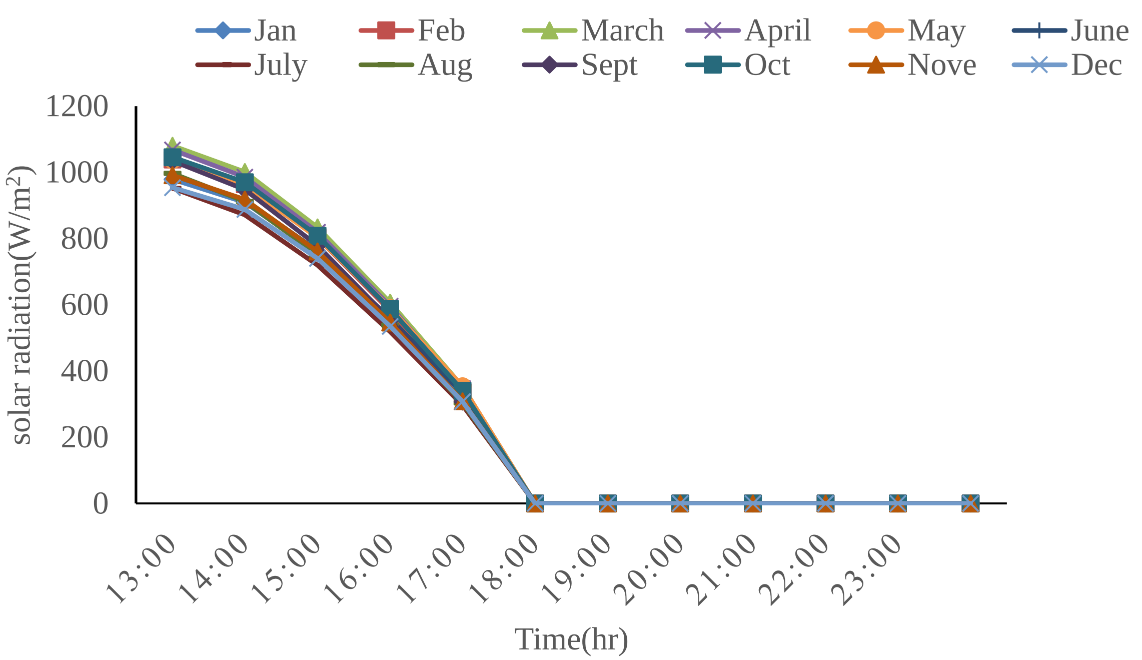

Figure: 3. 12 Global hourly solar radiation on 23.5° tilted surface (W.h/m^2) for West facing

3.8 Estimation of the Photovoltaic Module Absorptance on the Inclined Surface

The diffuse radiation model employed for the analysis was the isotropic sky model, which considers all components of radiation for calculating the incident radiation on the tilted plane whereas the optical model is used for calculating the solar radiation absorbed in the photovoltaic cell. The absorbed radiation calculated from the radiation and optical model is then coupled with the electrical model and the thermal model to determine the electrical power output and cell temperature. The major factor affecting the power output from a photovoltaic (PV) device is the solar radiation absorbed on the cell surface, which is a function of the incident radiation, air mass, and incidence angle. Similar to the situation with thermal collectors the needed radiation data are not normally known on the plane of the PV panel, so it is necessary to estimate the absorbed solar radiation using horizontal data and incidence angle information. The effective absorbed solar radiation for a PV system consists of beam, diffuse, and ground-reflected components and a spectral effect. Absorbed radiation, based on an isotropic photovoltaic module is given by (Kalogirou, 2014).

$$S_{PV} = M.\left((G_b R_b (\tau\alpha)_b + (\tau\alpha)_d G_d.\frac{(1+\cos\beta)}{2} + \rho_g G(\tau\alpha)_g \left(\frac{1-\cos\beta}{2}\right)\right) \quad (3.19)$$

Where: b -beam

d-diffuse

g- Ground

M –Air mass modifier

$(\tau\alpha)_b$ -Beam radiation transmittanceabsorptivity

$(\tau\alpha)_d$ –Diffuse radiation transmittance absorptivity

$(\tau\alpha)_g$ –Ground reflectivity transmittance absorptivity

An empirical relation that accounts for the changes in the spectral distribution resulting from changes the air mass of 1.5 at sea level is given by the following empirical relation developed by king et al.,1998, (Kalogirou, 2013).

$$M = a_o + a_1 m + a_2 m^2 + a_3 m^3 + a_4 m^4 \quad (3.19a)$$

$$m = \frac{1}{\cos\varphi + 0.505(96.08-\varphi) - 1.634} \quad (3.19a_1)$$

Where φ –Latitude

m- Air mass

For polycrystalline PV cell, the values of constants of the photovoltaic module are given as

a_o = 0.918093, $a_1 = 0.086257, a_2 = -0.024459, a_3 = 0.002816, a_4$= -0.000126

For a given incidence angle of θ_1, the refraction angle, θ_2 is given by:

$$\theta_2 = sin^{-1}\left(\frac{sin\theta_1}{n}\right) \quad (3.20)$$

Where: n –refraction index

The refraction index is 1.0 for air, 1.526 for glass, and 1.33 for water. For a given collector tilt angle, the following empirical relations, derived by Brandemuehl and Beckman(1980),can be used to find the effective incidence angle for diffuse radiation from sky and ground reflected radiation (Kalogirou,2014).

$$\theta_{e,d} = 59.68 - 0.1388\beta + 0.001497\beta^2 \quad (3.21)$$

$$\theta_{e,g} = 90.0 - 0.5788\beta + 0.002693\beta^2 \quad (3.22)$$

Where: β -the tilt angle

$\theta_{e,d}$ -Effective incidence angle for diffuse radiation from the sky

$\theta_{e,g}$ – Effective incidence angle for ground reflected radiation

For the beam radiation, transmittance absorptivity, the refraction and is given by the following equation (Kalogirou, 2013).

$$sin(\theta_r) = \frac{sin\theta}{n} \quad (3.23)$$

$$(\tau\alpha)_b = e^{-\left[KL/cos\theta_r\right]}\left(1 - \frac{1}{2}\left[\frac{sin^2(\theta_r - \theta)}{sin^2(\theta_r + \theta)} + \frac{tan^2(\theta_r - \theta)}{tan^2(\theta_r + \theta)}\right]\right) \quad (3.24)$$

For the diffuse radiation refraction and transmittance absorptivity calculated as follows:

$$\sin(\theta_{r)} = {\sin(\theta_{e,d})}/{n} \quad (3.25)$$

$$(\tau\alpha)_d = e^{-\left[KL/cos\theta_r\right]}\left(1 - \frac{1}{2}\left[\frac{sin^2(\theta_r - \theta_{e,d})}{sin^2(\theta_r + \theta_{e,d})} + \frac{tan^2(\theta_r - \theta_{e,d})}{tan^2(\theta_r + \theta_{e,d})}\right]\right) \quad (3.26)$$

For ground reflected radiation, the transmittance absorptivity and refraction were calculated as follows:

$$(\tau\alpha)_g = e^{-\left[KL/cos\theta_r\right]}\left(1 - \frac{1}{2}\left[\frac{sin^2(\theta_r - \theta_{e,g})}{sin^2(\theta_r + \theta_{e,g})} + \frac{tan^2(\theta_r - \theta_{e,g})}{tan^2(\theta_r + \theta_{e,g})}\right]\right) \quad (3.27)$$

$$\sin(\theta_{r)} = {\sin(\theta_{e,g})}/{n} \quad (3.28)$$

Where: τ-transmittance of the cover

α-absorptance of the cell

For most photovoltaic modules a typical value for *K* is 4 m−1, the value for ‘‘water white’’ glass, a typical value for the glazing thickness is 2 mm, and the refractive index is set to 1.526, the value for glass.

The monthly average hourly-absorbed solar radiation for south facing tilted PV from sunrise to sunset hour calculated using the above relation for the representative days of each month of Adama are shown in Figure 3.13. As the sample data for finding the experimental electrical and thermal performance of PV module, this data for May 15th for south facing module is shown in Figure 3.14.The monthly average hourly-absorbed solar radiation for East and west facing tilted PV from sunrise to sunset hour calculated using the above relation for the representative days of each month of Adama are shown in Figure 3.15 and Figure 3.16, respectively.

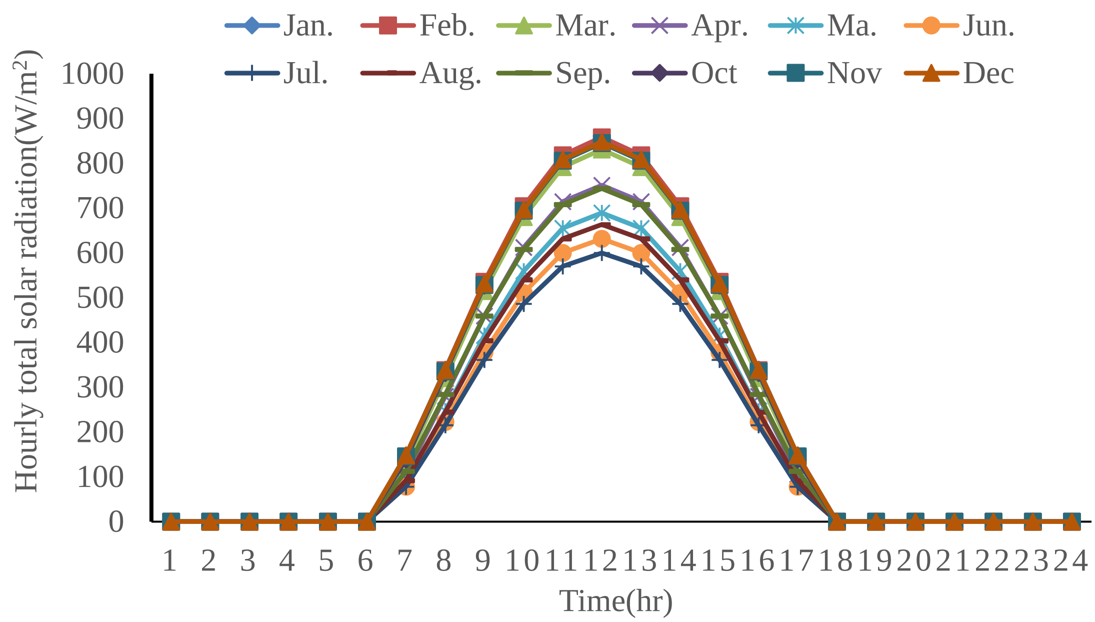

Figure: 3. 13 Graph of the monthly average hourly- absorbed solar radiation by PV panel on the tilted surface for South facing

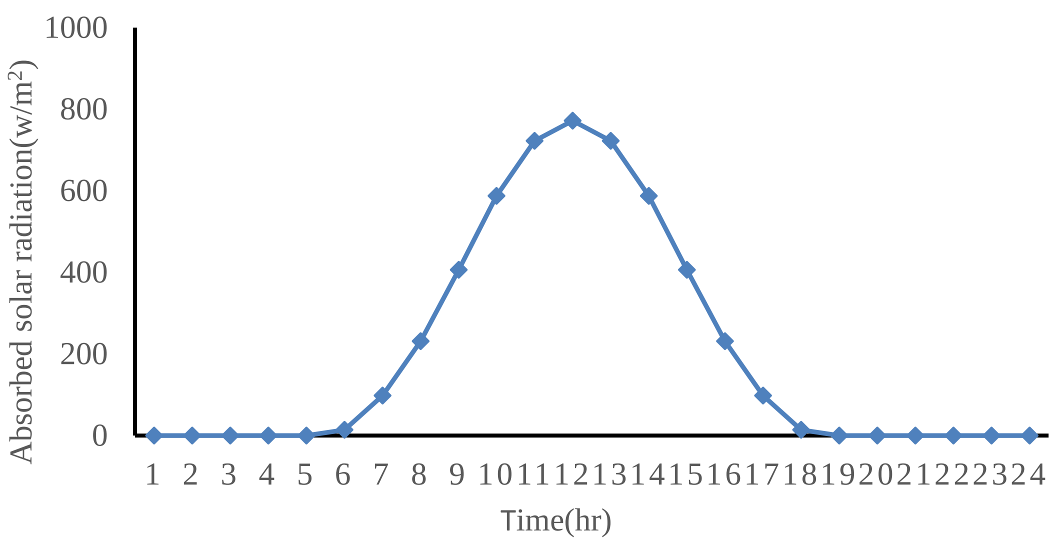

Figure: 3. 14 Graph of the monthly hourly-absorbed solar radiation by photovoltaic (PV) panel on tilted surface 23.5^0 for May 15th.

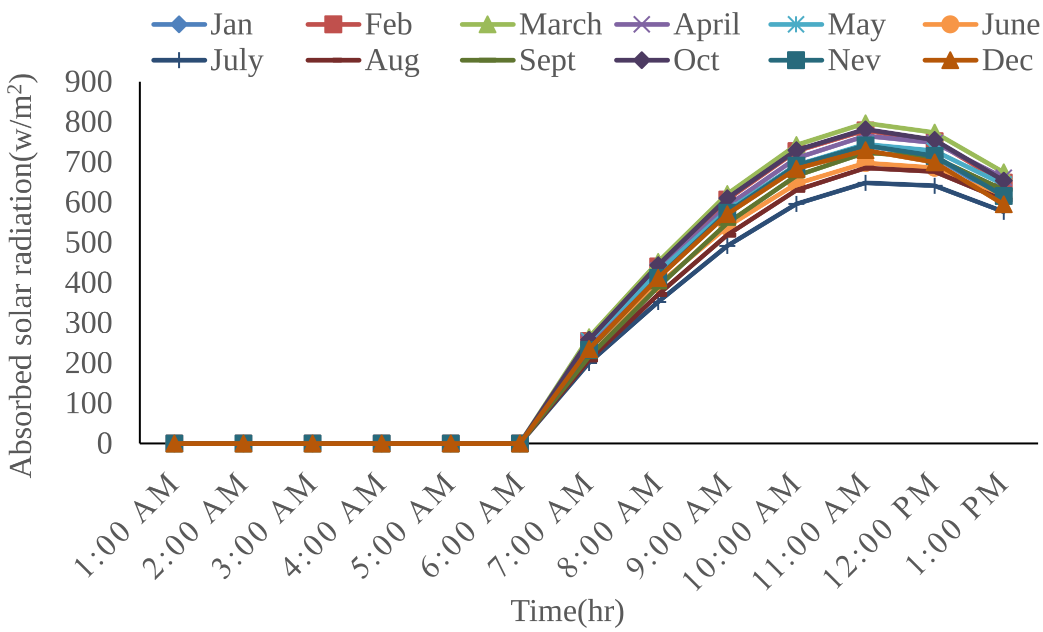

Figure: 3. 15 Graph of the monthly average hourly-absorbed solar radiation by PV panel on tilted surface for East facing.

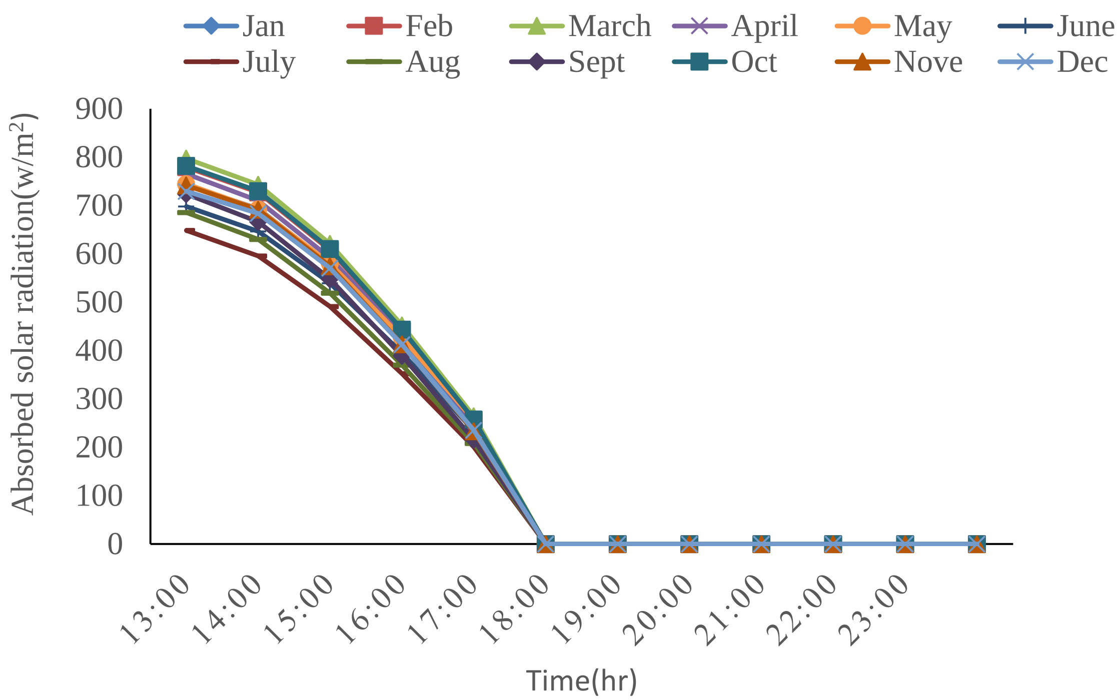

Figure: 3. 16 Graph of the monthly average hourly-absorbed solar radiation by PV panel on tilted surface for West facing.

3.9 Adama Metrological Temperature and Wind Speed Data

Adama is characterized by a climatic condition of the tropical region and it has a maximum of solar radiation intensity. In this research paper, ten years average climatic conditions of Adama are taken to evaluate the average monthly temperature and wind speed in addition to the sunshine duration. The monthly average ambient temperature of Adama ranges between18.9^{o} C (January) and 24.1^{o}C (June). The monthly average maximum and minimum wind speed are 4.42 and 2.62 m/s on December and September, respectively. The monthly average temperature and wind speed data are collected from Adama meteorology in order to estimate the heat loss analysis of photovoltaic module and these average values are shown in Table 3.2 and Figure 3.17 for each month.

Table 3. 2 Monthly average annual climatic condition (temperature and wind speed) of Adama (Source: East Shoa Zone Meteorology Agency)

Year		Months in years											
2011 2020		Jan	Feb	Mar.	Apr.	Ma.	Jun.	Jul.	Aug	Sept	Oct	Nov	Dec
Temperature (°C)	Ave Max	27.6	29.6	30.95	30.9	27.3	30.3	27.34	26.8	27.8	28.3	27.6	26.4
	Daily Mean	18.9	22.5	23.9	23.9	22.2	24.1	21.9	21.7	21.8	21.7	21.2	19.9
	Ave min	10.4	15.4	16.9	17.1	17.2	17.8	16.4	16.6	15.9	15.01	14.8	13.4
Wind(m/s) Speed		4.26	4.24	4.25	3.18	3.29	3.80	3.90	3.48	2.62	3.98	4.23	4.42

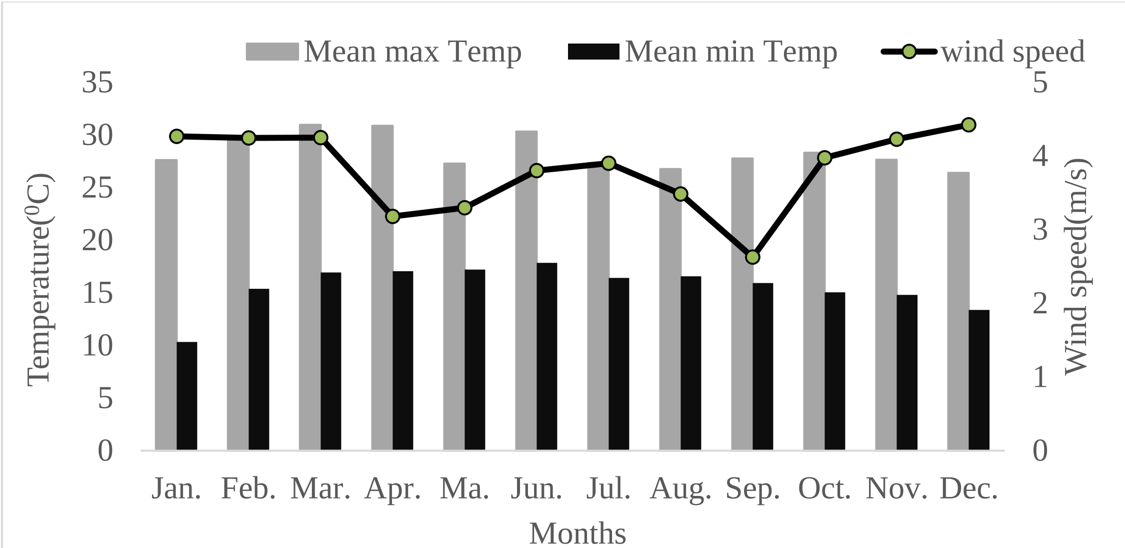

Figure: 3. 17 Graph of monthly average metrological data for wind speed and temperature of Adama of ten years.

3.9.1 Estimation of Hourly Ambient Temperature

A sinusoidal variation of the dry bulb temperature through the day and maximum temperature occurs at 15:00 hour sun time was assumed. $T_{(t)}$ represent the temperature variation at any time t as given by (Jones., 1994) (Nigussie, 2020).

$$T_{(t)} = \frac{T_{max}+T_{min}}{2} + \frac{T_{max}-T_{min}}{2}\left[sin\left(\frac{\pi(t-9)}{12}\right)\right] \quad (3.29)$$

Where : T_{max} -mean daily maximum temperature at 15:00hr sun time

T_{min} - Mean daily minimum temperature

t -Time of the day

Table 3. 3 Estimated average variations of ambient temperature of Adama

Months	Jan	Feb	Mar	Apr	May	Jun	Jul	Aug	Sep	Oct	Nov	Dec
T_a(2011-2020)	19.1	22.6	24.1	24.1	22.3	24.2	21.9	21.9	21.9	21.8	21.3	19.99

As shown in Table 3.3, the average monthly ambient temperature are variable across seasons. The maximum and the minimum estimated average ambient temperature are 24.2 and 19.1 ℃ for June and January respectively.

3.10 Summarize of Average Estimated Solar Radiation

As shown in Table 3.4, the maximum yearly average hourly, yearly mean hourly global tilted surface, beam and diffuse solar radiation are 0.998, 0.67 and 0.22 kWh/m^2/year, respectively. While the minimum yearly mean hourly global tilted surface, beam and diffuse radiation are 0.192, 0.107 and 0.056 kWh/m^2/year, respectively. In addition, the total maximum and minimum yearly average total absorbed solar radiation by photovoltaic on Adama are 0.763 and 0.117 kWh/m^2/year, respectively.

Table 3. 4 Comparison and summary of monthly mean daily, monthly mean hourly solar and the absorbed solar radiation by photovoltaic module.

Monthly average hourly solar radiation on tilt surface (kWh/m^2/year)	Total solar radiation on tilt(kWh/m^2/year)	Beam solar radiation (kWh/m^2/year)	Diffuse solar radiation(kWh/m^2/year)
	Maximum average solar radiation		
	0.998	0.67	0.22
	Minimum average solar radiation		
	0.192	0.107	0.056
Monthly average hourly solar absorbed radiation on tilt surface (kWh/m^2/year)	Maximum average solar radiation		
	0.763	0.67	0.22
	Minimum average solar radiation		
	0.117	0.107	0.056

CHAPTER FOUR

EXPERIMENTAL THERMAL AND ELECTRICAL PERFORMANCE EVALUATION METHOD OF THE SOLAR PHOTOVOLTAIC SYSTEM

4.1 Introduction

This chapter explains the experimental setup preparation, the data gathering techniques, and instrumentation and the electrical and thermal performance analyses methods used in the study. The experimental setups used were consisted of two photovoltaic modules, support frame, water tank, DC lamps (bulbs) and fan. These experimental setups were used to investigate the electrical and thermal performance of cooled and bare (uncooled) solar photovoltaic module to analyze the effect of the module surface temperature on the voltage and current characteristics during the generation of electric power over a period of a day. The preparation of the experimental setup, the different measuring instruments and experimental performances analysis methods used for the study are discussed.

4.2. The Experimental Setups

Generally the materials and instruments used in the preparation of the experimental setup were two identical a Photovoltaic (PV) module or a solar panel, a supporting structure for housing the photovoltaic module, fan blower, water tank or water can and pipe collections, connecting wires, tap water, and air as cooling fluid and measurement instruments such as thermocouple (K type), digital multimeter, and a potentiometer (rheostat). The preparation of the experimental setups and the instruments used are discussed below.

4.2.1 Photovoltaic (PV) Module

Two photovoltaic modules were purchased from the market. The two PV modules have the same size and the same electrical characteristics photovoltaic modules. The solar photovoltaic modules purchased are made of polycrystalline silicon-type cell. The solar photovoltaic modules have the following specifications. The standard test conditions (STC), of PV modules were a maximum 1000 W/m^2 solar intensity and 25 ℃ module temperatures. In addition to this, it has the following electric properties: Peak power (P_{max}) of 60 W, Fill factor (FF) of 0.68, Power tolerance of 0-3 %, Voltage (V_{mp}) of 18.0 V, Current (Imp) of 3.33 A, Open circuit voltage (Voc) of 21.5 V, Short circuit current (Isc) of 4.25 A and maximum system voltage of 1000 VDC. The solar photovoltaic module has overall size of 94.5 mm × 55 mm as shown in Figure 4.1

(a) (b)

(c)

Figure: 4. 1 Solar panel showing (a) packed panel, (c) backside of panel(c) front side of panel

4.2.2 Supporting (Frame) Structure

1. The supporting structure has been prepared as shown in Figure 4.2. Two supporting structures were made of the rectangular channel iron and angle iron welded for placing the photovoltaic (PV) module. The constructed frame structure is 94.5 mm × 55 mm areas and it can be adjusted manually to East, West, and South axes of the earth while facing the sun depend on the experiment done. The frame structure tilted was 23.5°.

Figure: 4. 2 Supporting structure

4.2.3 Fan

Fan is a machine whose primary function is to provide and accommodate a large flow of air or gas. This is achieved by rotating a number of blades, connected to a hub and shaft, and driven by a motor. The fan is shown in Figure 4.3. The fan used in this thesis has the following specifications: Power of 70 W, frequency of 50 Hz, voltage of 220 V. It is used as the active technique type cooling system in this thesis work.

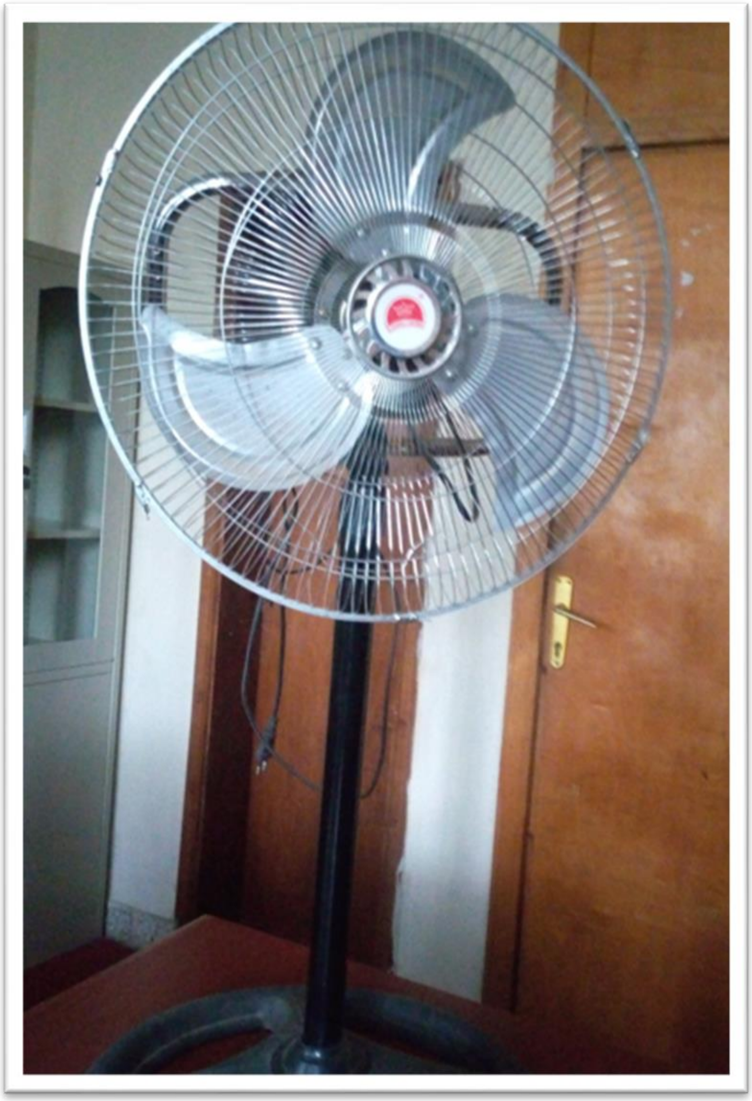

Figure: 4. 3 Fan

4.3. Experimental Setup Installation and Test Procedure

The two parallel setups contains a photovoltaic module, water tank (can), stainless steel as intermediate tank and garden hose were assembled as shown in Figure 4.4 and 4.5. The fittings of garden hose (Figure 4.5) is used to transmit cooling water from source to the water tank. The polyvinyl chloride (PVC) pipe are mounted at the end of water-cooled module to collect outlet water as shown in Figure 4.4 for used as cooled PV module.

4.3.1 Installation and Test Procedures of the Experimental Setup

The procedures used for getting ready the experimental set for experimentation were

- Fabrication of two supporting structures from locally available materials
- Fitted fan blower from the backside of a photovoltaic module
- Fabrication of a stainless steel water distributor manifold; this manifold is needed to distribute cooling water uniformly over the top surface of the PV module
- Preparation of manually controlled water storage tank above the PV module so that water can flow over the top surfaces after flowing through the distributor manifold
- PVC water collecting channel at the bottom of the PV module

4.3.2 Test Procedures

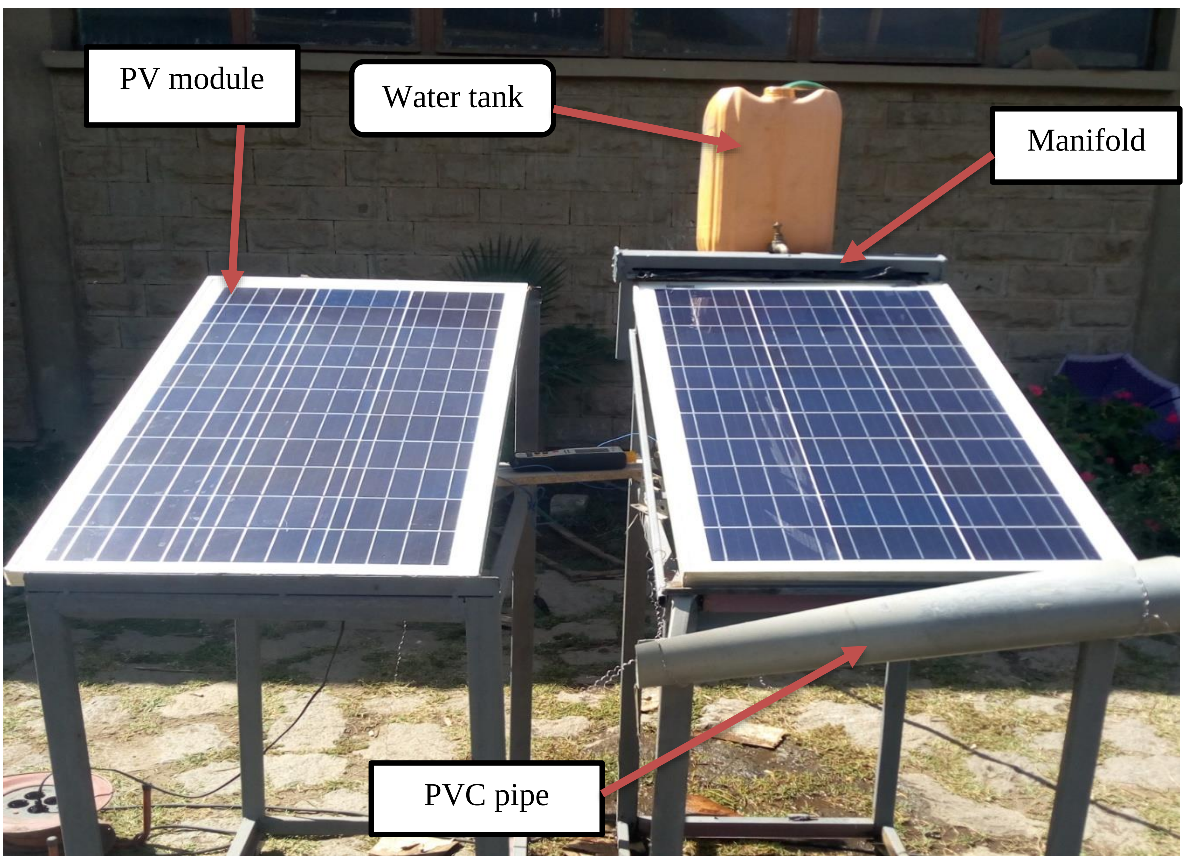

(a) (b)

Figure: 4. 4 Installation of the photovoltaic module set up (a) without cooling and (b) with film water- cooling system.

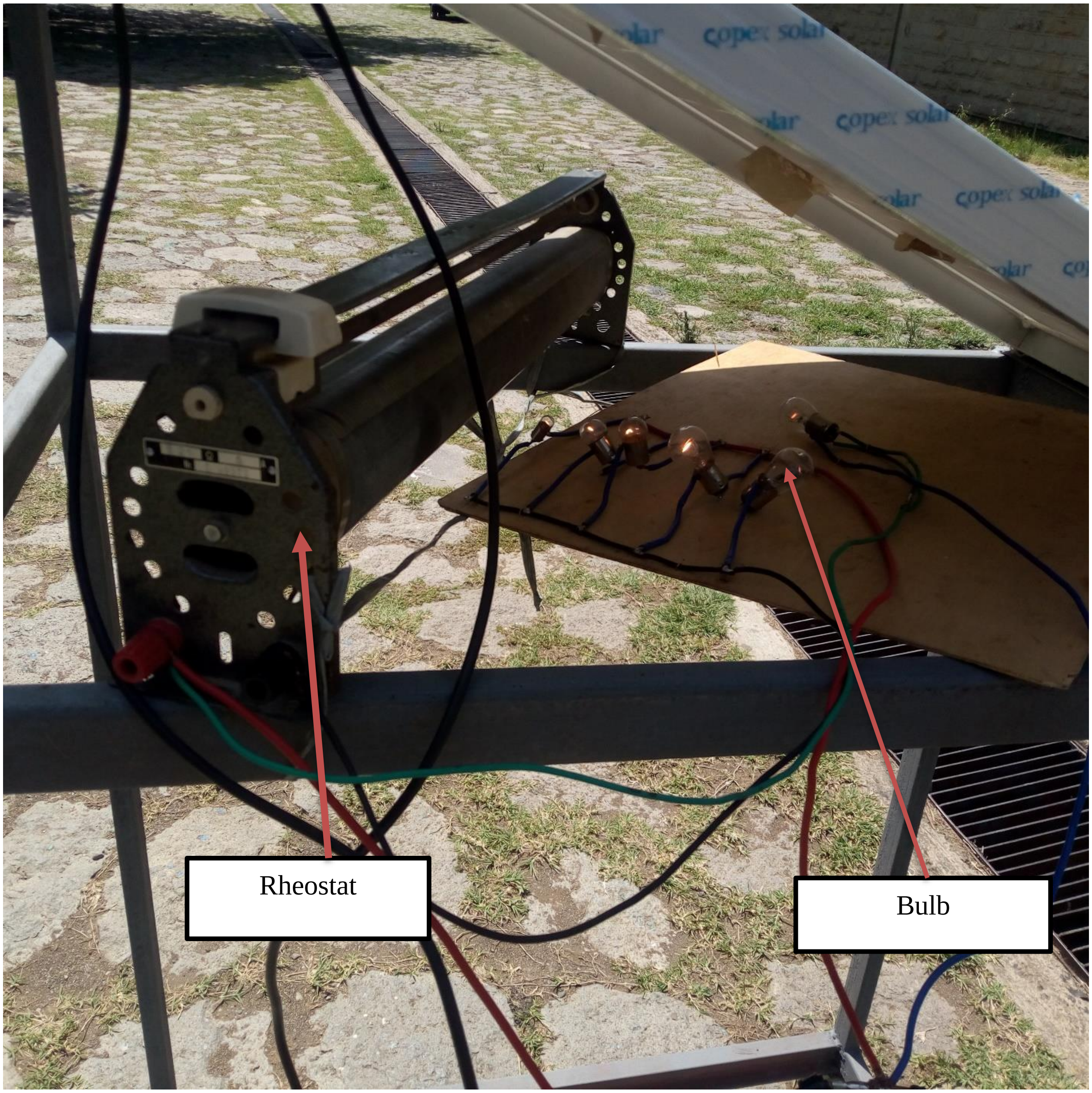

Figure: 4. 5 Installation of the DC bulb and potentiometer on photovoltaic modules.

Figure: 4. 6 Voltage and temperature measurement of photovoltaic modules cooled by water

Figure: 4. 7 Voltage and temperature measurement of PV modules cooled by air.

- ❖ Connect the port of the thermocouple on the backside of the photovoltaic module by Kapton tape to the photovoltaic module without and with cooling system at two positions for both photovoltaic modules to measure the temperature of the module
- ❖ Connect the photovoltaic module the negative terminal to the potentiometer (Rheostat) and negative terminal by adjusting rheostat at zero
- ❖ Connecting the negative terminal circuit from rheostat to negative terminal and positive terminal of the PV module.
- ❖ Connect six bulbs of each 3,5, 6, 10,12, and 24 power rating as the load between the rheostat and the PV module electric output
- ❖ The experimental set up was exposed to the sun in East or West or South earth axes from 9AM up to 3PM in a day

- ❖ Then after adjusting the digital multimeter on the ampere, the short circuit current has been measured every ten minutes
- ❖ The voltage has been measured after the digital multimeter was adjusted on voltage, by connecting the negative terminal from the module to the negative terminal of the multimeter and positive to positive has been measured by every ten minutes.
- ❖ Surface temperature of the solar PV module at two different points along the length were also recorded every ten minutes
- ❖ For all experimental tests, the same procedure is repeated

4.4. Instruments and Measurements

The instruments used during the experimentation and the measurements done for finding the thermal and electrical performances of the PV module are indicated in Table 4.1.

Table 4. 1 Measuring instruments and variables to be measured

Instrument	Measured variable
Multimeter	Current
Multimeter	Voltage
K- type thermocouple	Module Temperature
Digital thermometer	Ambient temperature
Potentiometer	Control of load

a. <u>Temperature measuring instruments</u>

Thermometer**-** A K-type Thermometer (thermocouple) (Figure 4.8) is used to measure the surface temperature of the PV module at different position. The specifications of the k-type thermocouple are listed below.

- ❖ K type thermocouple: Model : HT-9815
- ❖ Standard error of k type thermocouple: ±1℃
- ❖ Measurement Temperature range: - 200°C~1372°C (-328°F ~ 2501°F)
- ❖ Accuracy: ±1℃ for < -100°C

- ❖ Temperature resolution : 0.1°C for < 1000°C; 1°C > 1000°C
- ❖ Battery (Power supply): 9V
- ❖ Weight: Approx. 404g

Figure: 4. 8 Thermometer (Thermocouple)

b. <u>Electrical characteristics measuring instruments</u>

I. <u>Multimeter</u>

Multimeter- is a measuring instrument that can measure multiple electrical characteristics.

A typical multimeter used in this thesis work can measure voltage, resistance, and current. The digital multimeter used to measure, current and voltage is shown in Figure 4.9. The specifications of the digital multimeter are lists below.

- ❖ Digital multimeter model: VC890D
- ❖ DC Voltage range: 200mV/2V/20V/1000V (accuracy: ±(0.5%+3))
- ❖ DC Current range :2mA /200mA/20A (accuracy: ±(0.8%+10)
- ❖ Weight :270g
- ❖ Battery:9V

Figure: 4. 9 Digital Multimeter

II. **Potentiometer:**

The potentiometer is derived from the development of a rheostat. A rheostat was used for loading the PV module in order to get the current and voltage characteristics at a particular temperature value. A rheostat is shown in Figure 4.10.

Figure: 4. 10 Potentiometer

4.5 Evaluation Method of the Electrical Performance of the Solar Photovoltaic Module

The electrical performance of the solar photovoltaic module was evaluated after gathering data on the electrical characteristics of PV module exposed to the sun without cooling its surface and with cooling its surface. The electric short circuit current and open circuit voltage outputs of the photovoltaic module were the primary data gathering to evaluate the electric performance of the PV module operated with cooling and without cooling system integrated to it.

The current-voltage characteristic of the photovoltaic module in experimental test was measured in order to evaluate the power output and electrical efficiency generated. The electrical efficiency of the Photovoltaic module can be calculated by using the equation of Preet, (2018). The electrical efficiency η_e is depending on power output and solar radiation intensity and it can be calculated (Bhakre et al., 2021).

$$\eta_e = \frac{P_{out}}{P_{in}} \quad (4.1)$$

Where: P_{out} – PV Module power output (W)

P_{in} – Input power (W)

The power output and power input of the photovoltaic module are calculated as follows, respectively:

$$P_{out} = I_{SC} \times V_{OC} \times FF \quad (4.1a)$$

Where: I_{sc}-Short circuit current (A)

V_{OC}- Open circuit voltage (V)

FF- Fill factor

$$P_{in} = I_T A_a \quad (4.1b)$$

Where: $\mathbf{A_a}$– Is the actual area of the PV module $\mathbf{m^2}$

I_T – Is the total solar radiation intensity ($^{W}/_{m^2}$)

4.6. Evaluation Methods of the Thermal Performance of the Solar Photovoltaic Module

Using a similar setup arrangement, the thermal performance of the solar photovoltaic module was evaluated after gathering data on the module surface temperature along its length, in addition to collecting electrical characteristics of PV module exposed to the sun. Then energy balance principle was applied to the PV module to determine the thermal efficiency. The thermal performance of the photovoltaic module are depend on the thermal dissipation, the absorption properties of the materials, solar radiation intensity, ambient temperature, wind speed, and the accurate fixing (installation) of the PV module. Hence, it is essential to perform a quantitative analysis of the temperature impact on photovoltaic modules characteristics.

4.6.1 Evaluation of the Thermal Performance of the Solar Photovoltaic Module with Cooling

Heat loss analysis

The purpose of this part is to; analyze thermal performance of the photovoltaic module with water-cooling. The thermal efficiency of water-cooled solar photovoltaic depend on maximum useful heat energy generated and the solar radiation intensity. The thermal efficiency is calculated by equations below (Shahad et al., 2019). In addition to thermal efficiency, the heat losses on the photovoltaic module were analyzed.

In order to analyze the thermal efficiency of the photovoltaic module water-cooling system, the following assumptions were applied:

- The inlet water temperature is equal with ambient temperature.
- The outlet water temperature is equal with module surface temperature.
- Heat loss due to conduction is ignored
- The water mass is distributed uniformly over the PV module and water temperature was the same as the module temperature.
- Compared to water heat transfer (evaporative) radiation and convective heat transfer loss are negligible.

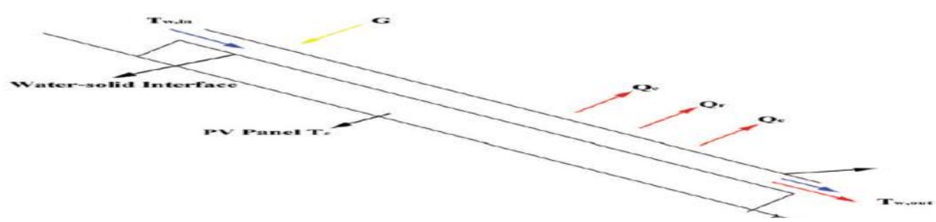

Figure: 4. 11 Heat transfer of the PV film water-cooled (Wu and Xiong, 2014).

The general energy balance of the photovoltaic module is:

$$\frac{dQ}{dt} = GA - Q_r - Q_e - Q_u \tag{4.2}$$

The steady energy balance equation are given from the above equation as:

$$GA - Q_r - Q_e - Q_u = 0 \tag{4.3}$$

Therefore, the useful heat gain can be find from:

$$Q_u = GA - Q_r - Q_e \tag{4.4}$$

Where Q_u –useful heat removal from PV (**W**)

G- Solar radiation (W/m^2)

Q_r- Radiation loss(**W**)

Q_e- Convection loss (W)

The thermal efficiency of water-cooled PV solar system is the ratio of the maximum useful heat energy generated by the module to solar irradiance. The thermal efficiency for the usage and circulation water of the module could be calculated as(Ceylan et al., 2014):

$$Q_u = m_w C_P (T_{fo} - T_{fi}) \tag{4.5}$$

m_w–Mass flowrate $\left({}^{kg}/_{s}\right)$

$\mathbf{C_P}$ -specific heat of water

T_{fo}- Outlet water temperature (°C)

T_{fi}-Inlet water temperature (°C)

$$\eta_{th} = \frac{Q_u}{I_T A_e} \qquad (4.6)$$

4.6.2 Evaluation of the Thermal Performance of the Solar Photovoltaic Module without Cooling

Heat loss analysis: The thermal performance of photovoltaic module also considered the overall heat transfer coefficient. The energy balance equations are based on one-dimensional and steady state assumptions. The total radiative heat loss from the photovoltaic module without cooling is given by(Sedaghat et al., 2020):

$$Q_r = \varepsilon_m \sigma\left({T_m}^4 - {T_s}^4\right) \qquad (4.7)$$

Where ground and sky temperature are given by the following equations

$$T_s = T_a - 6 \qquad (4.7a)$$

Where: $\boldsymbol{\varepsilon_g}$ emissivity of the glass (0.95)

$\boldsymbol{\sigma}$- Stefan Boltzmann constant $\mathbf{5.6697 \times 10^{-8}}(\boldsymbol{W/m^2K^4})$

T_m –module temperature (K)

T_s – Sky temperature (K)

$\mathbf{T_a}$-Ambient temperature (**K**)

The useful energy can also be calculated from energy balance by the following expression (Alobaid et al., 2018).

$$\mathbf{Q_u = Q_{ab} - Q_{loss}} \qquad (4.8)$$

Where: Q_{ab} –Absorbed heat

$\mathbf{Q_{loss}}$ –the total heat loss

$$Q_{ab} = SA_c \qquad (4.8a)$$

Where: **S** – The total absorbed solar radiation by PV module

A_c-Area of the photovoltaic module

$$\mathbf{Q_{loss} = U_L\left(T_{pm} - T_a\right)} \qquad (4.8b)$$

U_L- Overall heat loss coefficient

The convective heat transfer coefficient between glass cover and water for laminar flow can be estimated from:

$$N_u = \frac{h_w L}{k_w} = 0.664 {R_e}^{0.5} {P_r}^{0.333} \quad (4.9)$$

$\mathbf{N_u}$-Nusselt number

The convective heat transfer coefficient between glass cover and water for turbulent flow can be estimated from:

$$N_u = \frac{h_w L}{k_w} = 0.037 {R_e}^{0.8} {P_r}^{0.33} \quad (4.10)$$

The radiative heat transfer coefficient between glass cover and sky can be estimated from:

$$\mathbf{h_{r_{c-a}} = \varepsilon_g \sigma (T_c + T_s)({T^2}_c + {T^2}_s)} \quad (4.11)$$

Where $h_{r_{c-a}}$- Radiative heat transfer coefficient

The convective heat transfer takes place by two methods, which is natural and forced convection. Therefore, the total heat loss by convection at each surface of the panels is expressed(Sedaghat et al., 2020):

$$Q_c = h_c A(T_m - T_a) \quad (4.12)$$

The Nusselt number in free convective cooling mainly depends on the angle of inclination, Rayleigh number and the critical Grashof number. Among different available correlations, the following expressions for tilted (Kaplani and Kaplanis, 2014).

$$N_u = \left(0.825 + \frac{0.387 {R_a}^{\frac{1}{6}}}{\left(1+\left(\frac{0.49}{pr}\right)^{\frac{9}{16}}\right)^{\frac{8}{27}}}\right)^2 \quad 0 < \beta < 60° \quad (4.13)$$

$$\mathbf{G_r = \frac{gB(T_m - T_a)l^3}{v^2}} \quad (4.14)$$

Where: G_r – Grashof number

B- Volumetric thermal expansion coefficient

$$B = \frac{1}{T_{av}} \quad (4.14a)$$

The Rayleigh number is determined from the following equation below.

$$R_a = G_r P_r \quad (4.15)$$

$$P_r = \frac{v}{a} \tag{4.15a}$$

Where: **v**-Kinematic viscosity ($\mathbf{m^2/s}$)

a-Thermal diffusivity (m^2/s)

l -Length of the panel (m)

Finally, the natural convection coefficient can be obtained from the Nusselt number.

$$h_n = \frac{N_u l}{k} \tag{4.16}$$

Where: $\mathbf{N_u}$ -is Nusselt number

k_a - The thermal conductivity of the air ($W/m.K$)

The forced heat transfer convection coefficient at the top of the solar panel from as reported by (Watmuff et al.,1977) (Duffie and Beckman, 2013).

$$\mathbf{h_f = 2.8 + 3v} \tag{4.17}$$

Where: v -Wind speed (m/s)

The useful energy is calculated by the following expression (Alobaid et al., 2018).

$$\mathbf{Q_u = Q_{ab} - Q_{loss}} \tag{4.18}$$

Where: Q_{ab} –Absorbed heat

$\mathbf{Q_{loss}}$ –the total heat loss

$$Q_{ab} = S_{ab} A_c \tag{4.19}$$

Where: $\mathbf{S_{ab}}$ -The total absorbed solar radiation by PV

A_c-Area of the photovoltaic module

$$\mathbf{Q_{loss} = U_L(T_{pm} - T_a)} \tag{4.20}$$

$$\boldsymbol{U_L = \left(\frac{1}{h_{r_{g-a}}} + \frac{1}{h_w} + \frac{1}{h_c}\right)^{-1}} \tag{4.20a}$$

These efficiencies usually include the ratio of the useful thermal gain and electrical gain of the system to the incident solar irradiation on the collector gap within a specific time or period (Arefin, 2019).The overall efficiency of the photovoltaic module given as follows:

$$\eta_{th} = \frac{Q_u}{I_T A_e} \tag{4.21}$$

CHAPTER FIVE

RESULTS AND DISCUSSIONS

5.1 Introduction

Photovoltaic module performance analysis is depending on several climatic factors. These are incident solar radiation intensity, absorbed solar radiation, module surface temperature, wind speed and ambient temperature. In this part, the results of measurements accomplished from May 15 up to 25 May 2021 on two PV modules (one cooled and the other bare) have been presented and analyzed. In the experiments two cooling fluids medium were used: water and air. Electrical and thermal performances of the PV modules were tested with water or air cooling system from 9:00 AM to 3:00 PM under lower level of radiation intensity to higher radiation intensity. The experimental were carried out by facing bare and water or air-cooled PV modules in parallel arrangements (in the same day) towards West, East, and South axes of the earth. Cooling of the PV modules was done by blowing air from backside; by continuous flowing water film on top surface and by flowing water intermittently on top surface. This chapter discusses the experimental thermal and electrical performances results of the modules for four cases of experimentation: film water flow cooling versus bare module, fan-cooling module versus bare module, intermittent water-cooling versus bare module, and film water-cooling versus fan cooling. All these experiments were done by inclining the PV modules at about 23.5^o. The results of the estimated solar radiation intensity and absorbed solar radiation needed to evaluate the energy conversion performances of the module for east; west and south facing PV modules are also presented and discussed.

5.2. Hourly Total Incident Solar Radiation on Inclined Surface

The monthly average hourly incident solar radiation on the tilted surface in Adama for all months is calculated. The recommended tilt angle for Adama that is 23.5^o was used for all axes. The surface azimuth angle used were zero , negative ninety and positive ninety degree, for PV module facing the sun in the South, West and East axes of earth, respectively. This estimation depends on the number of brightness days. Figure 5.1, Figure 5.2 and Figure 5.3 shows the estimated hourly incident solar radiation for the South, East and West facing tilted surfaces in Adama for the days (May 15 to May 25, 2021) of experimentation, respectively.

The monthly total hourly average incident solar radiation on the inclined surface of Adama for all months of the year was estimated using Eq.3.17. These estimated total solar radiations for the South, East, and West were used to estimate the electrical efficiency of the PV modules.

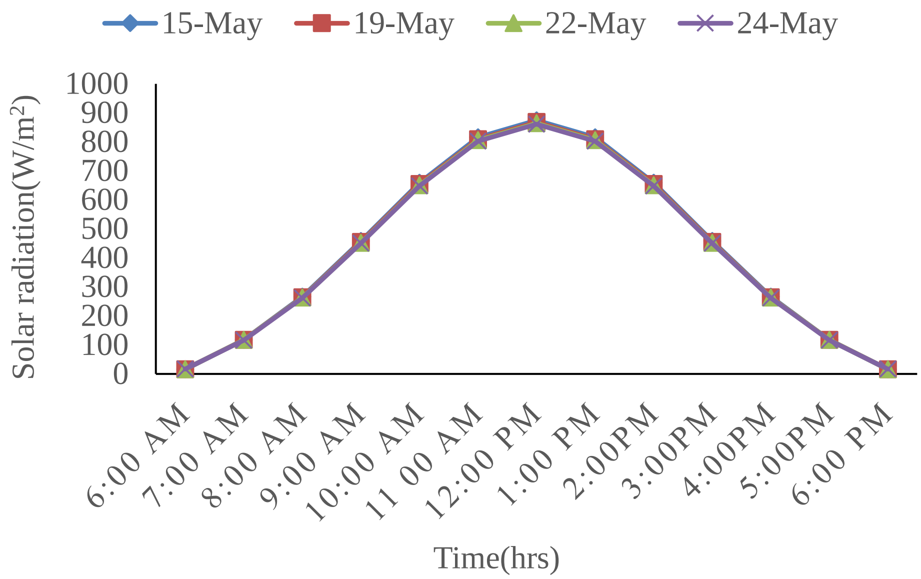

Figure: 5. 1 Estimated hourly incident solar radiations on the inclined surface for days of experiments in May -South facing

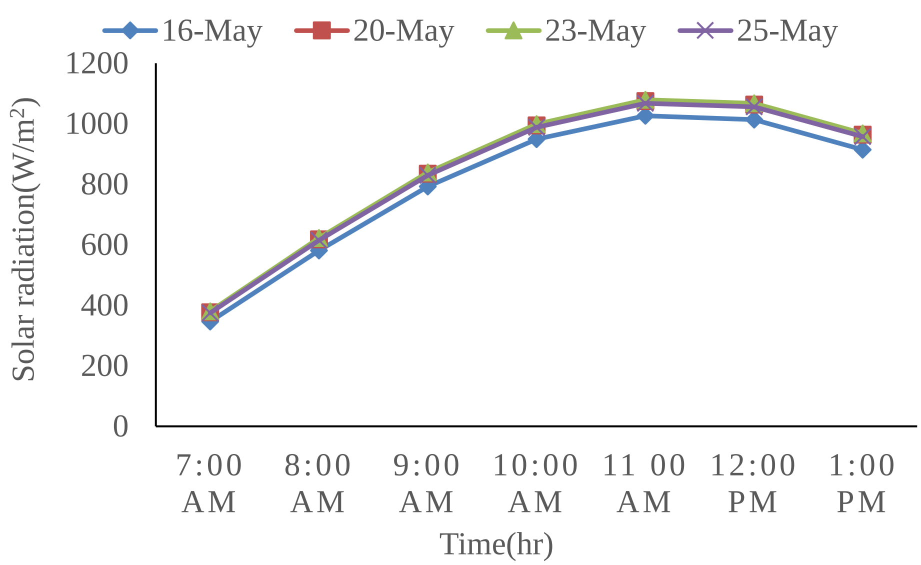

Figure: 5. 2 Estimated hourly incident solar radiations on the inclined surface for days of experiments in May - East facing

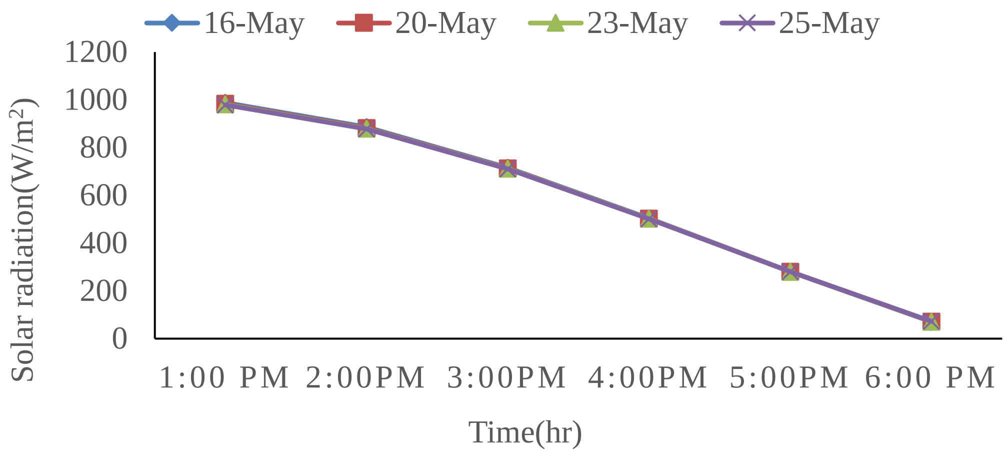

Figure: 5. 3 Estimated hourly incident solar radiations on the inclined surface for days of experiments in May -West facing

5.3. Hourly Total Absorbed Incident Solar Radiation on Inclined Surface

Figure 5.4, Figure 5.5 and Figure 5.6 shows the estimated hourly-absorbed solar radiation for the South, East and West facing of tilted PV modules in Adama weather condition. The monthly hourly average absorbed incident solar radiation of Adama for all months of the year was estimated using Eq.3.19.These estimated total absorbed solar radiations for the South, East, and West were used to estimate the thermal efficiency of the PV modules.

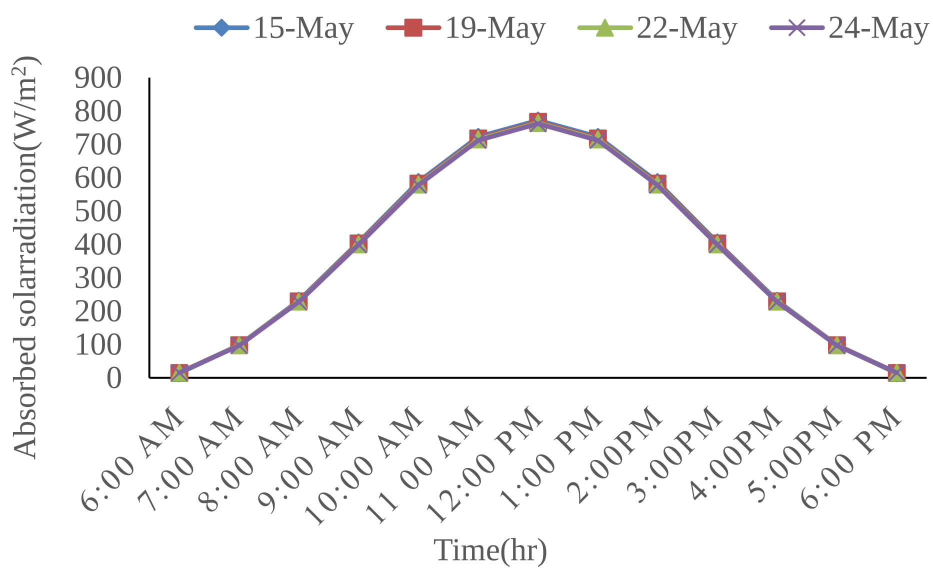

Figure: 5. 4 Estimated hourly-absorbed solar radiation by inclined PV modules for days of experiments in May- South facing

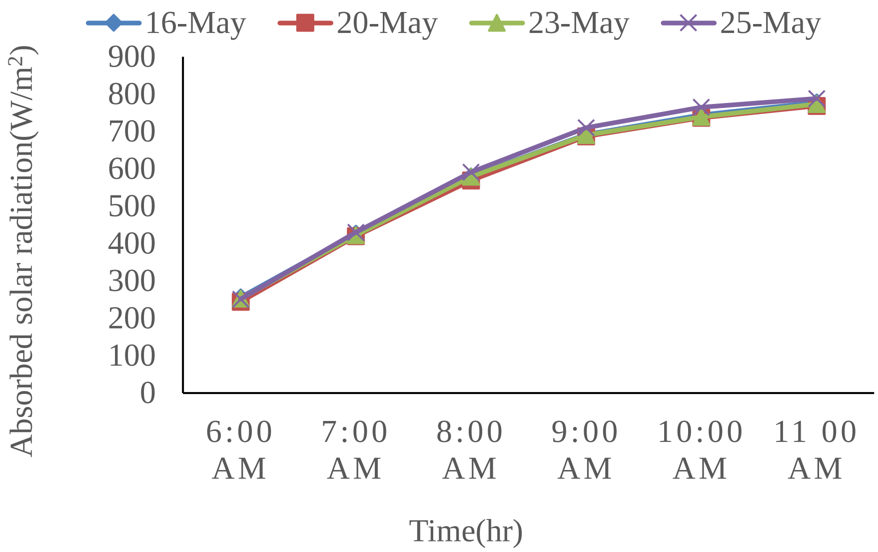

Figure: 5. 5 Estimated hourly-absorbed solar radiation by inclined PV modules for days of experiments in May- East facing

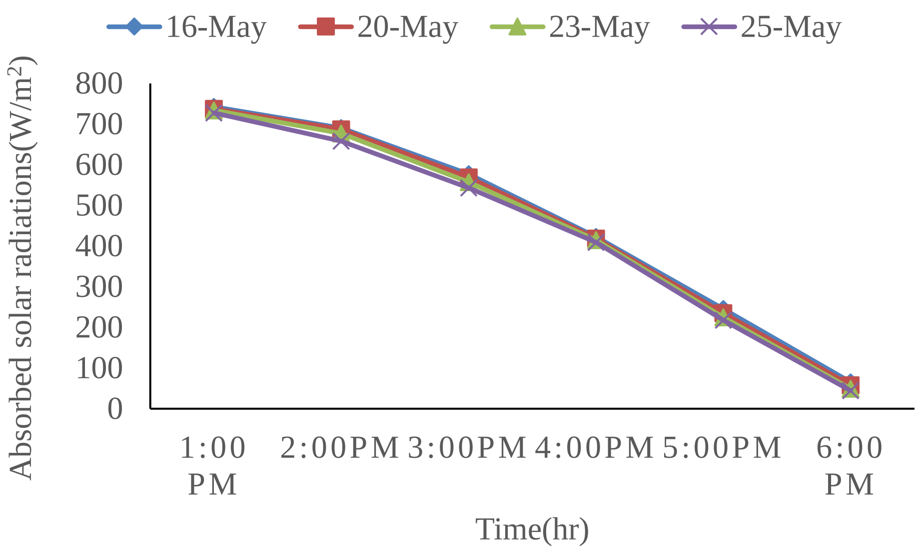

Figure: 5. 6 Estimated hourly-absorbed solar radiation by inclined PV modules for days of experiments in May- West facing

5.4 Thermal and Electrical Performance of South Faced Photovoltaic Module

Two PV modules were exposed to solar radiation facing the sun in the south axis to investigate the effect of cooling on the electricity generated. When cooled continuously on the top surface by water; continuously cooled on the back surface by air; intermittently cooled by water on the top surface, and lastly, comparative performance of the PV modules when one was cooled by air and the other by water continuously. The thermal performances of these arrangements were determined in terms of measured surface temperature and thermal efficiency of the cooled and uncooled module. The electrical performances of these arrangements were determined in terms of current, voltage, power generated and electrical efficiency. For estimating the electrical and thermal efficiency of the modules, the estimated hourly solar radiation and absorbed solar radiation by the PV modules were use

5.4.1 Performance of South Faced Bare Photovoltaic Module

To have a better understanding of the performance of PV modules without cooling (bare) compared to cooled PV module, the experimental collected thermal and electrical characteristics data and the calculated thermal and electrical efficiencies of bare PV module in generating electricity are discussed separately in this section.

5.4.1.1 Thermal Performance of South Faced Bare Photovoltaic Module

Experimentation on the south-faced bare PV module was conducted for three consecutive days. Figure 5.7 shows that the photovoltaic module average surface temperature was recorded every 10 minutes throughout the experimental day on May 15/2021.The maximum and minimum value of the bare PV module hourly average surface temperature was 50.5 and 40.3°C, respectively. The surface temperature of the PV module was high at peak solar radiation intensity (11AM-12PM).

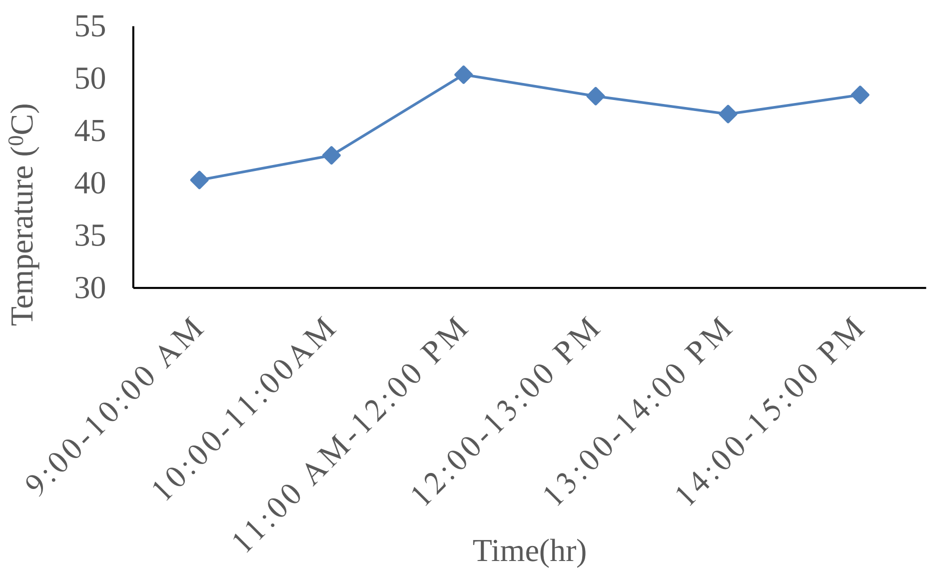

Figure: 5. 7 Hourly average surface temperature of Bare PV module versus time

Figure 5.8 shows the bare PV module thermal efficiency throughout the experiment day on May 15. The thermal efficiency of the photovoltaic module was fluctuating due to variation in temperature and solar radiation (Eq. 4.21). The bare PV module's maximum and minimum value of thermal efficiency were of 80 and 73%, respectively.

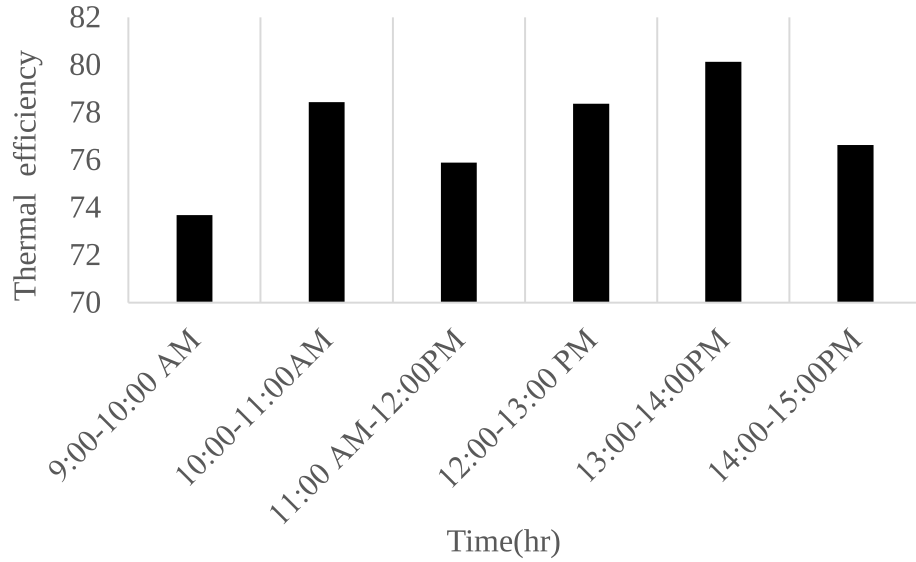

Figure: 5. 8 Bare PV module thermal efficiency versus time

5.4.1.2 Electrical Performance of South Faced Bare Photovoltaic Module

Figure 5.9 shows the short circuit current output produced by the photovoltaic module throughout the experiment on May 15. The current output for operation observed begins to be an increased value from 9:00 AM to 12:00 PM, which is at the peak solar radiation intensity. The current output is high, around noon, which has a value of 3.04 A.

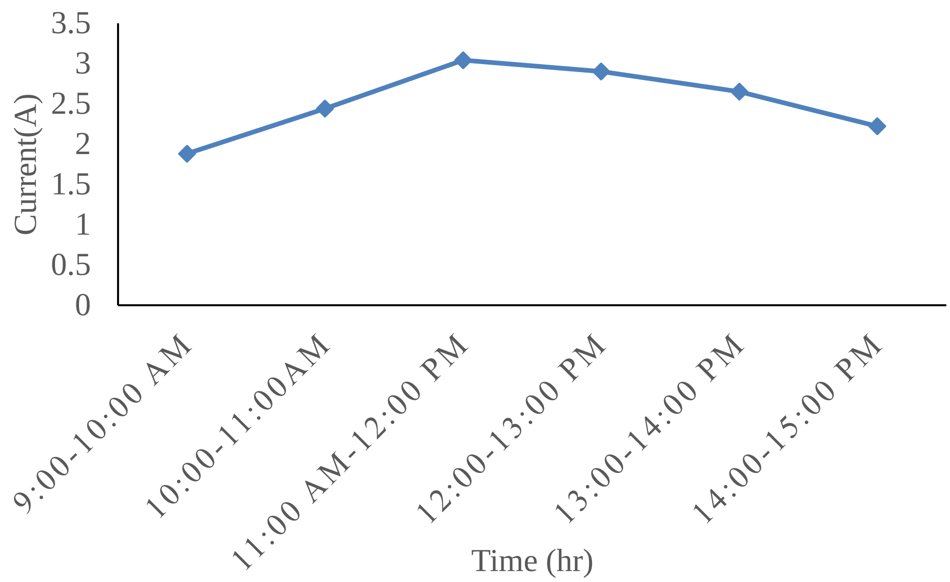

Figure: 5. 9 Current of bare photovoltaic module versus time

The open circuit voltage of the PV module versus time graph on May 15,2021is shown in Fig 5.10.This Figure shows the variation in voltage. Due to rise in module temperature as shown in Figure 5.7 the module, voltage was decrease. During the time 11:00 to 12:00 PM due temperature reaching peak point the voltage output was minimum. The voltage is low, around noon, due to rise in temperature. The maximum and minimum value of the bare PV module voltage was of 18.54 and 18 V, respectively.

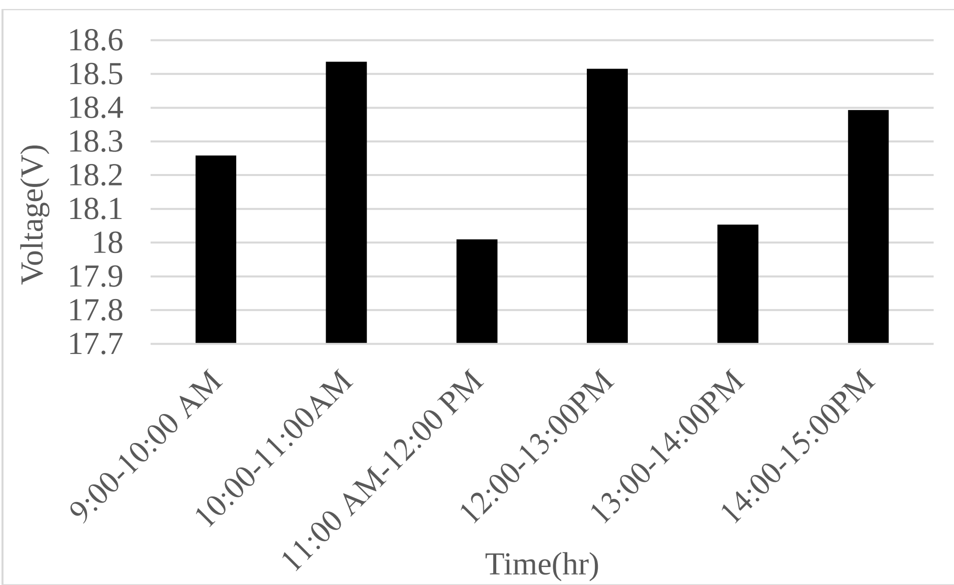

Figure: 5. 10 Voltage of bare photovoltaic module versus time

The electrical power output of the panel for the power versus time graph on May 15, 2021 is shown in Fig 5.11. The power out of the photovoltaic is increased, as the solar intensity is high, even if the raised surface module temperature drops the power output. The maximum value of the power output of the module for the non-cooling case was 36.67 W (Eq.4.1) from 11:00 AM to13:00 PM, whereas the minimum power output 9:00 to 10:00 AM was 23.03 W.

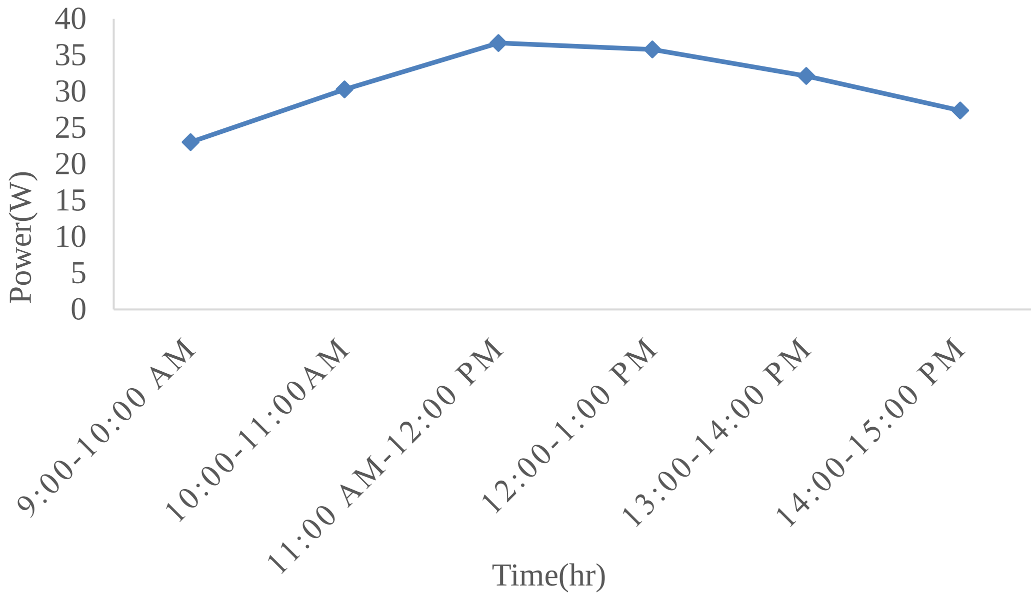

Figure: 5. 11 Power output of bare photovoltaic module versus time

As shown in Figure 5.12, as the surface temperature of the photovoltaic is increased (as shown in Figure5.7) the electrical efficiency was decreased. The experiment has been done on May 15, 2021. This is due to the reduction of short circuit current and open-circuit voltage. Without cooling as the ambient temperature and radiation intensity, reach maximum the module surface temperature was increased. The maximum efficiency was gained at a low surface module temperature that is 9.63 %(Eq.4.1a). In addition to this, the minimum electrical efficiency was gained during the maximum temperature is 7.83%.

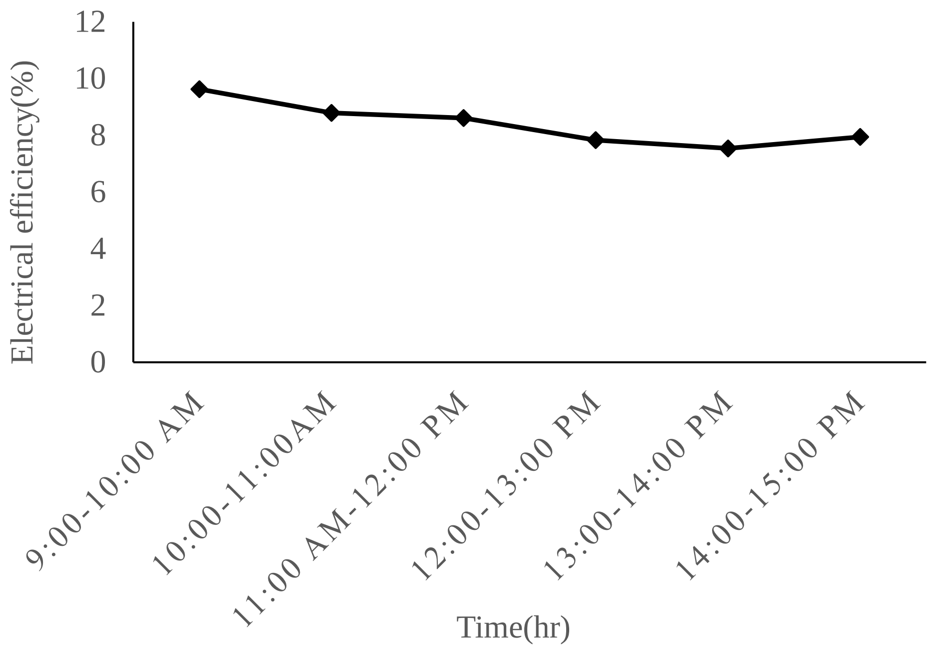

Figure: 5. 12 Electrical efficiency of bare photovoltaic module versus time

Table 5. 1 Comparison of performance characteristics of PV module at 9 AM and 12 PM

Considered performance	Time(hr.)		Difference
	9 AM	12 PM	
Temperature (^{0}C)	35.2	48.75	13.55
Current (A)	1.54	3.22	1.68
Voltage (V)	18.2	17.1	-1.1
Power (W)	18.78	37.32	18.54
Electrical efficiency (%)	9.65	7.83	-1.82

Table 5.1 shows the performance comparison of the bare photovoltaic module at 9 am and at noontime. As shown in this table, the surface PV module temperature was increased by 13.55^{0}C and the electric current was increased by 1.68 A. This is due, as the solar radiation reaches the peak point PV module surface temperature, and the current was increased. In other ways, the electrical efficiency and voltage were decreased due to the rise in surface PV module temperature.

In addition to this, the power output increase due to an increase in electric current. Similarly, the electrical and thermal performance of the bare PV module was determined for the remaining days (May 19 to 25 May 2021) and the data are given in Appendix B.

5.4.2 Performance of South Faced Continuously Water Cooled Photovoltaic Module

5.4.2.1 Thermal Performance of South Faced Continuously Water Cooled Photovoltaic Module

Figure 5.13 indicates that the temperature difference between the photovoltaic modules cooled by water film and the bare photovoltaic module. As seen from the graph, the maximum heat removal obtained by water film flow on the PV front face because this is due to the uniform flow of water on the top of the photovoltaic panel. The maximum temperature (temp) removal obtained by the top water film was 20.45℃, and the minimum was 3.4℃ as shown in Figure 5.13, has been tested on May 15, 2021. The average removal of the temperature of the photovoltaic module was around 11.09℃.

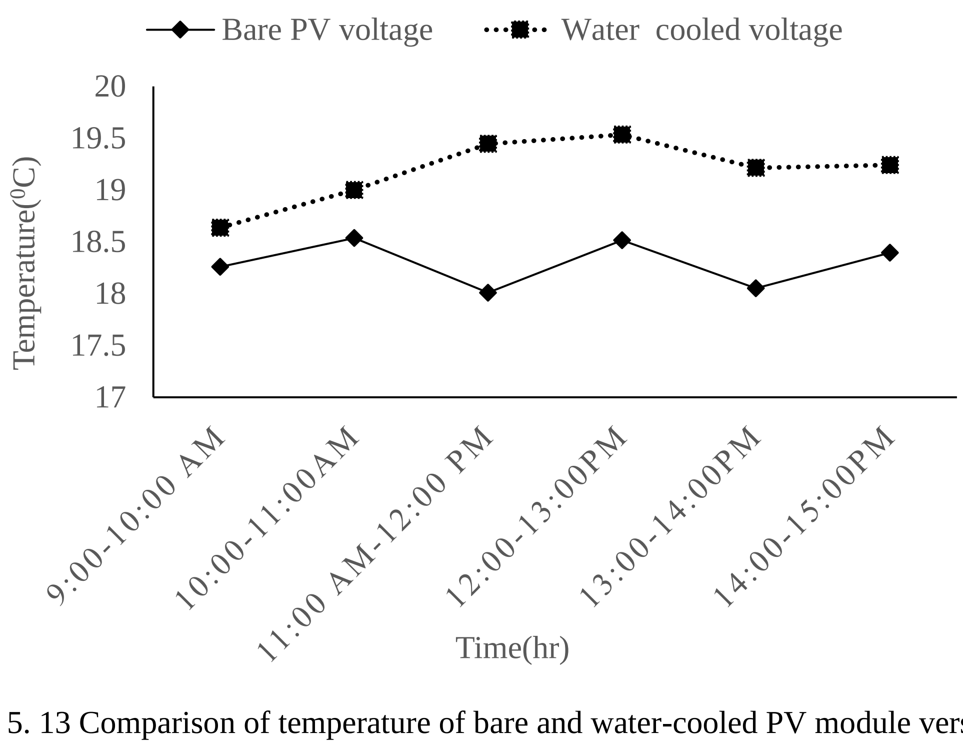

Figure: 5. 13 Comparison of temperature of bare and water-cooled PV module versus time.

Figure 5.14 indicates the comparison of thermal efficiency of bare and water-cooled PV modules. The maximum thermal efficiency of bare and with water-cooling was 80 and 52.2%, respectively (Eq. 4.21). As water-cooling is applied to the photovoltaic module, its thermal efficiency was decreased.

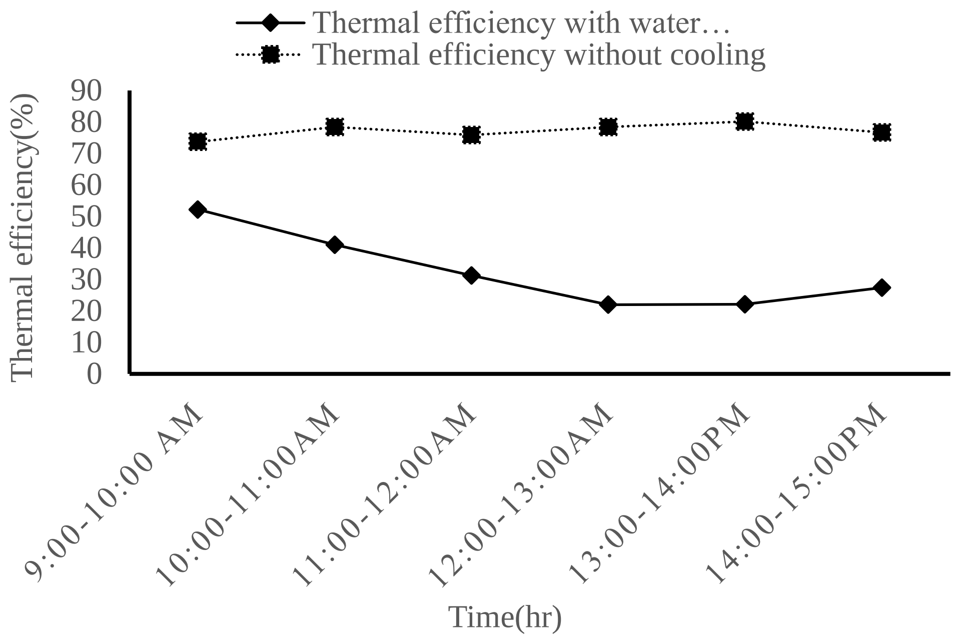

Figure: 5. 14 Comparison of thermal efficiency of bare and water-cooled PV module versus time

5.4.2.2 Electrical Performance of South Faced Continuously Water Cooled Photovoltaic Module

Figure 5.15 shows with the existing water cooling mechanism, the current output obtained slightly increased with the decreasing module temperature. The experimental test has been done on May 15, 2021. The highest current was observed to produce by using $0.23\ kg/_{min}$ water-cooling flow rate was 3.18 A during noon, with the highest solar intensity. Only 3 A is produced without cooling (bare) at the same condition.

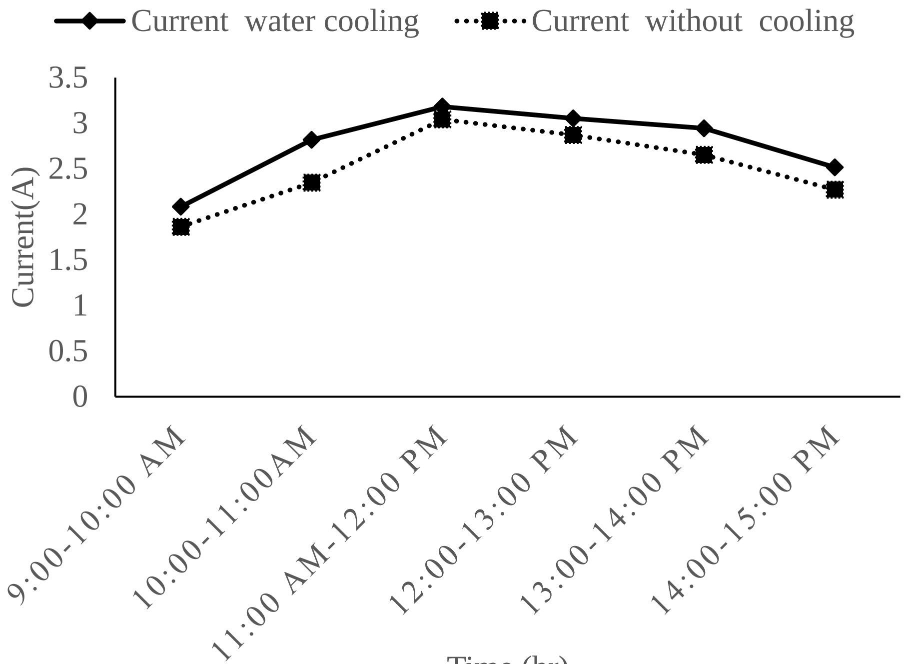

Figure: 5. 15 Comparison of current of bare and water-cooled PV module

Figure 5.16 indicates the voltage outputs of the bare PV module and water-cooled. As shown in this Figure, by using water-cooling, the average maximum and the minimum voltages were 19.534 and 18.637 V, respectively. With applying water-cooling, about 8.03% maximum increasing in voltage output was observed.

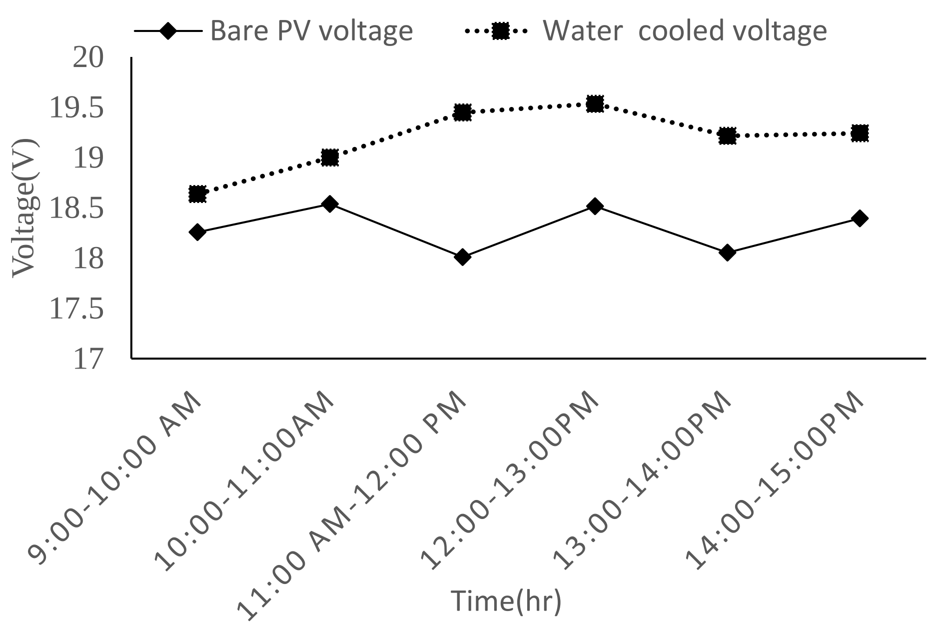

Figure: 5. 16 Comparison of voltage output of bare and water-cooled PV module

Figure 5.17 describes the power output generated with and without cooling. As shown in this Figure, by using water-cooling, a remarkable increase in power output was found. The experiment was done on May 15/2021. Without applying cooling to the PV panel, only 36.67 W of the power output can be produced at high ambient temperature and solar intensity (Eq.4.1a). At the same conditions, the result notice that the power output is increased by about 11.40 % by introducing 0.23kg/min a flow rate of water for cooling photovoltaic module and produced a maximum of around 42.55 W (Eq.4.1a). The average increment of power output by the cooling system was 17.028%.

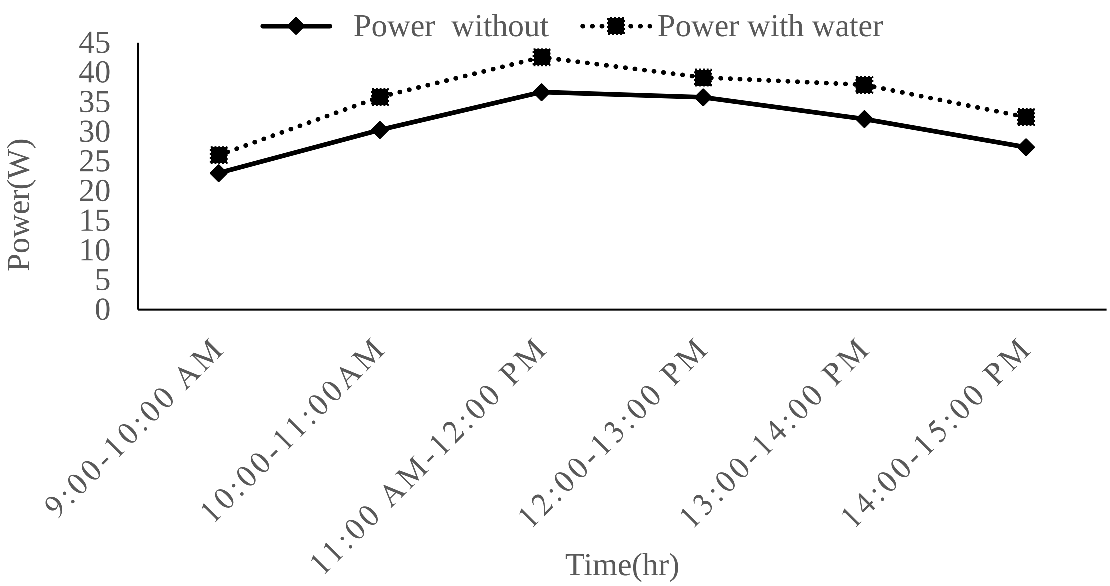

Figure: 5. 17 Comparison of power output of bare and water-cooled PV module.

Figure 5.18, shows the plot of the electrical efficiency of the photovoltaic module with water and bare investigated experimentally on May/15/2021. The maximum electrical efficiency water-cooled and bare were 10.88 and 9.6%, respectively (Eq.4.1). It was observed that the electric efficiency of the module with water-cooling increases maximally by 23.15% and on average by 16.26%.Similar work from the literature review has been validated, the result of the study was the maximum temperature removed 22^{o}C (Bhakre et al., 2021).

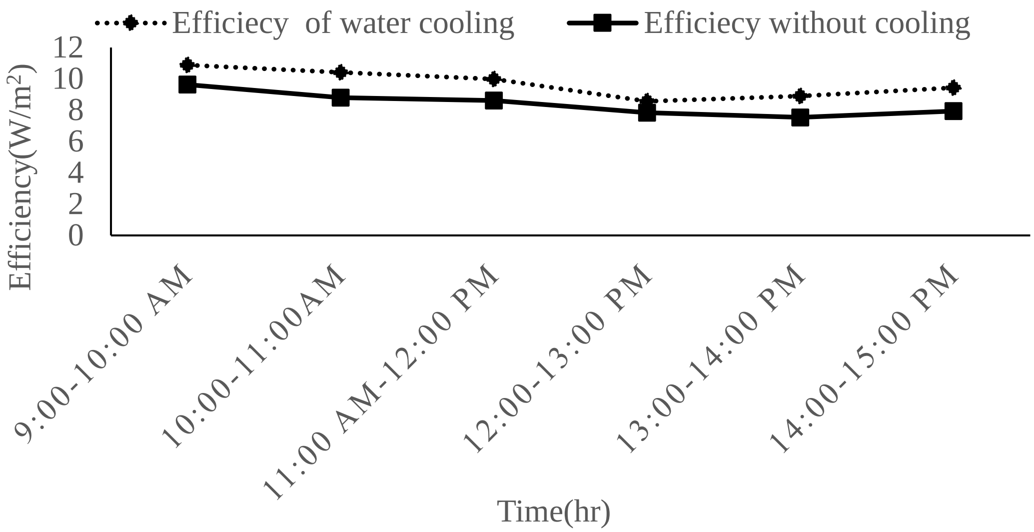

Figure: 5. 18 Comparison of electrical efficiency of bare PV and water-cooled

5.4.3 Performance of South Faced Air Cooled Photovoltaic Module

5.4.3.1 Thermal Performance of South Faced Continuously Air Cooled Photovoltaic Module

Figure 5.19, described the temperature variation over the surface of the module. The experimental test was accomplished on May 19/2021. The result reported that measured average temperature ranges increased from 30.87 ^{0}C to maximum values 46^{0}C. The temperature of the photovoltaic module was fluctuating depending on the solar radiation intensity. The flow rate of air over the PV module was 0.000763kg/s.

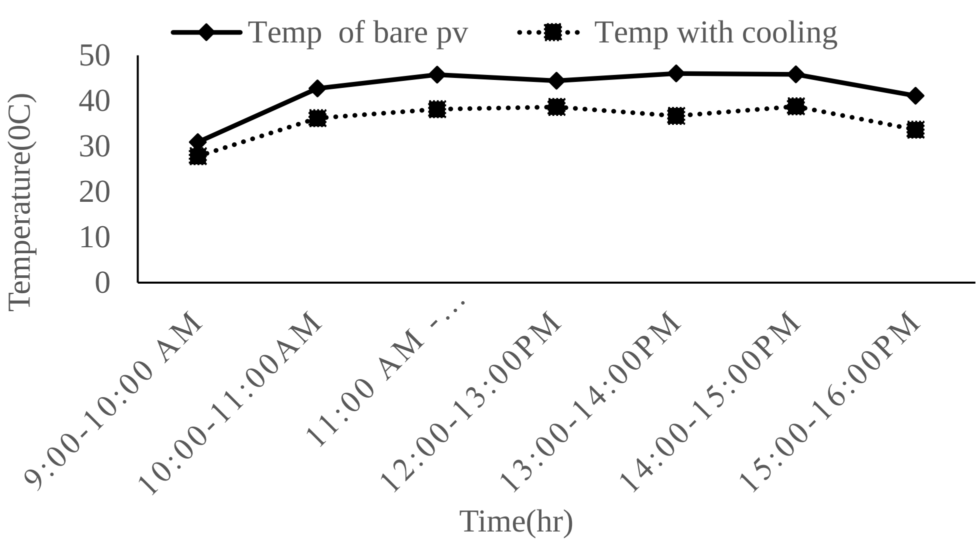

Figure: 5. 19 Comparison of bare and air-cooled PV module temperature versus time

Figure 5.20 illustrates the thermal efficiency of the photovoltaic module without and with air-cooling. This experimental test was done on May 19/2021. The maximum thermal efficiency without cooling was 82% and with air-cooling was 25 % (Eq.4.21).

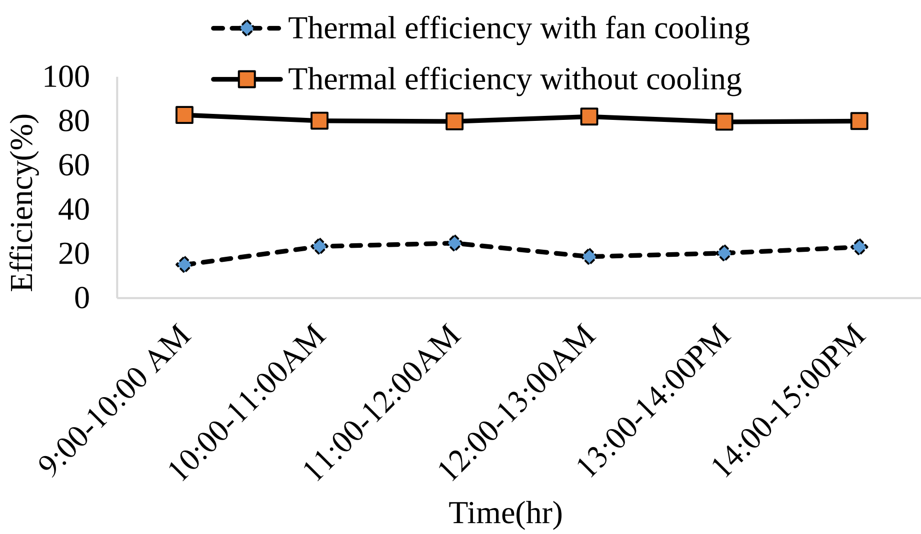

Figure: 5. 20 Comparison of bare and air-cooled photovoltaic module thermal efficiency versus time

5.4.3.2 Electrical Performance of South Faced Continuously Air Cooled Photovoltaic Module

The effect of the fan on the current output of the PV module is illustrated in Figure 5.21. The maximum average current produced by using fan blower operation 3.04 A at 12:00 PM to 1:00 PM. Even if in the same condition, only 2.93 A has been produced for the bare photovoltaic module.

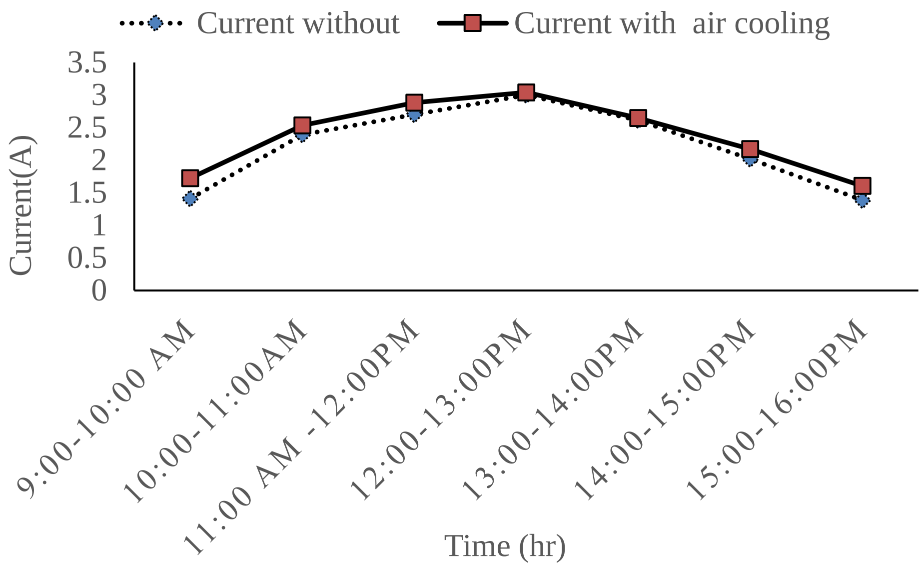

Figure: 5. 21 Comparison of the current of bare photovoltaic module and air-cooled

The voltage output of the photovoltaic module for bare and air cooled PV modules was shown in Figure 5.22. As shown in this Figure, the voltage output was decreases due to a rise in surface temperature at peak solar radiation, during noontime the cooled voltage was 19.08 V and uncooled was around 18.2 V. Due to cooling by air, the increase in 5% increase in voltage of the photovoltaic module.

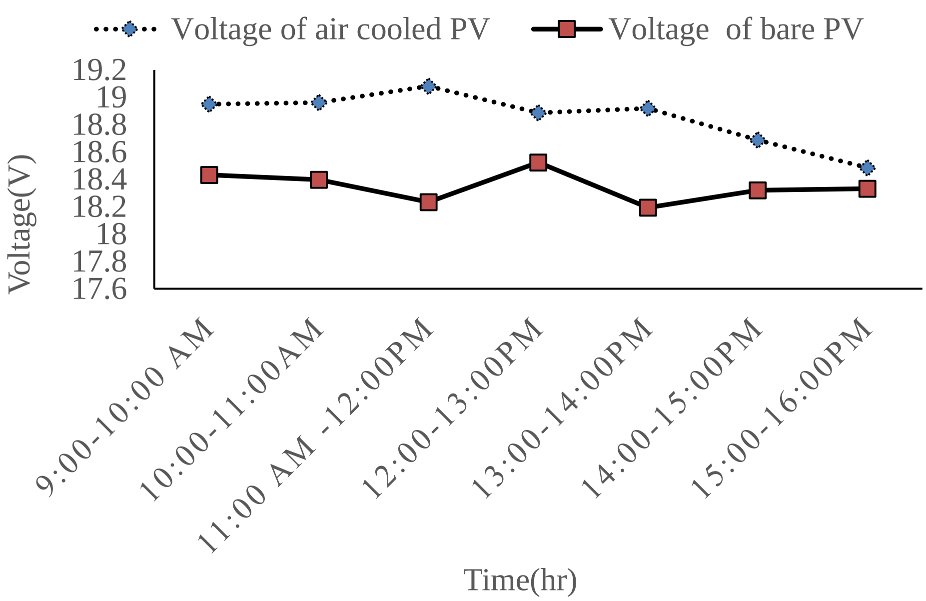

Figure: 5. 22 Comparison of voltage of bare and air-cooled photovoltaic module versus time

Figure 5.23, illustrated the comparison of power output of bare and air-cooled on May 19, 2021. The experimental tested during noontime the maximum air-cooled and bare power of PV module 39.08 and 37.31 W, respectively (Eq.4.1a). Because of air-cooling, there was an increment of output power by 4.18%.

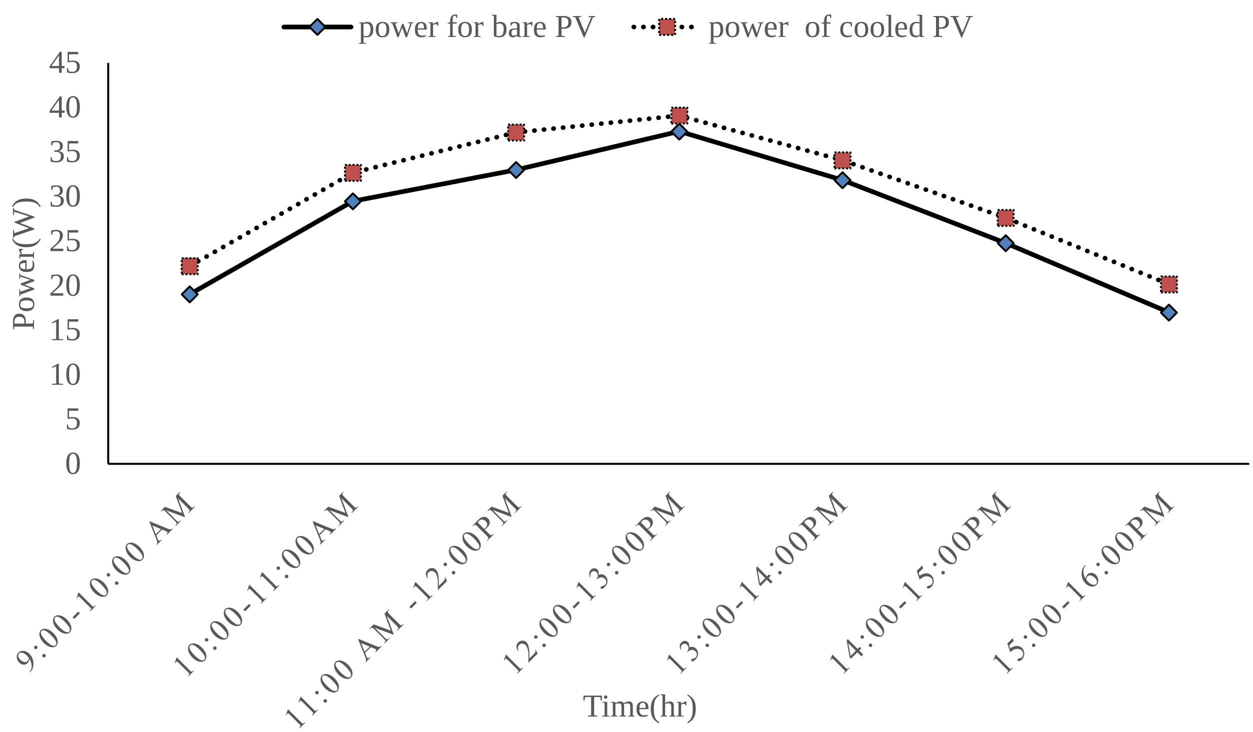

Figure: 5. 23 Comparison of power output for bare and air-cooled PV module versus time

Figure 5.24, shows that the increment of electrical efficiency by air-cooling. The maximum electrical efficiency due to cooling was 9.55% and bare efficiency was 8.6% (Eq.4.1). The maximum and average increment of electrical efficiency was 18.5 and 11.1%, respectively.

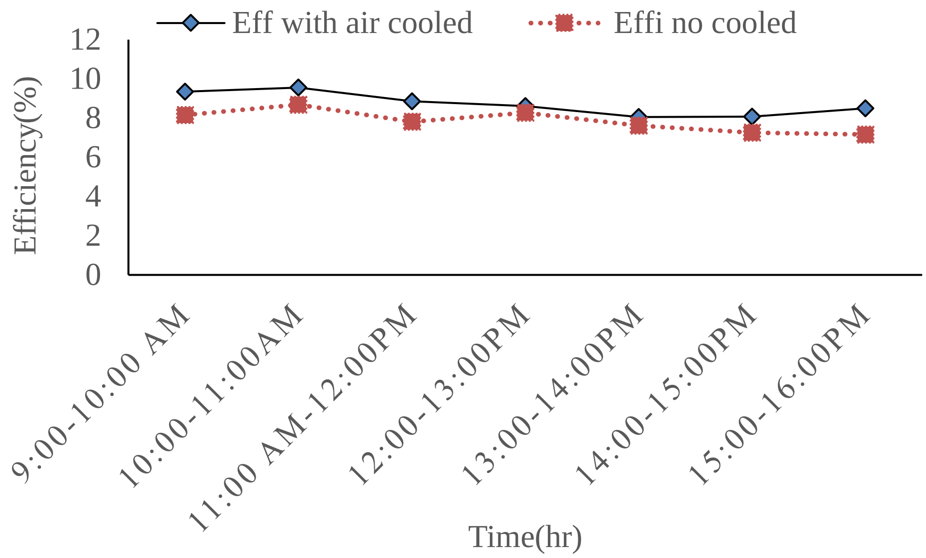

Figure: 5. 24 Comparison of electrical efficiency of bare and air-cooled PV module versus time**.**

5.4.4 Performance of South Faced Intermittent water Cooled Photovoltaic Module

5.4.4.1Thermal Performance of South Faced Intermittent water Cooled Photovoltaic Module

The bare photovoltaic module system is operating at maximum average temperature as shown in figure 5.25. The maximum operating temperature of the intermittent water-cooled and the bare module was 43.1 and 50.1^{0}C, respectively. The overall result implied the working temperature maximum, minimum and average dropped by 15.8, 3, and 7.8 ^{0}C, respectively.

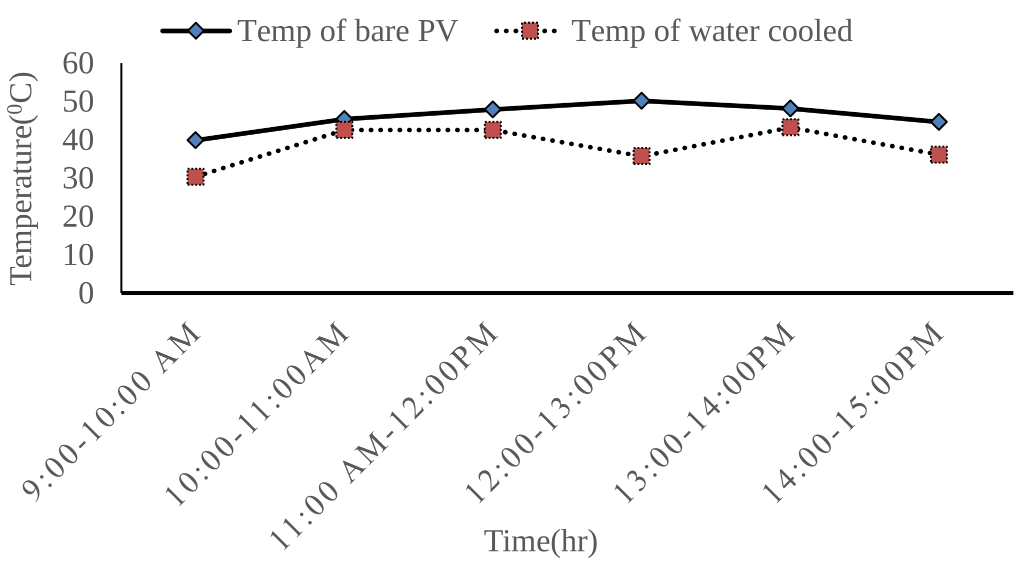

Figure: 5. 25 Comparison of PV module surface temperature of bare and intermittent water-cooled versus time

Figure 5.26 shows the thermal efficiency for bare and intermittent water-cooling versus time. As shown in this Figure, thermal efficiency for bare was maximum. The maximum thermal efficiency without cooling was 80.85% (Eq.4.21). In addition to this, the maximum intermittent water-cooling was 39.9 % (Eq.4.6).

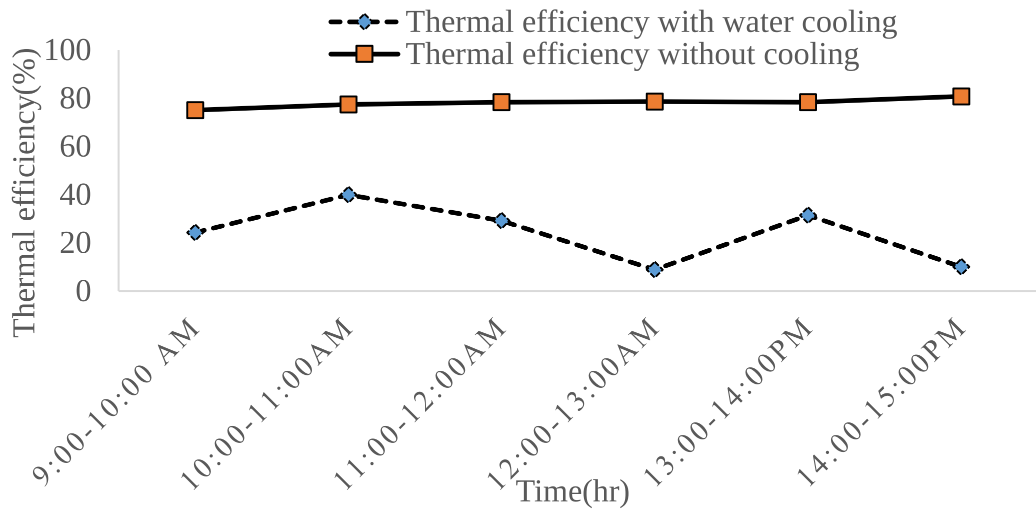

Figure: 5. 26 Thermal efficiency bare and intermittent water-cooling versus time

5.4.4.2 Electrical Performance of South Faced Intermittent water Cooled Photovoltaic Module

Figure 5.27 illustrates the comparison of experimental result of the current output of the bare photovoltaic module and intermittent water-cooling. With applying water-cooling mechanism, about 12.3 and 7.25% maximum, and average output current have improved, respectively.

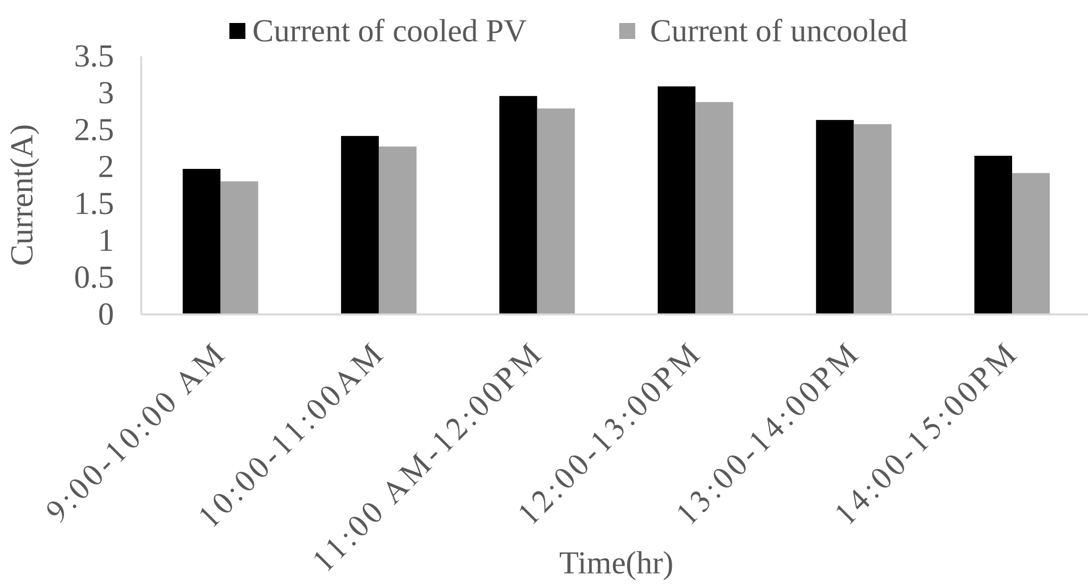

Figure: 5. 27 Comparison of current with intermittent water-cooling and bare versus time

The comparison of the voltage output of the bare and intermittent water-cooled PV module was presented in Figure 5.28. The result showed the maximum and average increment due to the cooling system is 8 and 5.25%, respectively. During noontime, bare and cooled voltage was 18.15 and 19.57 V, respectively. There was 7.52% increase in voltage output due cooling system.

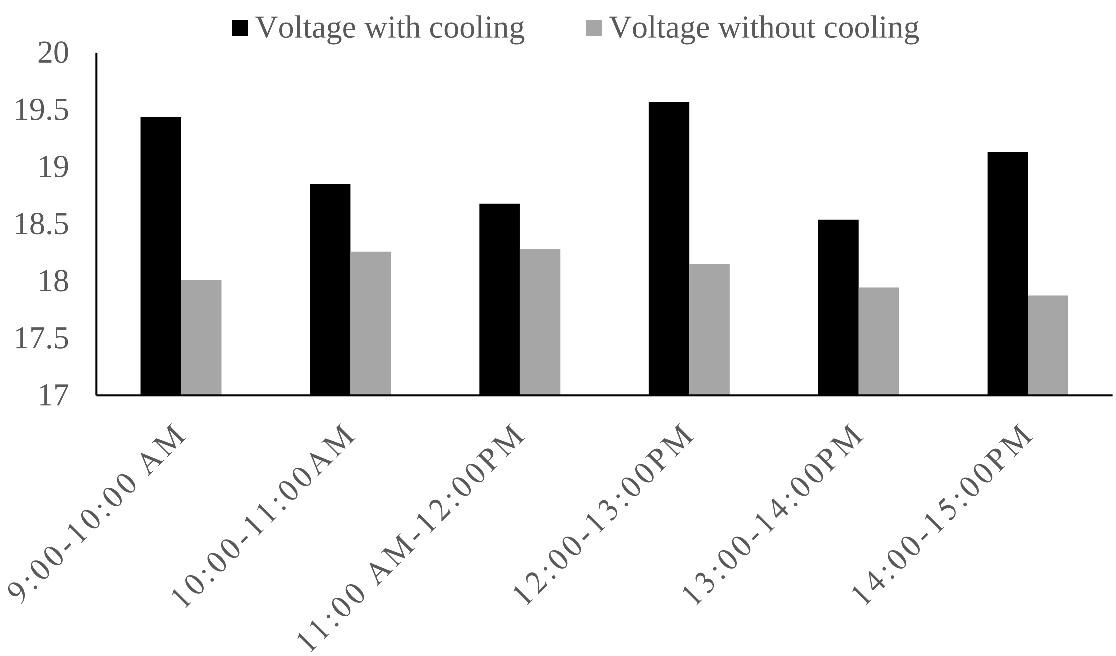

Figure: 5. 28 Comparison of the PV module voltage with intermittent water cooled and bare versus time

As shown in Figure 5.29, during the experiment the module power is maximum for the cooling case. At the same time, during noon, the maximum output power with and without cooling, is 41.5 and 35.8 W (eq.4.1a), respectively. The increment in power output is due to intermittent water is the maximum and an average of 5.64 and 3.73 W, respectively.

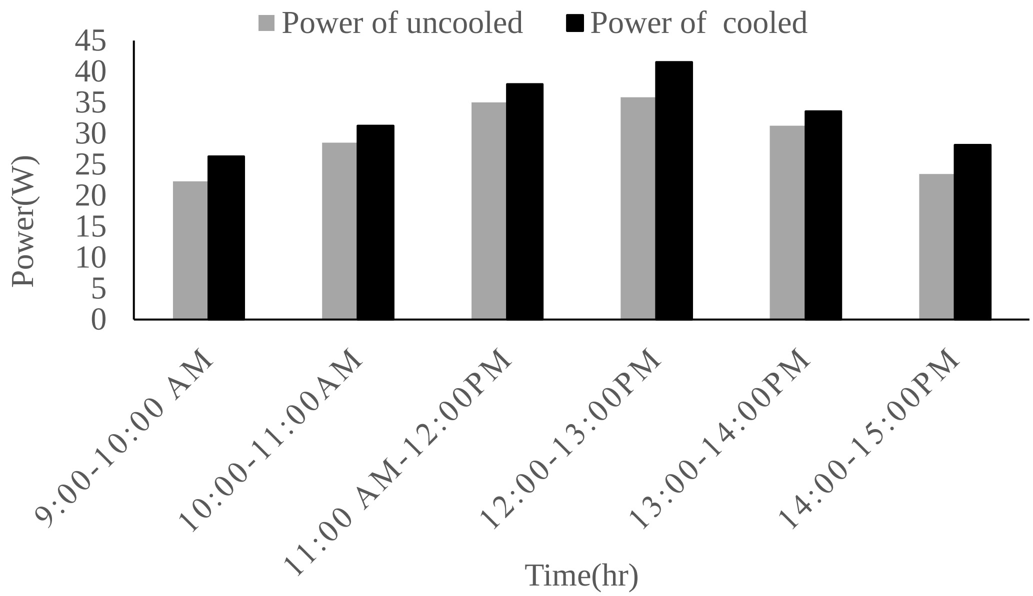

Figure: 5. 29 Comparison of the power of bare PV module and intermittent water-cooled versus time

As shown in Figure 5.30, that the increment of electrical efficiency is due to water-cooling. This experiment was carried out on May 22/2021 for south facing. The maximum and average increments of electrical efficiency were 20.149 and 13.5%, respectively. The maximum produced electrical efficiency due to intermittent water-cooling was 9.79% (eq.4.1).

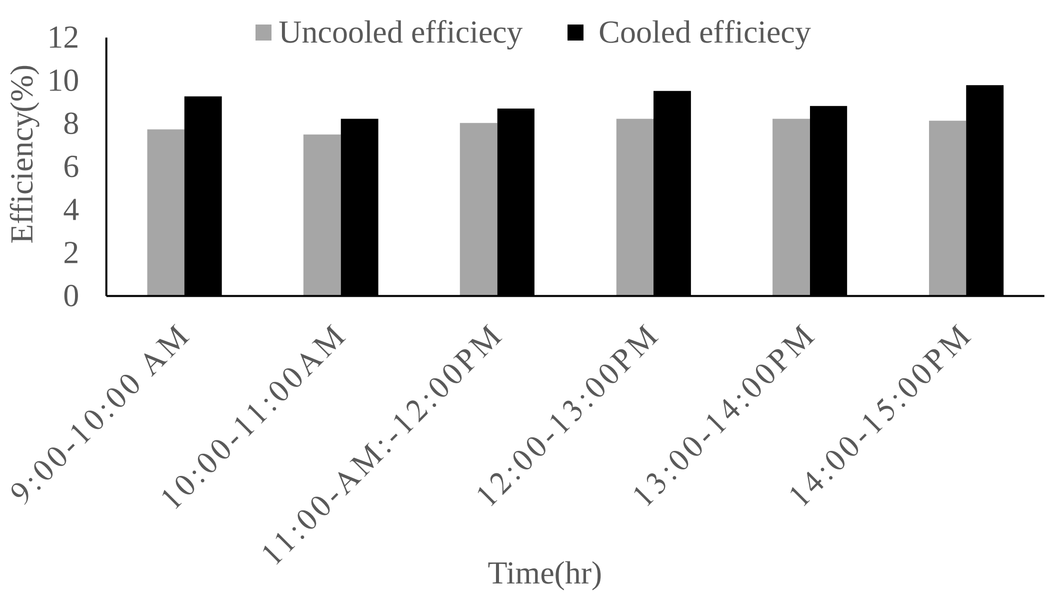

Figure: 5. 30 Comparison of the electric efficiency of bare PV module and water intermittent cooling versus time

5.4.5 Performance of South Faced Continuously Water and Air Cooled Photovoltaic Module

5.4.5.1 Thermal Performance of South Faced Continuously Water and Air Cooled Photovoltaic Module

The comparison of the module temperature cooled with air and water is illustrated in Figure 5.31. A PV module cooling is more effective for water than air. In addition to this, the front water-cooling was removing the dust and impurities from the photovoltaic surface. The average module temperature is decreased by water was 6 ^{0}C. The maximum and minimum PV water-cooled were 33.59 and 29 .3^{0}C respectively. In addition to this, 41.5 and 32.2 ^{0}C were the maximum and the minimum air-cooled PV module surface temperature respectively.

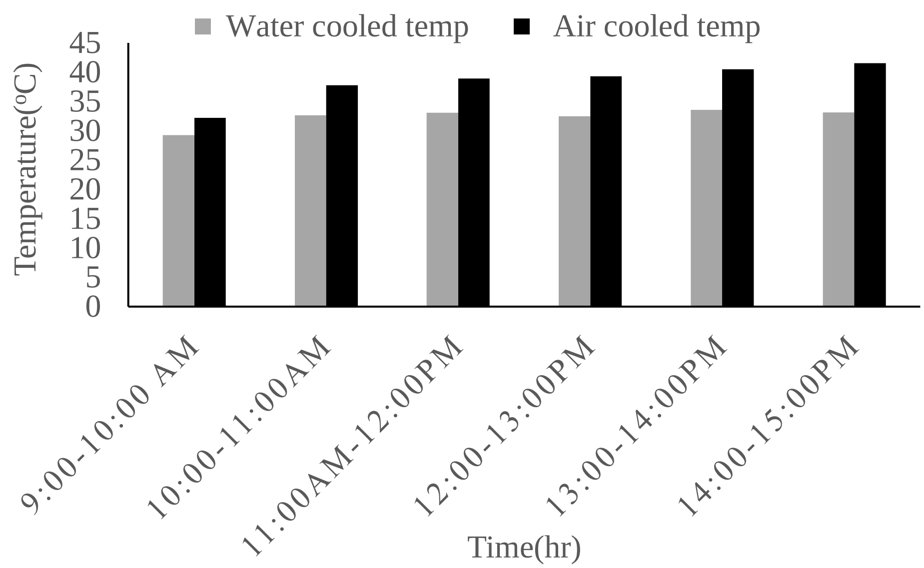

Figure: 5. 31 Comparisons of average PV module temperature with air and water-cooled versus time

The comparison of the module thermal efficiency cooled with air and water is illustrated in Figure 5.32.When compared thermal efficiency of air and water; the air-cooled efficiency was high.

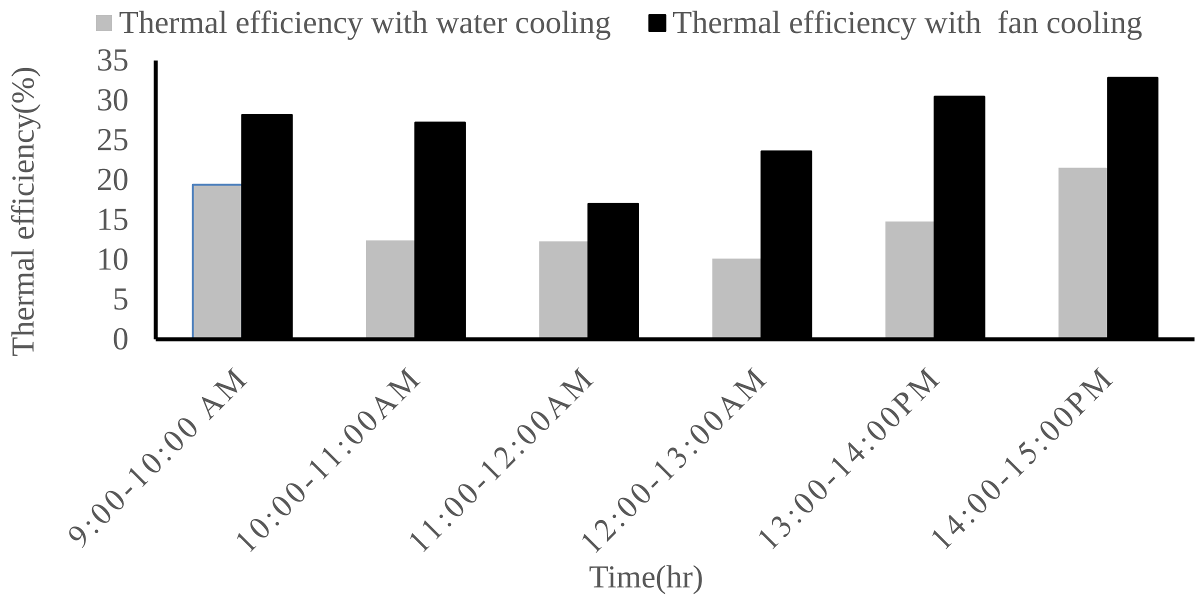

Figure: 5. 32 Comparison of thermal efficiency of water and air-cooled PV module

5.4.5.2 Electrical Performance of South Faced Continuously Water and Air Cooled Photovoltaic Module

Figure 5.33 shows the current of the PV module increases with an increase in solar radiation for both air and water-cooled. The PV module with water heat removal has a lower module surface temperature and generated a higher current than air-cooling. The maximum increment in output current by water -cooling was, 7.54% when compared to the air-cooling module.

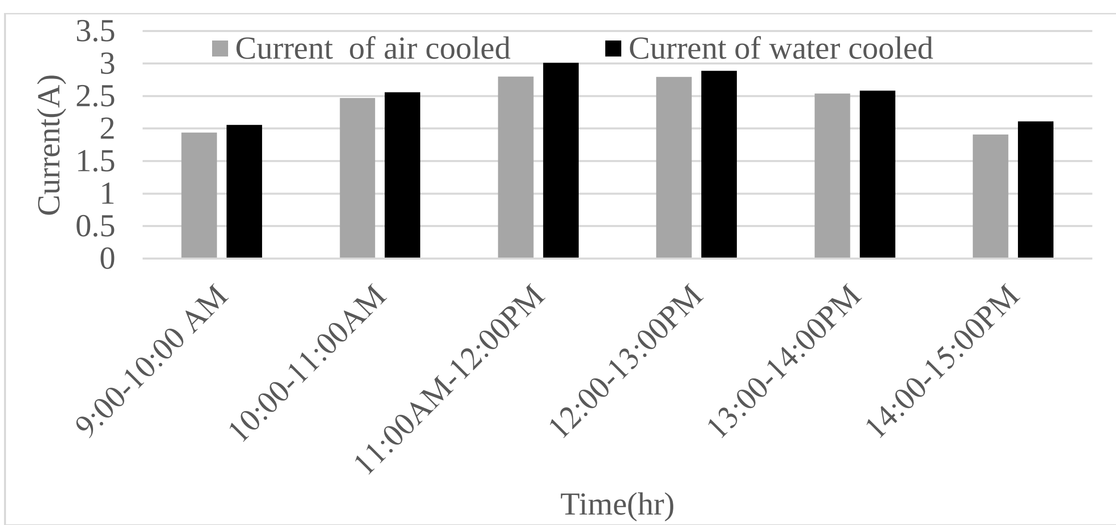

Figure: 5. 33 Comparisons of the current output cooled by air and water versus time

As already mentioned, an increase in the PV module temperature leads to a decrease in their voltage generation. This truth is clearly, explained in Figure 5.34. According to this Figure, the PV module cooled with water and has about 6.04% more output voltage compared with air- cooling photovoltaic module. The maximum water and air-cooled PV module voltage was 19.7 and 19.1 V, respectively.

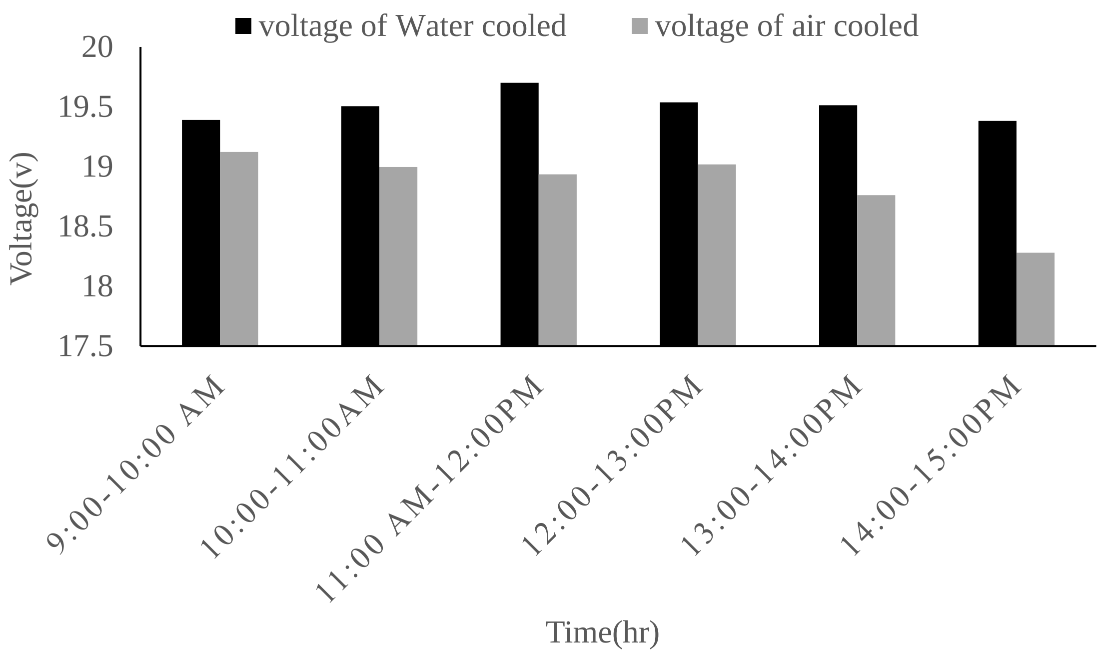

Figure: 5. 34 Comparison of voltage of the PV module with water and air-cooled

Figure 5.35 shows the comparison of the air and water-cooled power output of the photovoltaic module. The Figure for the cooled PV module stands higher than for the air-cooled PV module, which indicates that cooling of the module by water, produces more output power. The maximum water-cooled power was 40 W (eq.4.1a).The water-cooled PV module has a maximum of 17% higher output power than the air-cooled PV modules while flowing water at a mass flow rate of 0.333 kg/min.

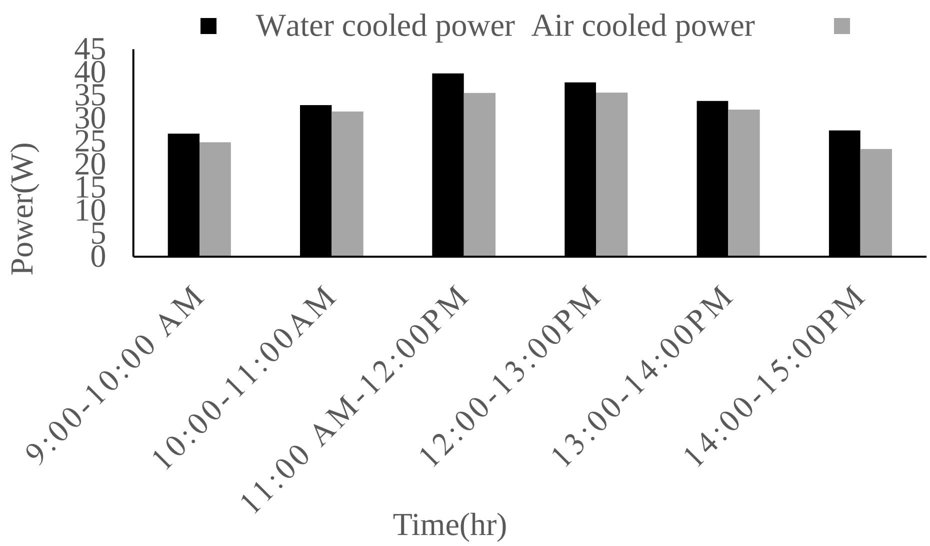

Figure: 5. 35 Comparison of the output power of the PV module with water and air-cooled

Figure 5.36 shows the electrical efficiency produced by the PV module through the experiment of air and water-cooled. As shown in this Figure the maximum and minimum water-cooled efficiency is 11.33 and 8.07 %(Eq.4.1) respectively. As a whole, the maximum increase in efficiency by water-cooled was 17.09%. From experimental results, concluded that the water-cooling system is more effective than the air-cooled photovoltaic modules.

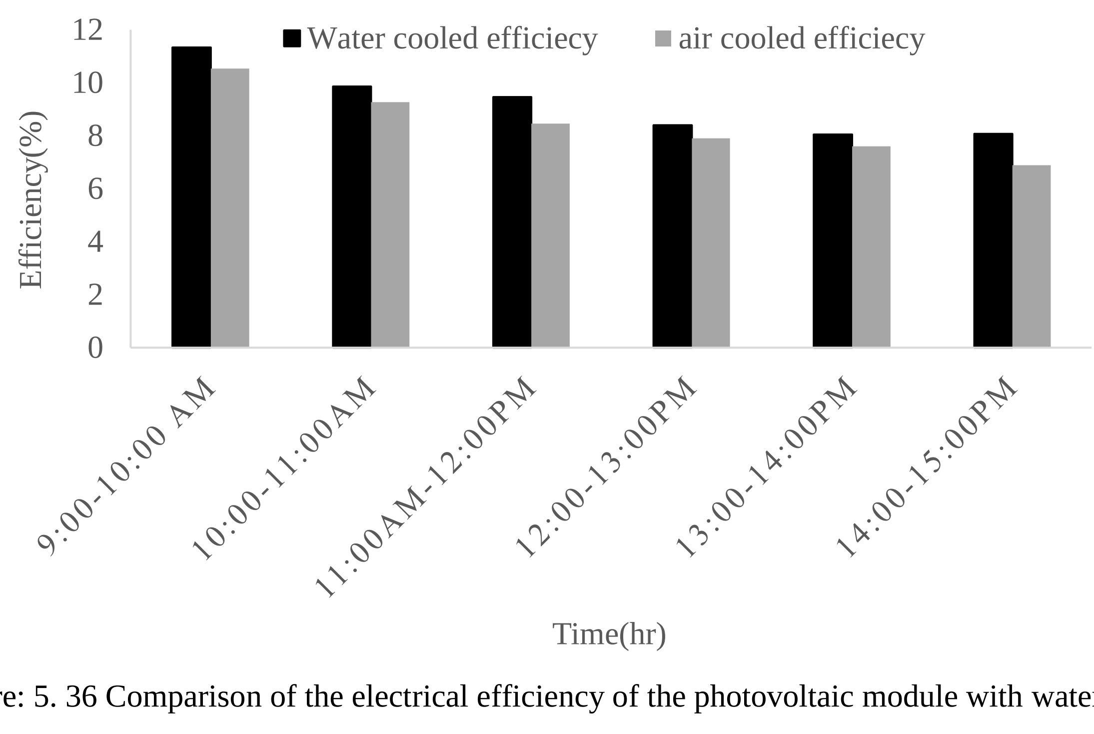

Figure: 5. 36 Comparison of the electrical efficiency of the photovoltaic module with water and air-cooled PV module.

5.5 Thermal and Electrical Performance of East Faced Photovoltaic Module

Two PV modules were exposed to solar radiation facing the sun on the East axis to investigate the effect of air and water-cooling on the electricity generated. The thermal and electrical performance results of these experiments are discussed in this section.

5.5.1 Performance of East Faced Bare Photovoltaic Module

5.5.1.1 Thermal Performance of East Faced Bare Photovoltaic Module

Figure 5.37 shows the results of the bare PV module surface temperature on May 23, 2021, for east facing. The Figure illustrates for the east case the temperature of the module was high when compared to the south case. The maximum average temperature without cooling was 55.43^{0}C.

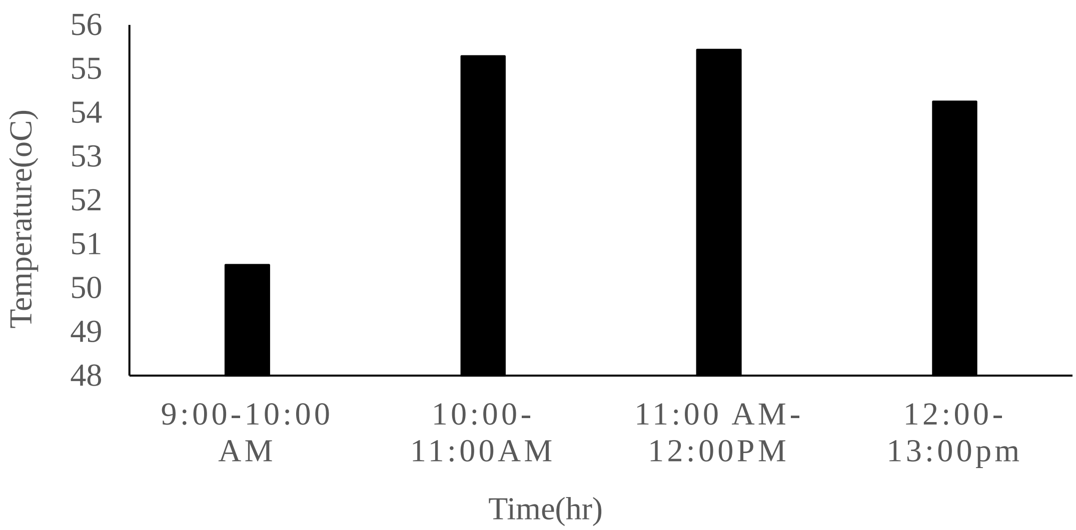

Figure: 5. 37 Bare PV module surface temperature versus time

Figure 5.38 shows the thermal efficiency of the East faced bare photovoltaic module. As shown in this Figure the maximum thermal efficiency of the bare PV was 70 % (Eq.4.21). The bare thermal efficiency was increased due to increase in surface temperature.

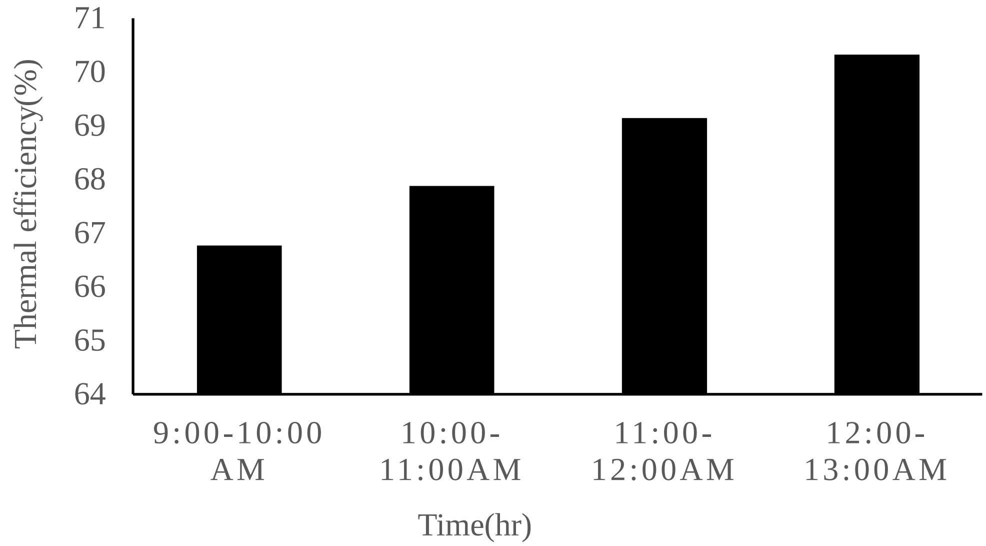

Figure: 5. 38 Thermal efficiency of the bare photovoltaic module versus time

5.5.1.2 Electrical Performance of East Faced Bare Photovoltaic Module

The bare photovoltaic module current East faced on May 23/2021 was illustrated in Figure 5. 39. The output maximum current was 3.1 A for the bare PV module and the average minimum was 2.8 A.

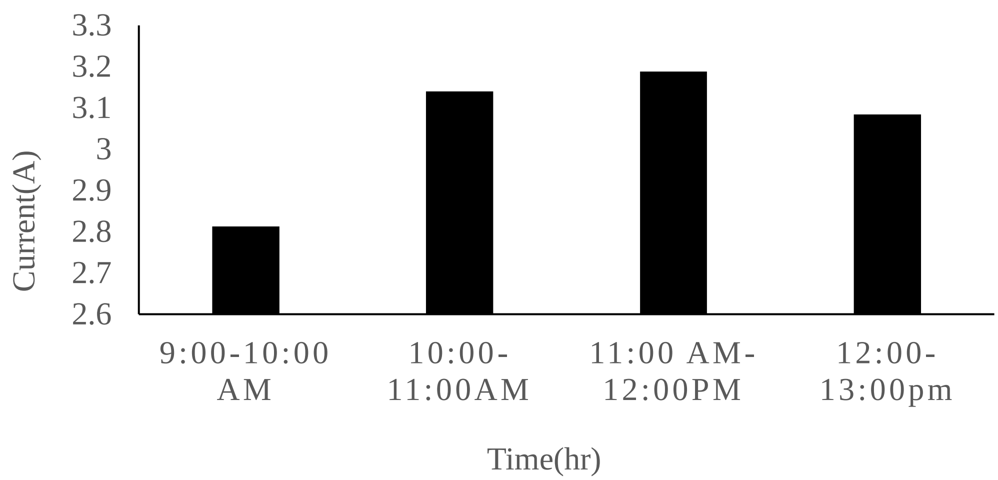

Figure: 5. 39 Current of the bare photovoltaic module versus time

Figure 5.40 shows bare PV module voltage on May 23, 2021, for east facing. As shown in this, figure the maximum average voltage was 18.43 V. As shown in this Figure the voltage drop is happened due to arise in surface PV module temperature shown in Figure 5.37.

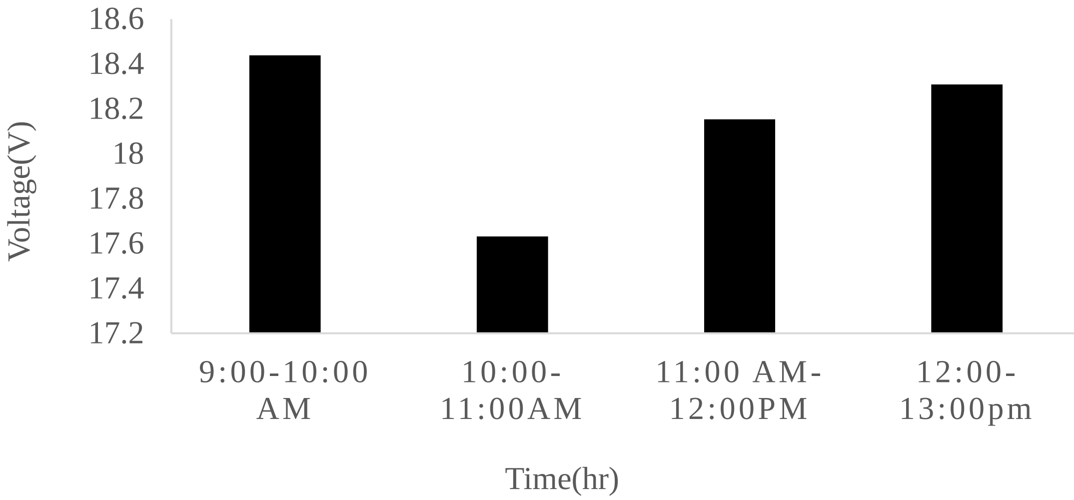

Figure: 5. 40 Voltage of the bare photovoltaic module versus time

The hourly experimentation electrical power output is plotted in Figure 5.41. The experiment was carried out on May 23/2021. The values of the power output varied slightly with changes in solar radiation and module surface temperature. The maximum power output of the bare PV module was 39.6 W (Eq.4.1a) is a low value due to the decrease in voltage of the module.

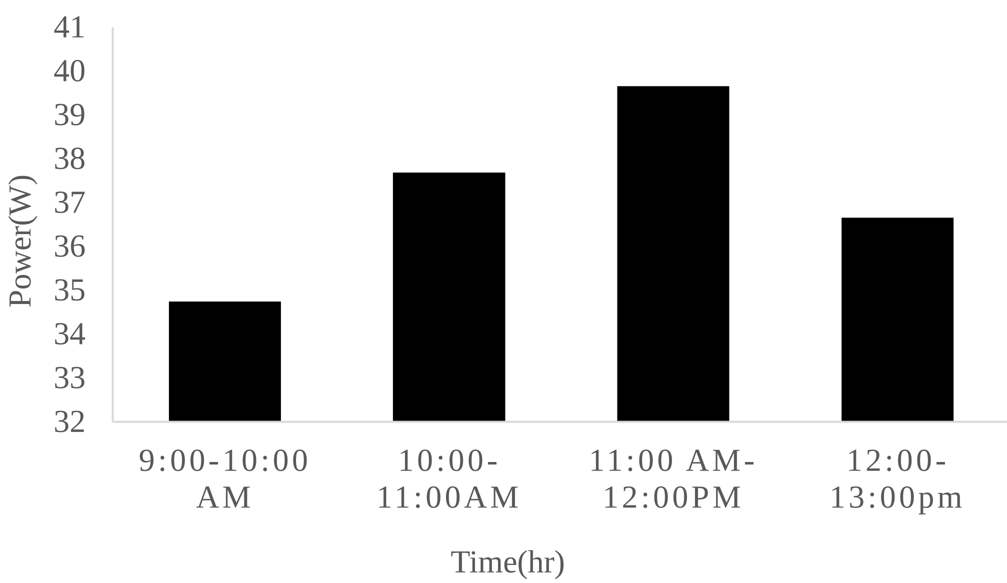

Figure: 5. 41 Power output of the bare photovoltaic module versus time

The comparison of the electric efficiency for dry was shown in Figure 5.42. The maximum electrical efficiency of the bare PV module was 7.94 %(eq.4.1).

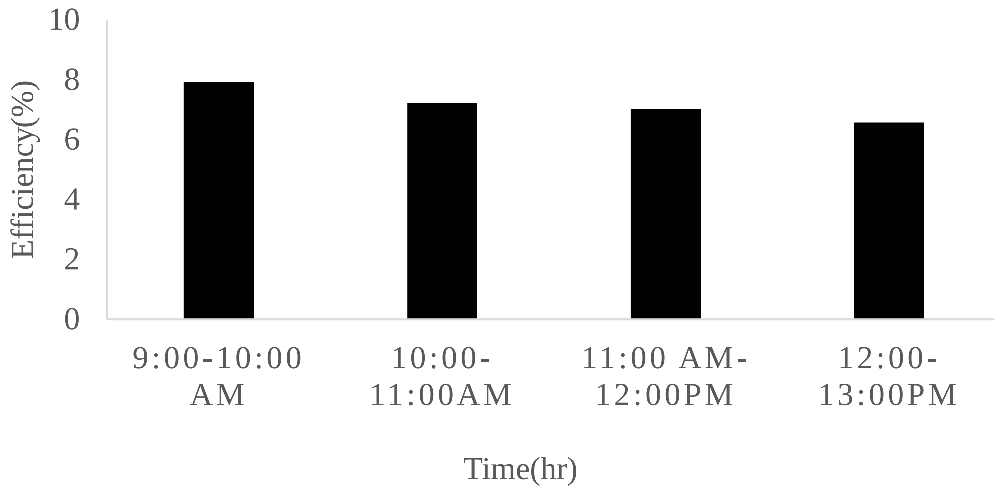

Figure: 5. 42 Electrical efficiency of the bare photovoltaic module versus time

5.5.2 Performance of East Faced Continuously Cooled Photovoltaic Module

5.5.2.1 Thermal Performance of East Faced Continuously Water Cooled Photovoltaic Module

Figure 5.43 shows the results of the bare and water-cooled PV module average surface temperature on May 16, 2021, for east facing. As shown in this Figure the maximum bare and water-cooled temperature were 54.39 and 35.35 ^{0}C during the time 11 to 12 PM respectively. This implies there was 19.04 ^{0}C in temperature removal.

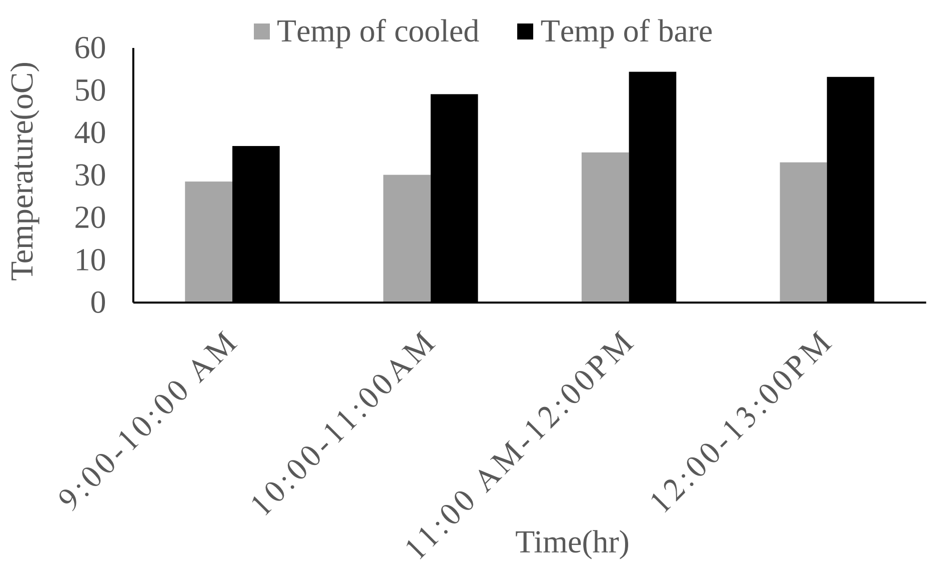

Figure 5. 43 Comparison of the bare and water-cooled PV temperature versus time

Figure 5.44 shows the results of the bare and water-cooled PV module thermal efficiency. The maximum thermal efficiency of the bare PV module was 70.5%.

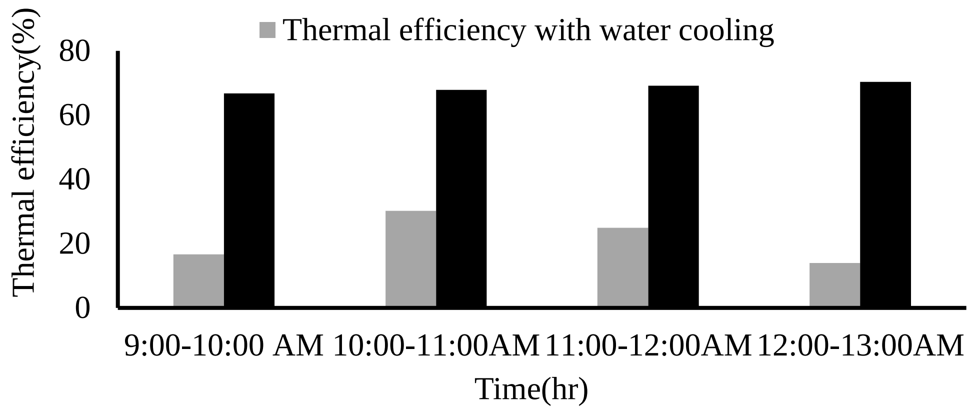

Figure: 5. 44 Comparison of the bare and water-cooled PV thermal efficiency versus time

5.5.2.2 Electrical Performance of East Faced Continuously Water Cooled Photovoltaic Module

Figure 5.45 shows the comparison of the bare and water-cooled PV module average electric current on May 16, 2021, for east facing. The maximum current of the bare and water-cooled PV module were 3.3 and 3.38 A respectively.

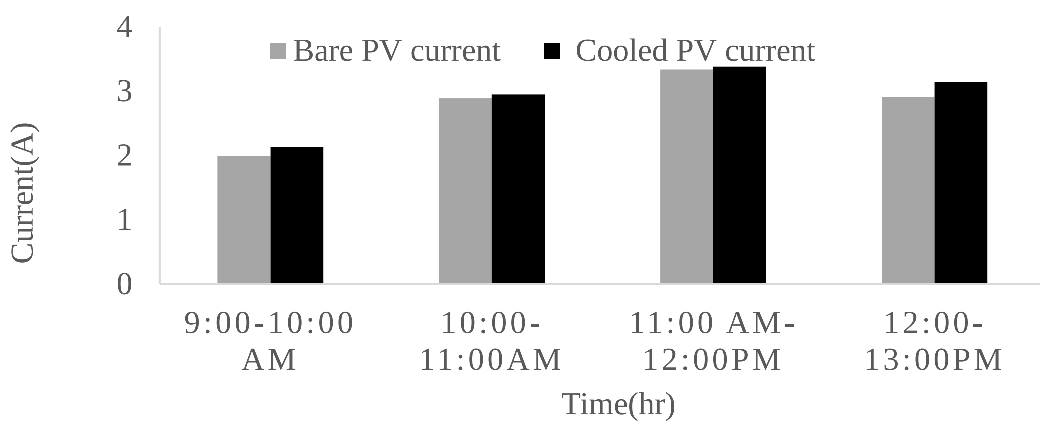

Figure: 5. 45 Comparison of the water-cooled and bare PV module current versus time

The comparison of average of the bare and water-cooled PV module average electric voltage was illustrated on Figure 5.46. The Figure 5.45 show that 19.9 V was the maximum average voltage of the water-cooled PV module and at the same condition the maximum bare PV module voltage was 18.58 V. At this condition, there was 7.1% increment in voltage output.

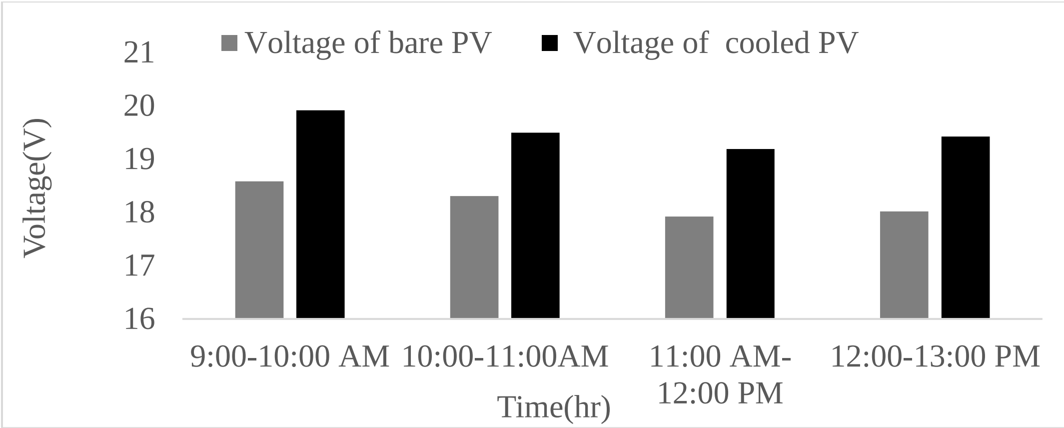

Figure: 5. 46 Comparison of the water-cooled and bare PV module voltage versus time

Figure: 5.47 illustrates the variation bare and water-cooled output power versus time of the PV module. It can be observed from the graph that the power generated gradually increases over time increase. From 11:00 AM to 12:00 PM, the maximum power output was 43.56 and 41W (Eq.4.1a) for cooled and bare PV modules respectively.

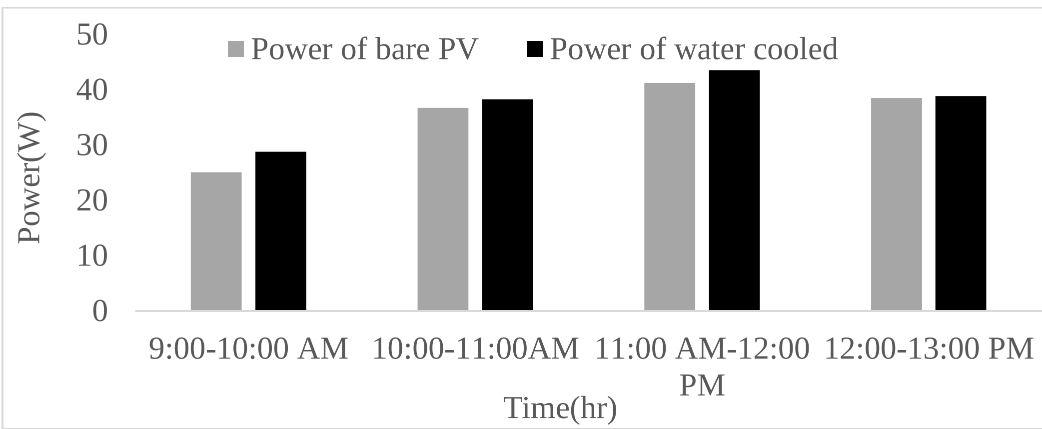

Figure: 5. 47 Comparison of the water-cooled and bare PV module power versus time

Figure: 5.48 shows the variation bare and water-cooled of the PV module electrical efficiency of east facing. The maximum bare and water-cooled electrical efficiency were 7.68 and 8.13% respectively.

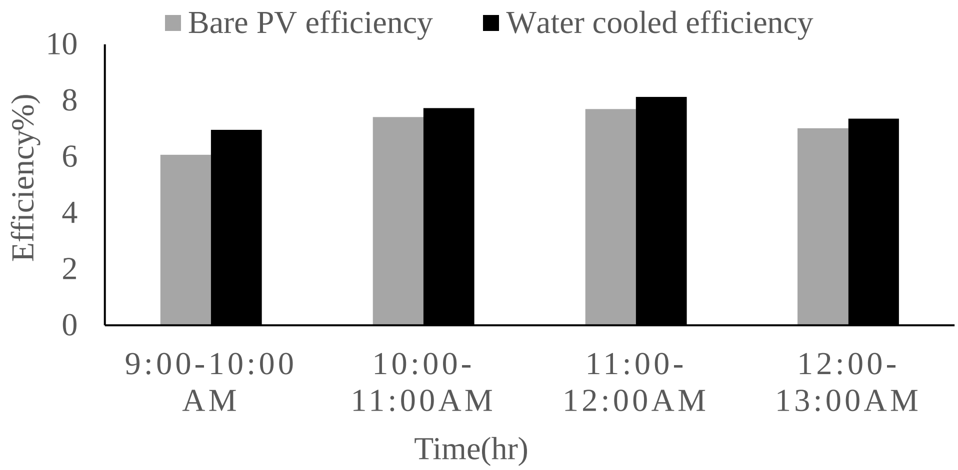

Figure: 5. 48 Comparison of the water-cooled and bare PV module electrical efficiency versus time

5.5.3 Performance of East Faced Continuously Air Photovoltaic Module

5.5.3.1 Thermal Performance of East Faced Continuously Air Photovoltaic Module

Figure 5.49 shows a graph for the variation of temperature of bare and air-cooling versus time on May 20, 2021, for the east-faced photovoltaic module. It can be observed from the graph that the photovoltaic module with air is moderately cooler than a conventional photovoltaic module. As shown in this figure, the maximum average temperature of the uncooled and cooled modules are 47.92 and 41.07^{o}C respectively. The maximum and average temperature reduction by air was 7.87 and 7.12^{o}C, respectively

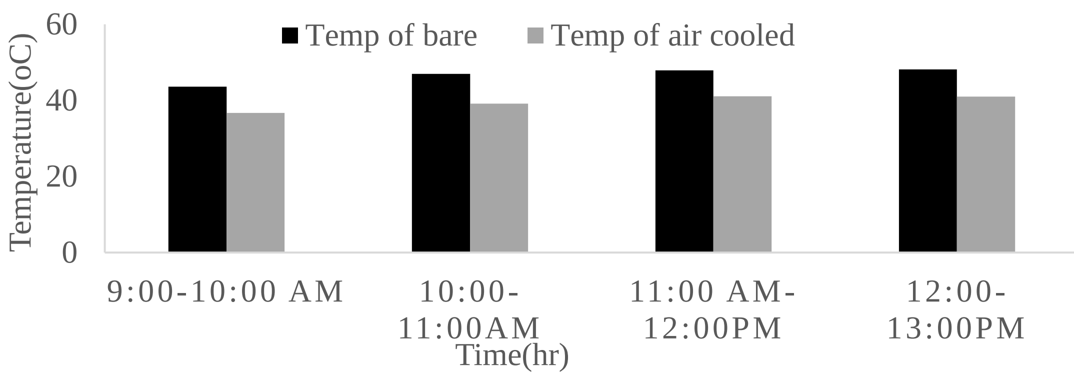

Figure: 5. 49 Comparison of bare and air-cooled PV module surface temperature versus time

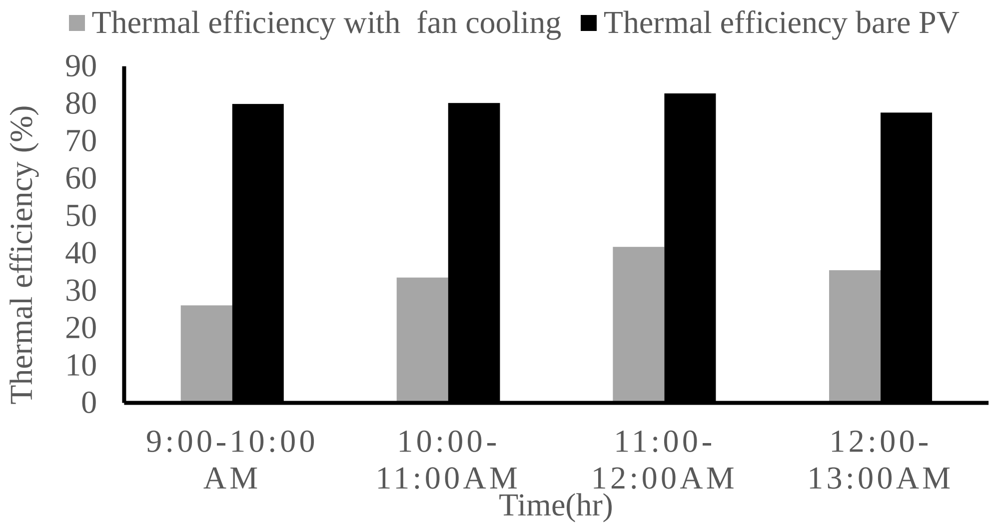

Figure: 5. 50 Comparison of bare and air-cooled PV module thermal efficiency versus time

Figure 5.50 shows a graph for variation of bare and air-cooled of the PV module thermal efficiency versus time. This Figure shows that the maximum thermal efficiency were obtained for the bare PV module.

5.5.3.2 Electrical Performance of East Faced Continuously Air Photovoltaic Module

Figure 5.51 shows a graph for variation of bare and air-cooled current versus time of the photovoltaic module faced to east. As shown in the figure, the current is increased as the solar intensity was increased. From the graph below the maximum current for both case were high at 12 am to 1 pm at peak solar radiation, even if the bare panel current was decreased due maximum temperature of the surface module and it was increased due to high solar radiation intensity. The average increment in electric current due to air-cooling was 2.7%.

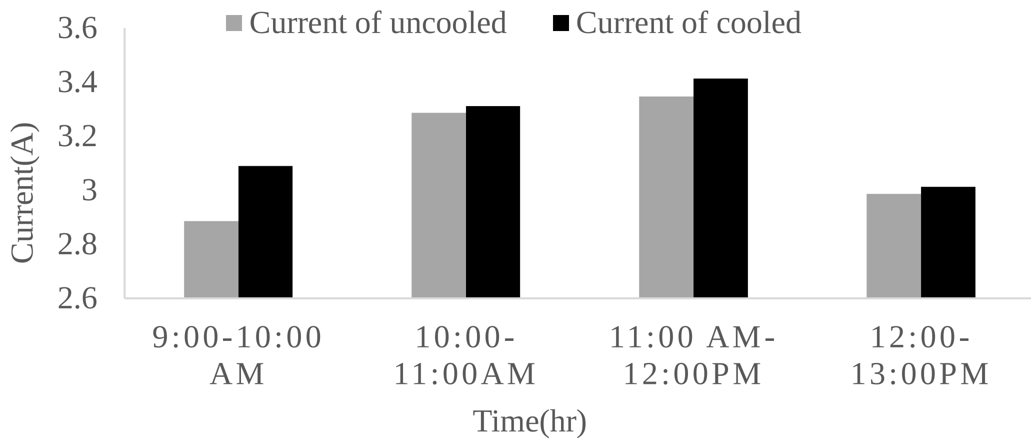

Figure: 5. 51 Comparison of the PV module current for bare and air-cooling versus time

Figure 5.52 shows a graph for variation of bare and air-cooled voltage versus time of the PV module of the air-integrated system and bare PV module system. It can be observed from the graph that voltage was dropped due to the increase in surface temperature of the module. The average increment due to air-cooling was around 2.73%.

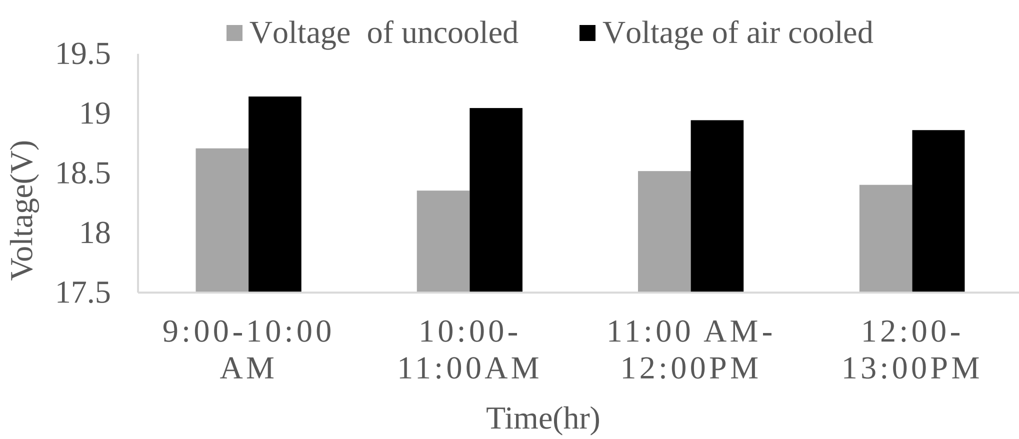

Figure: 5. 52 Variation of the module voltage without and with air-cooling versus time

Figure 5.53 illustrates the variation of output power versus time of the PV module of both air integrated and bare systems. It can be observed from the graph that the power generated gradually increases over time increase. From 11:00 am to 12:00 pm, the maximum power output was 43.33 and 41.5 W (Eq.4.1a) for cooled and uncooled modules respectively.

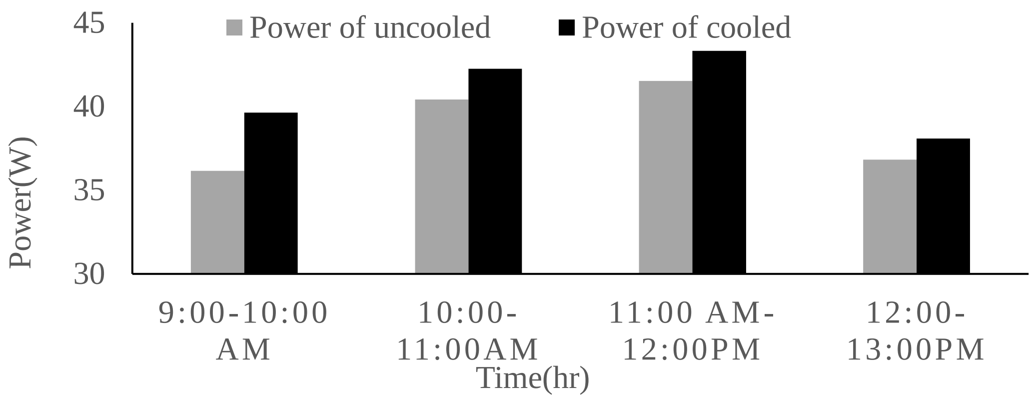

Figure: 5. 53 Comparison of the module power without and with air-cooling versus time

Figure 5.54 shows the comparison between the efficiency without and with air-cooling for the east on May 20/2021 during the experimental test (Eq.4.1). As shown in this figure as the air-cooling is applied, the electrical efficiency is increased. The maximum increase in efficiency was 9.6%.

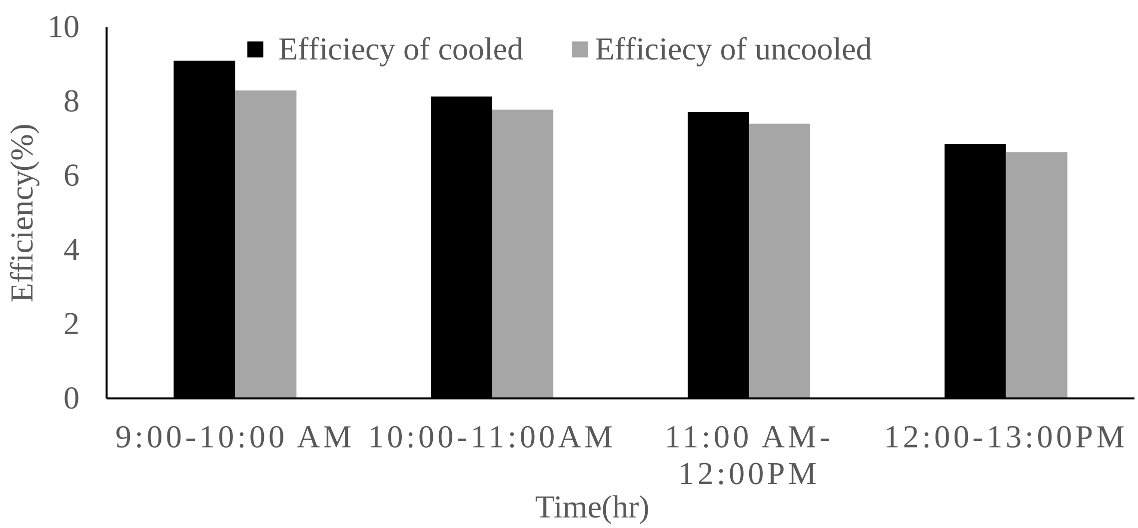

Figure: 5. 54 Comparison of the module efficiency without and with air-cooling versus time

5.5.4 Performance of East Faced Intermittent Water Cooled Photovoltaic Module

5.5.4.1 Thermal Performance of East Faced Intermittent water Cooled Photovoltaic Module

Figure 5.55 shows the results of the uncooled and cooled temperature on May 23, 2021, for east facing. The Figure illustrates for the east case the temperature of the module was high when compared to the south case. The maximum average temperature without cooling was 55.43^{0}C. The module average temperature is varied between 32 and 45^{0}C with water-cooling and the maximum decrement in temperature was 18.45^{0}C.

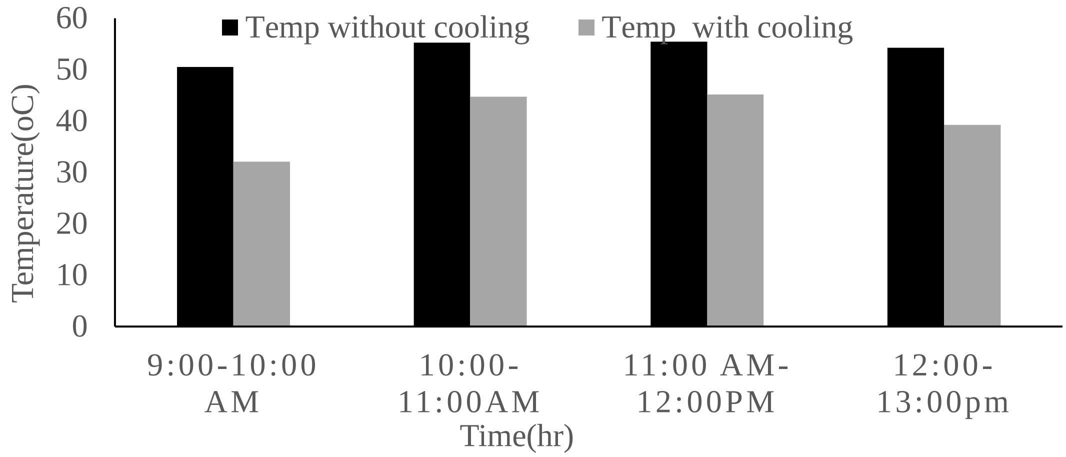

Figure: 5. 55 Temperature of the bare PV module and intermittent water-cooling versus time

Figure 5.56 shows the thermal efficiency of the photovoltaic module with and without cooling system.70 and 30% (Eq.4.21) were the maximum uncooled and water-cooled efficiency respectively. The reason behind is that thermal efficiency and temperature was directly proportional.

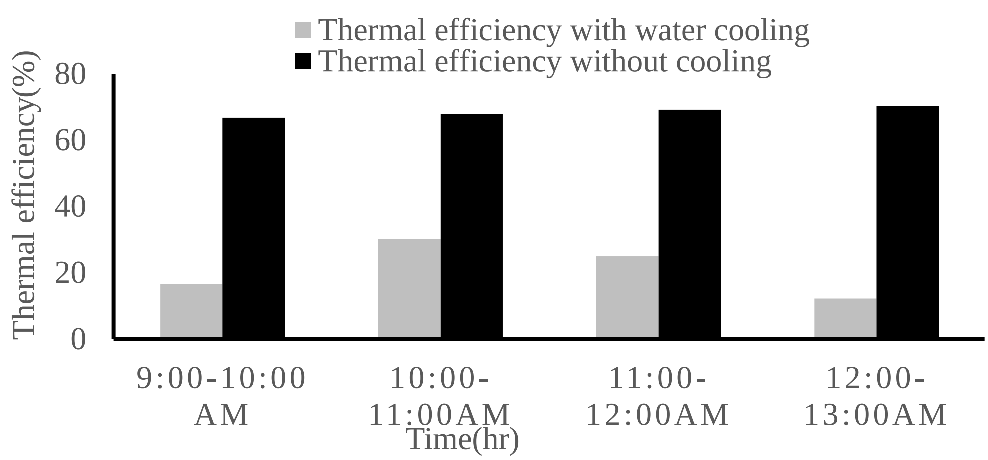

Figure: 5. 56 Comparison of the bare PV module and intermittent water-cooled thermal efficiency versus time

5.5.4.2 Electrical Performance of East Faced Intermittent water Cooled Photovoltaic Module

The effect of water-cooling on the current output of the PV module compared bare was illustrated as in Figure 5.57. As shown in this figure, the cooling of the module by water was increased the output current. Instead, at the same condition, uncooled modules experienced low current at peak values of solar intensity. The output current was 3.26 and 3.1 A for cooled and uncooled modules respectively. As a whole, the average increment in output is current 3.24%.

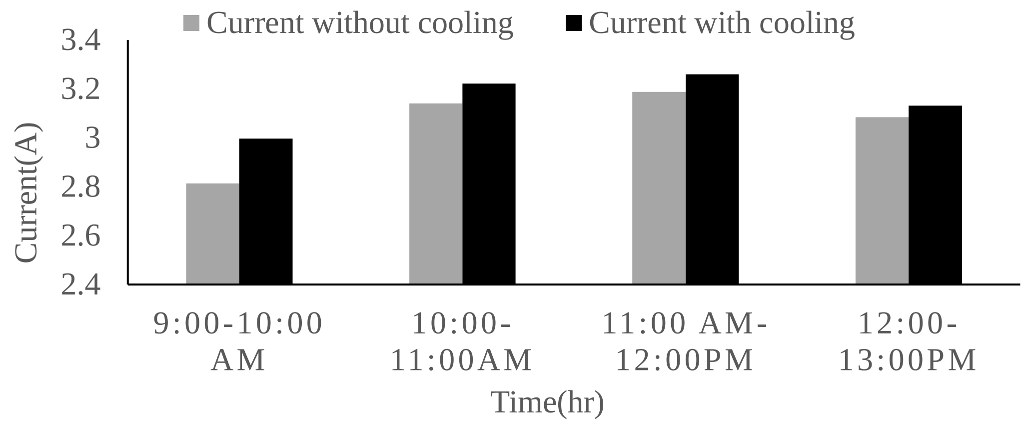

Figure: 5. 57 Comparison of the current of the bare PV module and water –cooled versus time

Figure 5.58 shows the comparison of the uncooled and cooling of the voltage on May 23, 2021 for east facing. As shown in this, figure the maximum average voltage for both cooled and uncooled was 19.58 and 18.43 V respectively. This implies a 6.67% increment in the output voltage. The maximum voltage due to intermittent water-cooling, when compared to uncooled PV module was 7.34%.

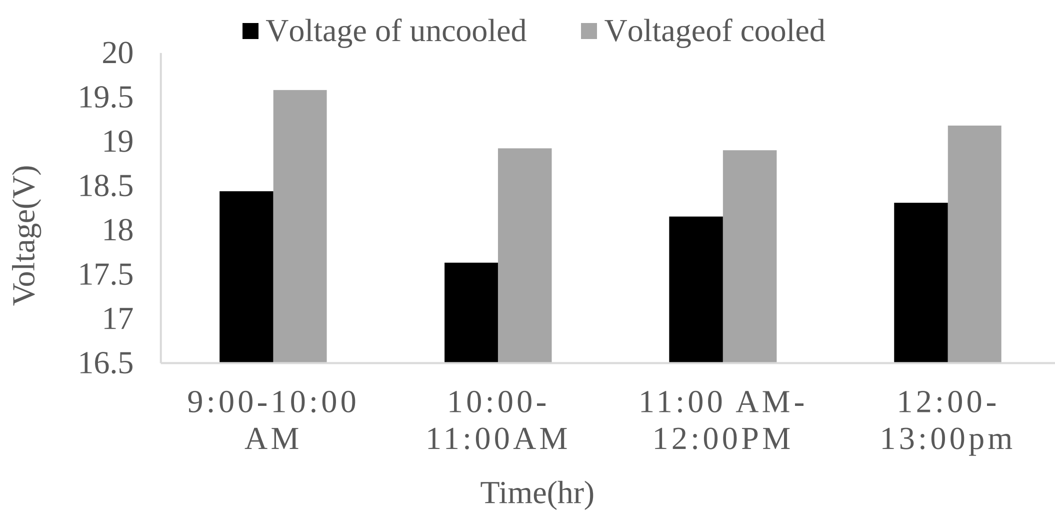

Figure: 5. 58 Comparisons of the voltage with and without cooling versus time

The hourly electrical power output is plotted in Figure 5.59. The values of the power output varied slightly with changes in solar radiation and module surface temperature. The maximum and the average increase in power by intermittent water-cooling were 13 and 8.29 W. The maximum increased power was around 41.32 W for cooled and 39.6 W (Eq.4.1a) for the uncooled module.

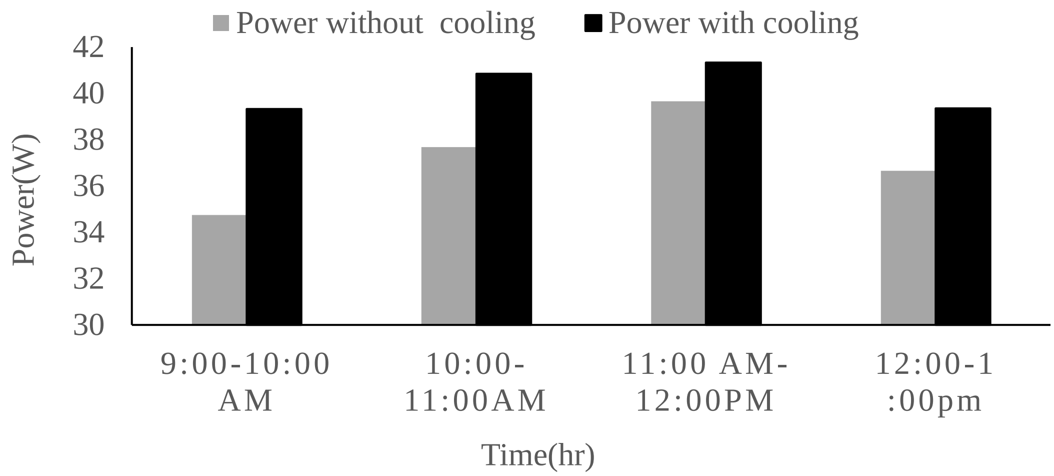

Figure: 5. 59 Comparison of the power without and with cooling water versus time

The comparison of the electric efficiency for bare (dry) and intermittent water-cooled was shown in Figure 5.60.The maximum electrical efficiency for cooled and uncooled were 9.11 and 7.94% (Eq.4.1), respectively. Due water is applied to the PV module the maximum increase in efficiency was 14.9%.

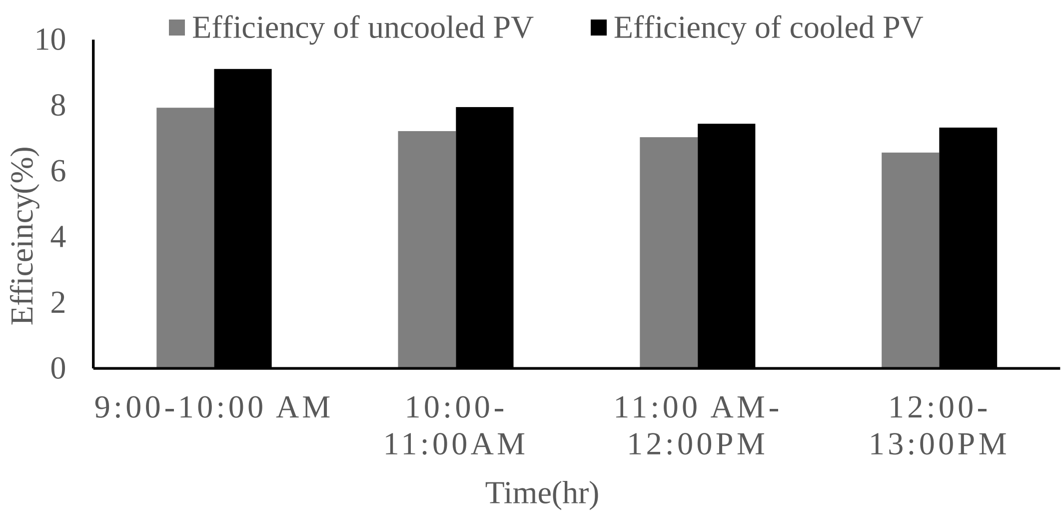

Figure: 5. 60 Comparison of electrical efficiency with and without cooling versus time

5.5.5 Performance East Faced Continuously Water and Air Cooled Photovoltaic Module

5.5.5.1 Thermal Performance of East Faced Continuously Water and Air Cooled Photovoltaic Module

The comparison of the photovoltaic module surface temperature cooled by air and water is shown in Figure 5.61.The maximum difference between air and water-cooled surface module temperature is 5^{o}C. Due to the cooling system is applies the temperature of the PV module varied slightly.

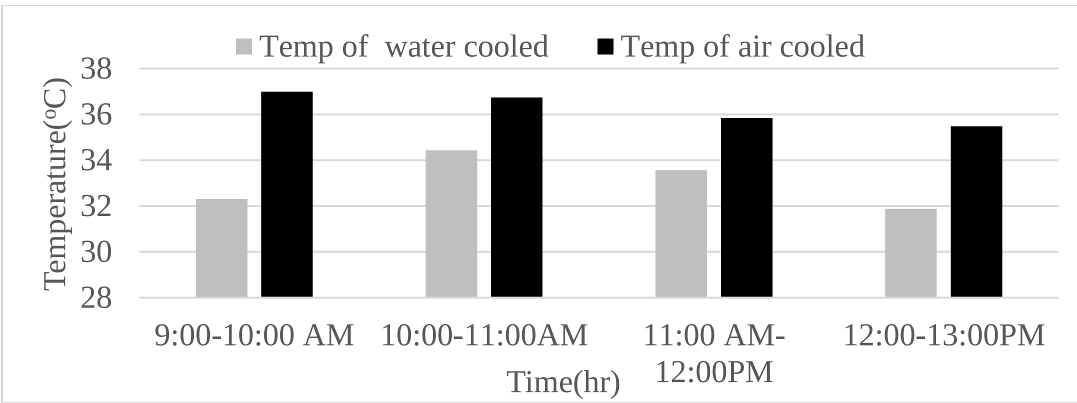

Figure: 5. 61 Comparison of the Temperature water-cooled and an air-cooled versus time

The comparison of thermal efficiency of the PV module surface temperature cooled by air and water is shown in Figure 5.62. As shown in this Figure, the thermal efficiency cooled by air was maximum for all times which indicates that water-cooling is better in reducing the heat absorbed.

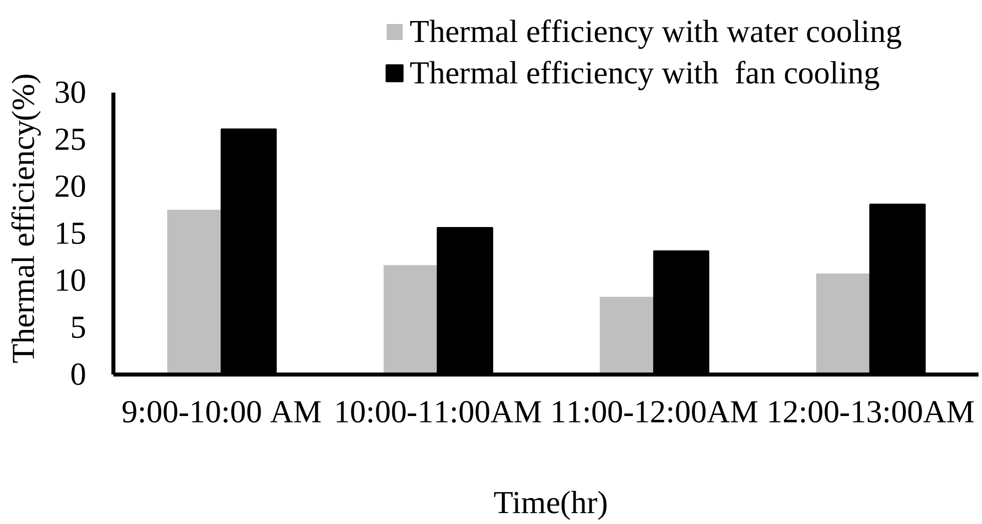

Figure: 5. 62 Comparison of the thermal efficiency of water-cooled and an air-cooled versus time

5.5.5.2 Electrical Performance of East Faced Continuously Water and Air Cooled Photovoltaic Module

Figure 5.63, shows the comparison of the current cooled by air and water during the experimental tests for east facing. For the east, facing the electric current was high from 3 to 6 a.m. The maximum current for water and air-cooled are 3.33 and 3.1A, respectively.

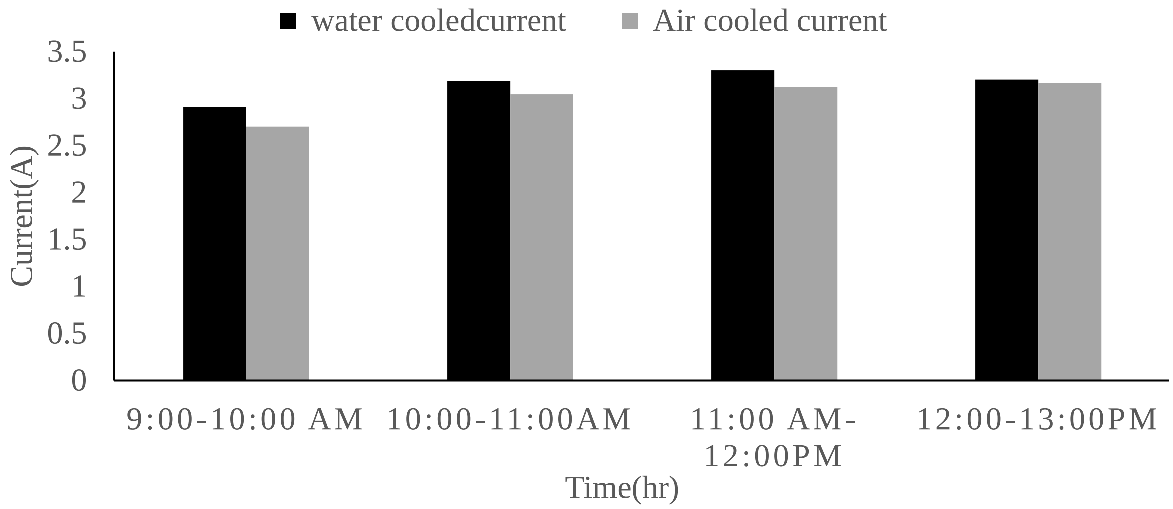

Figure: 5. 63 Comparisons of the current output cooled by air and water versus time

The result of the air and water-cooled voltage are shown in Figure 5.64. The maximum voltage is created during the maximum solar intensity is 19.72 V from 11 to 12 am. While at the same condition, the maximum air-cooled is 18.9 V.

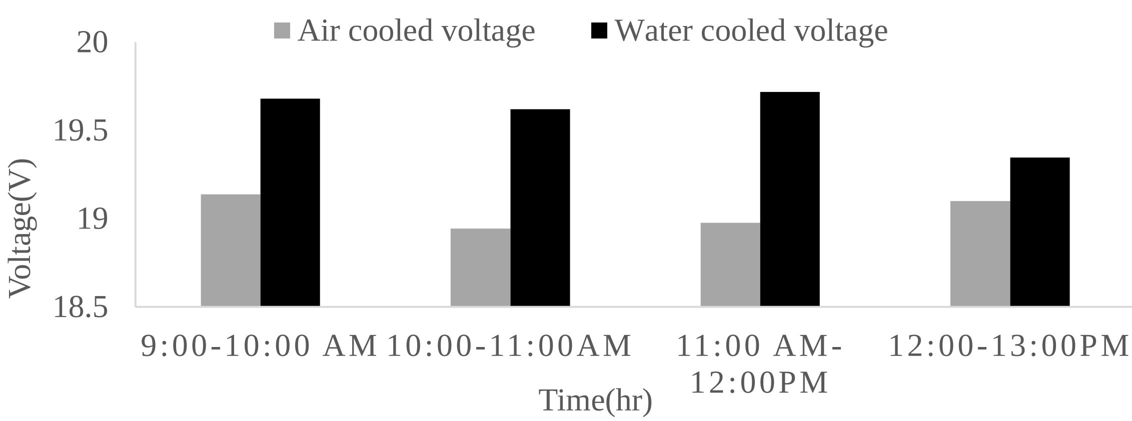

Figure: 5. 64 Comparisons of the voltage cooled by air and water versus time

In Figure 5.65, the power of air and water-cooled versus time is illustrated. As shown in this figure the photovoltaic module that cooled by water is more effective compared to the air-cooled module. The maximum increased in output power is 7.5%.

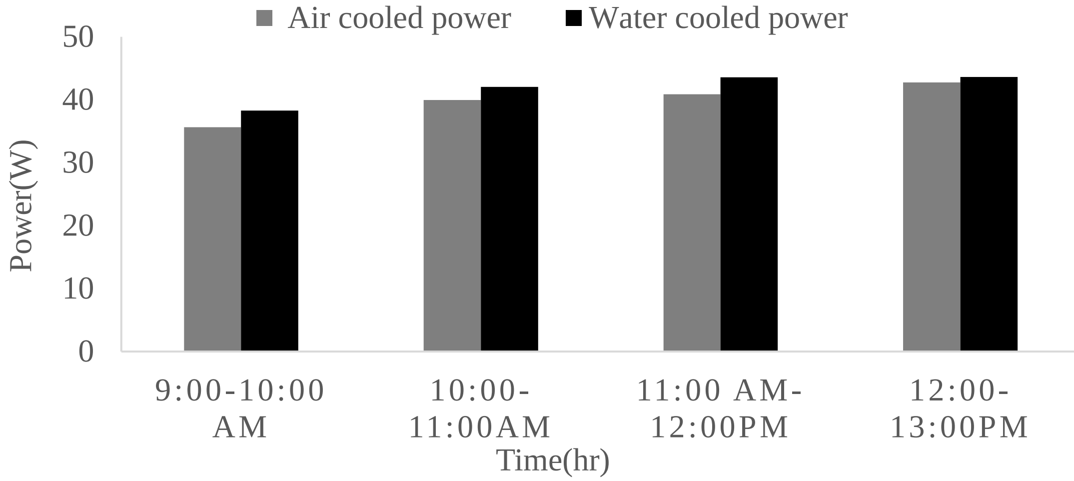

Figure: 5. 65 Comparison of the water and air-cooled PV module Power versus time

Figure 5.66, shows the comparison of air and water-cooled PV module electrical efficiency.as show in this Figure the maximum air and water cooled electrical efficiency were 8.9 and 7.9% respectively.

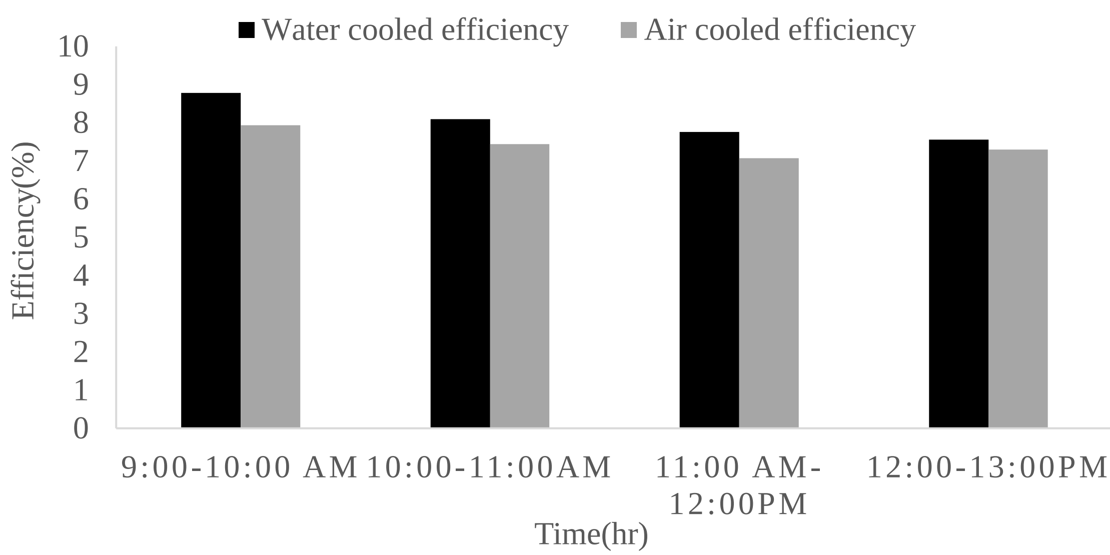

Figure: 5. 66 Comparison of the water and air-cooled electrical efficiency versus time

5.6 Thermal and Electrical Performance of West Faced Photovoltaic Module

Two PV modules were exposed to solar radiation facing the sun in the west axis to investigate effect of air and water-cooling on the electricity generated for the four cases already discussion in similar procedure.

5.6.1 Performance of West Faced Bare Photovoltaic Module

5.6.1.1 Thermal Performance of West Faced Bare Photovoltaic Module

The bare PV module average surface temperature was illustrated in Figure 5.67. This experiment was done on May 23, 2021, for west facing. The highest average surface temperature of the bare PV module is 54.79 and at the peak solar radiation temperatures.

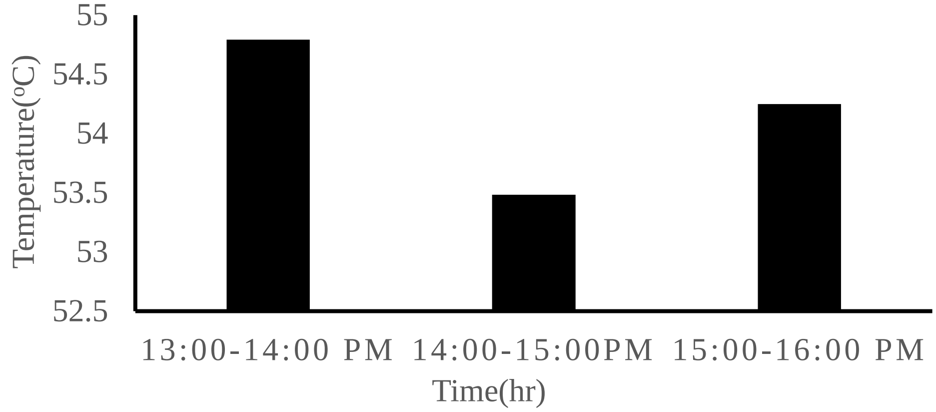

Figure: 5. 67 Bare PV module surface temperature versus time

Bare PVmodule thermal efficiency for west facing was shown in Figure 5.68. The maximum and the minimum bare thermal efficiency were 69 and 63% respectively.

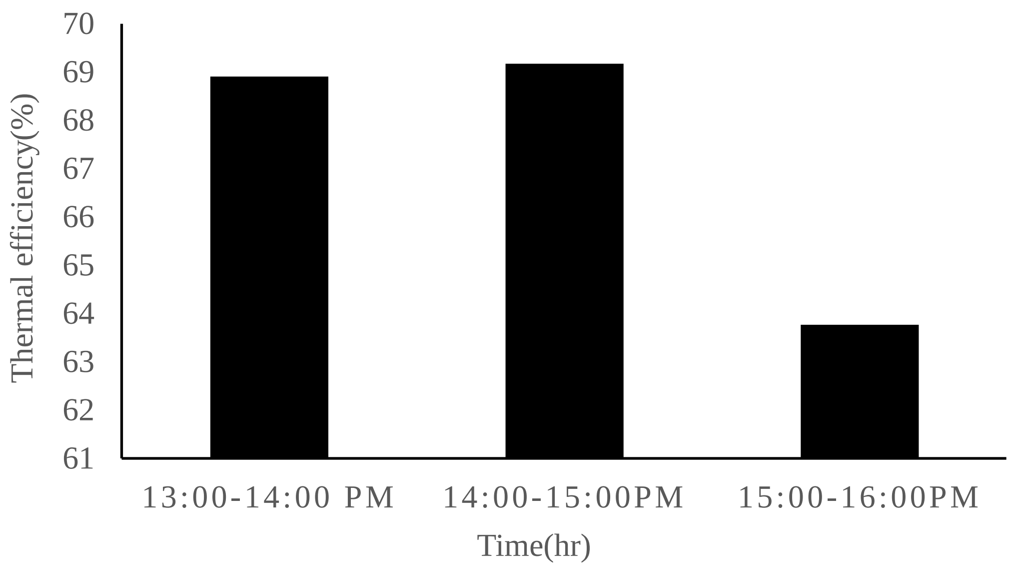

Figure: 5. 68 Thermal efficiency of the bare PV module versus time

5.6.1.2 Electrical Performance of West Faced Bare Photovoltaic Module

A bare PV module current was given in Figure 5.69. For the period of the peak solar radiation PV module only 3.15 A have been produced when no cooling mode was attached.

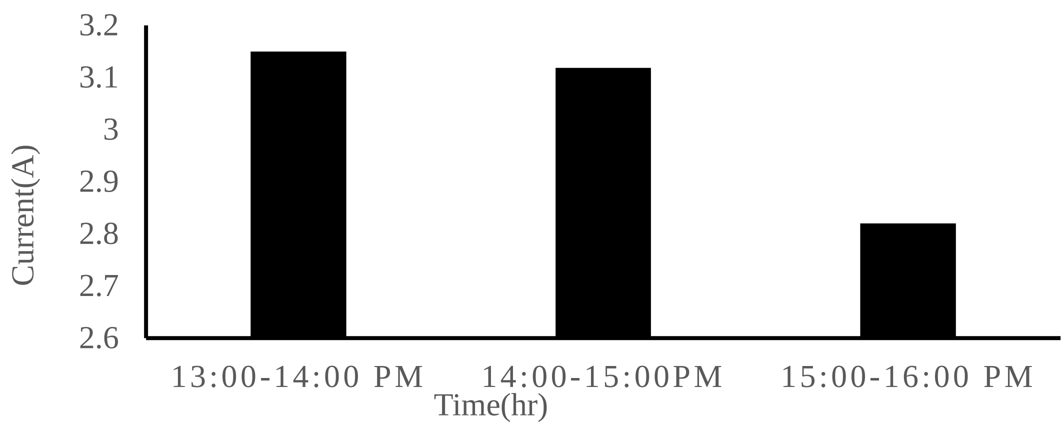

Figure: 5. 69 Bare PV module current versus time

The electric voltage of bare PV module conditions is illustrated in Figure 5.70. At the peak solar intensity and at higher ambient temperature the maximum and minimum uncooled voltage are 18.1 and 17.9 V, respectively.

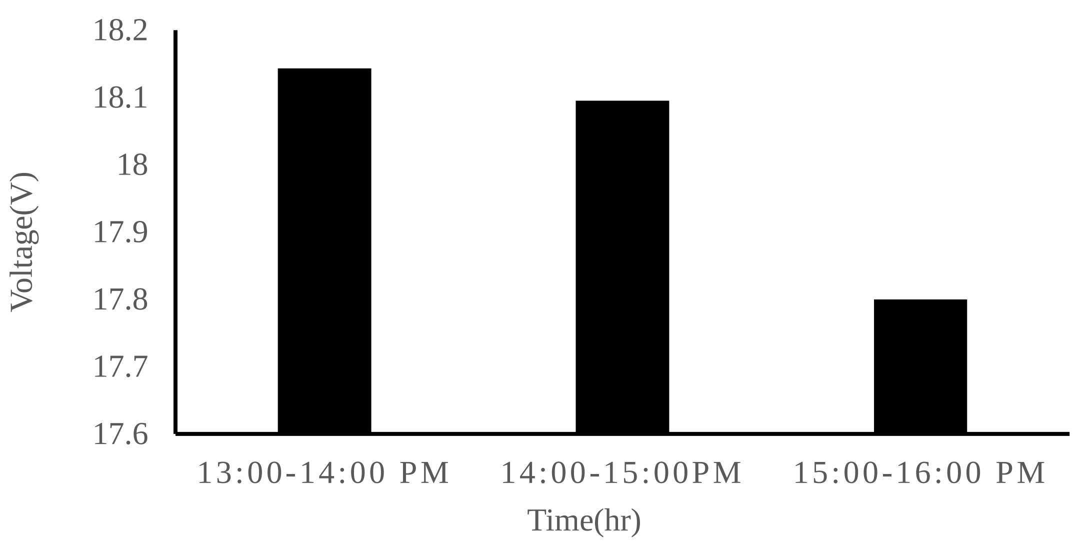

Figure: 5. 70 Variation of the electric voltage of bare PV module versus time

Figure: 5.71 shows the power output of the photovoltaic module without cooling. As shown in this figure, power output of the photovoltaic module is decreased. The Maximum power produced was 39.5 W (Eq.4.1a) was produced at 1 to 2 PM.

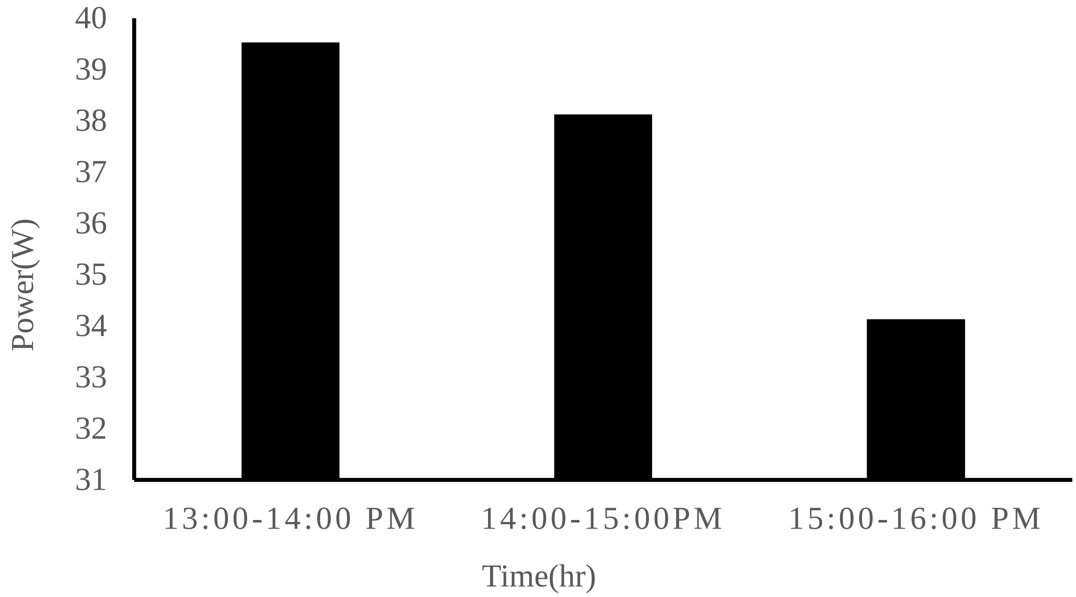

Figure: 5. 71 Power output of the bare PV module versus time

Figure: 5.72 shows the electrical efficiency of the photovoltaic module without cooling (Eq.4.1). As shown in this figure, as the PV module efficiency was increased. The Maximum and the minimum values of 9.18 and 7.72%, respectively.

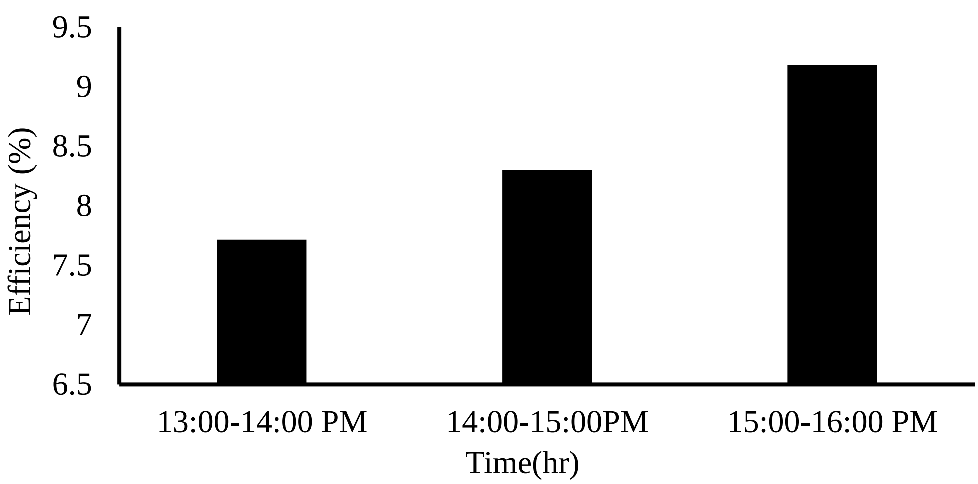

Figure: 5. 72 Electrical efficiency of the bare PV module versus time

5.6.2 Performance of West Faced Continuously Water Cooled Photovoltaic Module

5.6.2.1 Thermal Performance of West Faced Continuously Water Cooled Photovoltaic Module

Figure 5.73 shows the comparison of the bare PV module and water-cooled temperature for west faced PV module. As shown on this figure the maximum and the minimum bare and water cooled temperature was 58.6 and 33.35°C, respectively. Due to water cooling the maximum average removed in temperature was 25.25 °C.

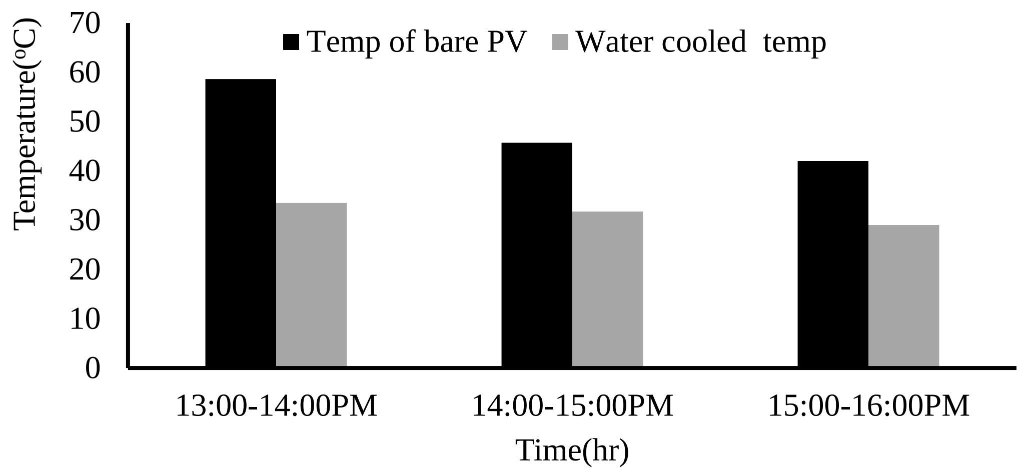

Figure: 5. 73 Comparison of the bare and water-cooled PV module temperature versus time

5.6.2.2 Electrical Performance of West Faced Continuously Water Cooled Photovoltaic Module

Figure 5.74 shows comparison of the bare and water-cooled PV module current versus time. This graph shows the cooled current was maximum values 3.25 A and bare maximum current was 3 A.

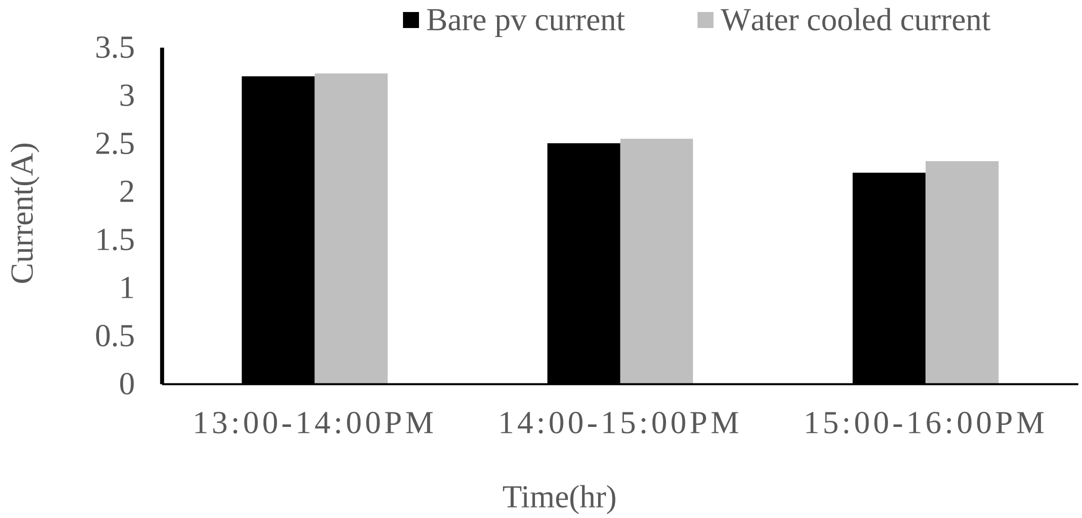

Figure: 5. 74 Comparison of the bare and water-cooled PV module current versus time

The comparison of the bare and water-cooled voltage of the PV module was shown in Figure 5.75. This figure illustrates the bare and water cooled west faced PV module voltage on May 16/2021. The maximum water-cooled and bare PV module voltage was 19.28 and17.98 V**,** respectively. At the same situation, there was 7.23% increments in electric voltage due to cooling.

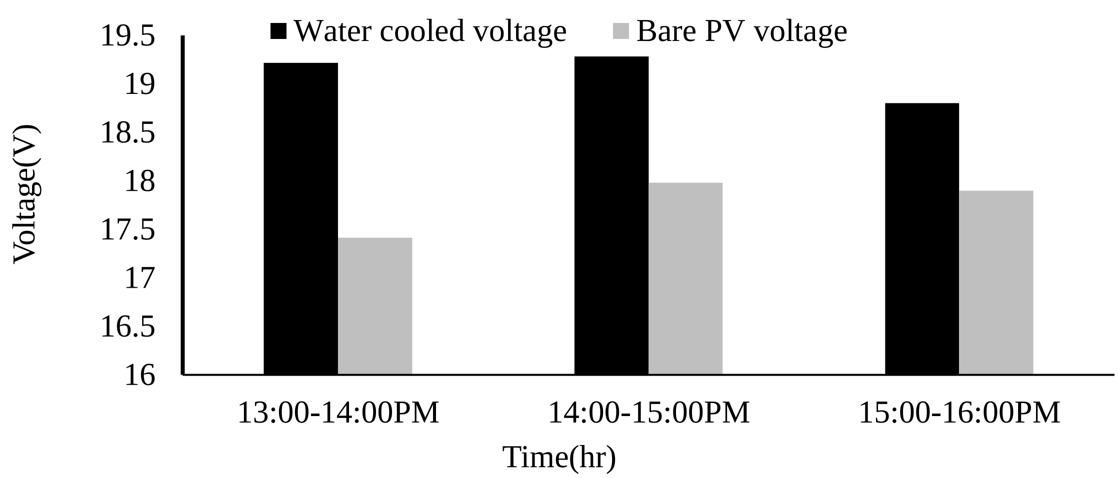

Figure: 5. 75 Comparison of the bare and water-cooled PV module voltage versus time

The comparison of the bare and water-cooled power of the PV module was illustrated in Figure 5.76. Ass seen, the maximum water-cooled power was 41.7 W (Eq.4.1a).

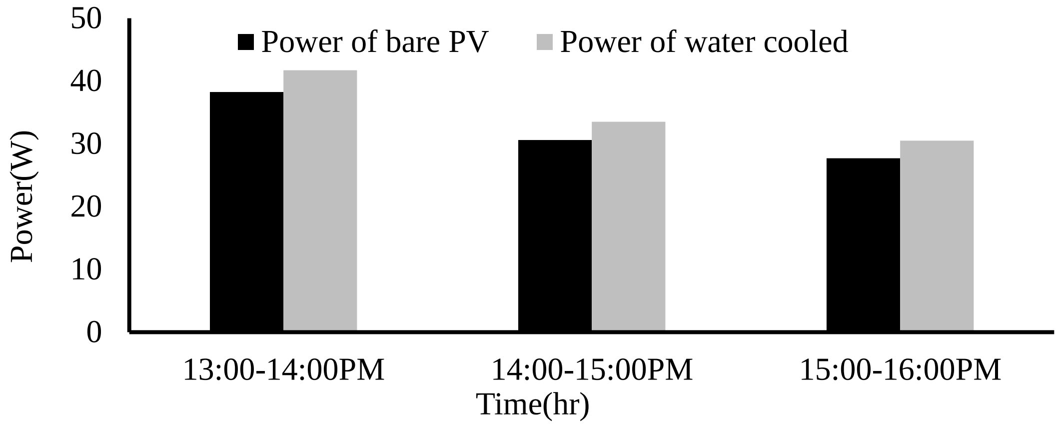

Figure: 5. 76 Comparison of the bare and water-cooled PV module Power versus time

5.6.3 Performance of West Faced Continuously Air Photovoltaic Module

5.6.3.1 Thermal Performance of West Faced Continuously Air Photovoltaic Module

Figure 5.77 compares the surface temperature of the bare PV module and air-cooling conditions. The maximum average temperature of the PV module with air-cooling and without were 55.64 and 45.1^{o}C, respectively. The average removed temperature of the module was 8.74^{o}C.

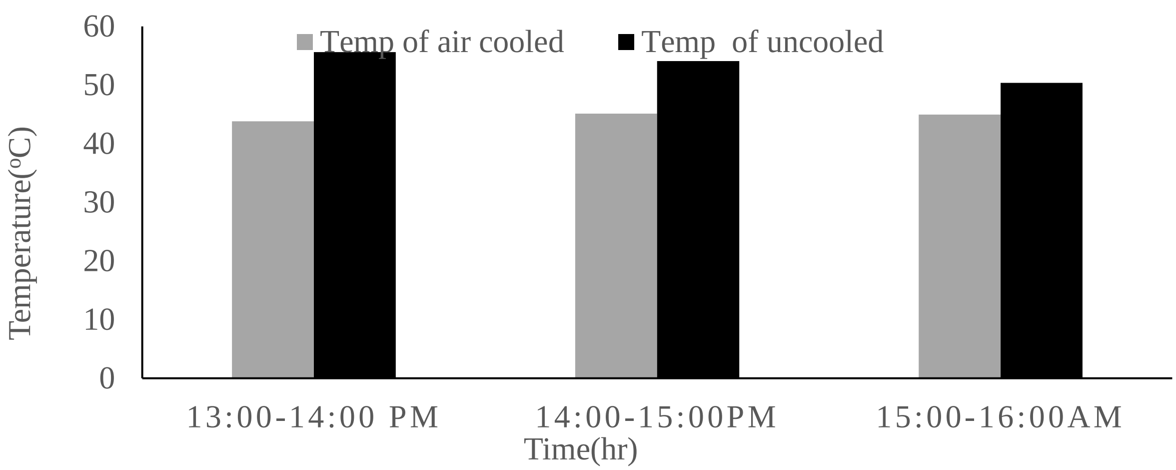

Figure: 5. 77 Comparison of the bare PV module temperature and air-cooling versus time

5.6.3.2 Electrical Performance of West Faced Continuously Air Photovoltaic Module

Figure 5.78, shows the variation of electric current of PV module with and without a cooling system. In this Figure, the maximum and the minimum electric current for cooled are 3.34 and 2.55 A respectively. The maximum and the average increase in current was 6.5 and 3.8% respectively

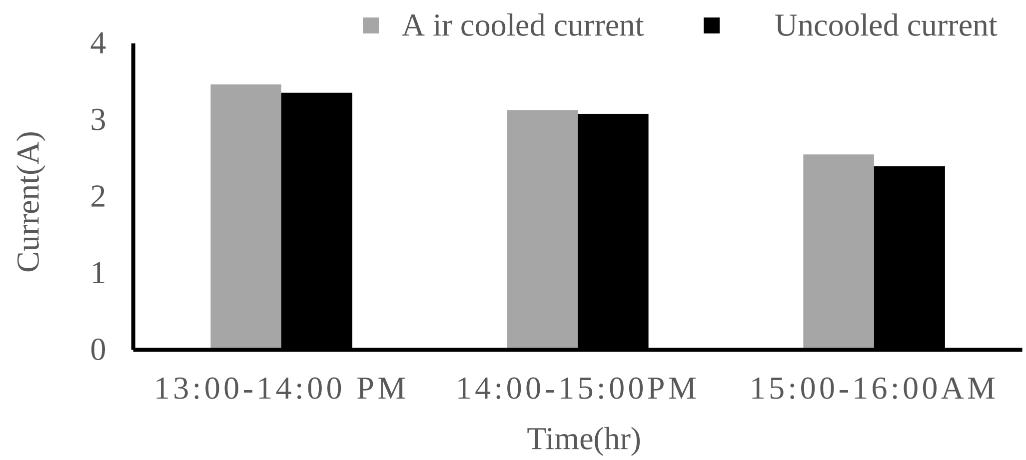

Figure: 5. 78 Hourly variation of the bare PV module current and air-cooling versus time

Figure: 5.79 shows a comparison of the module voltage of the bare PV and air-cooling versus time. As shown in this figure, the voltage output with the cooling condition has a maximum value than bare. The maximum air-cooled voltage is 18.9 V and the maximum bare module voltage was 18.1 V. The maximum increase in electric voltage was 4.4%.

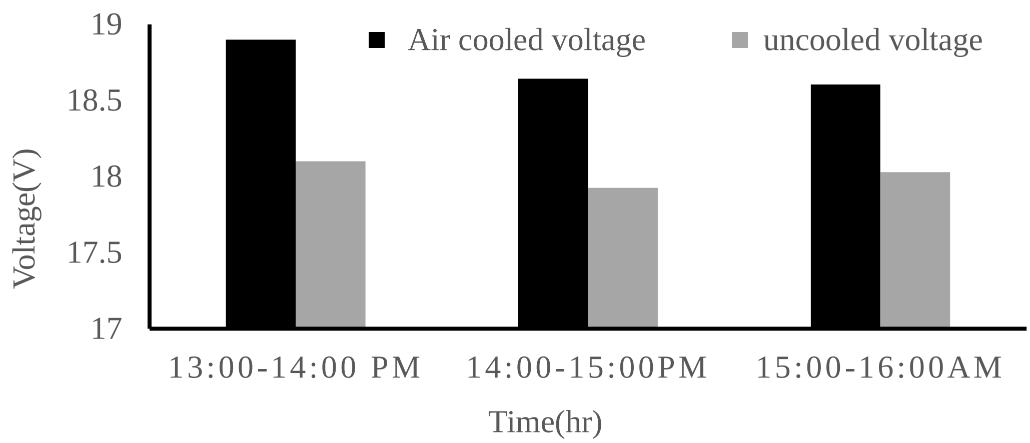

Figure: 5. 79 Comparison of the bare PV module voltage with air-cooled versus time

The comparison of hourly output power is given in Figure 5.80. The value of power varied slightly with changes in solar radiation intensity and module surface temperature. It has been expressed that power was the maximum for the photovoltaic cooled by air since its surface temperature is dropping and the maximum power yielded is 43.2 W (Eq.4.1a). At the same time, the maximum output power without cooling was 39.3 W. increased by 10.01% due to cooling.

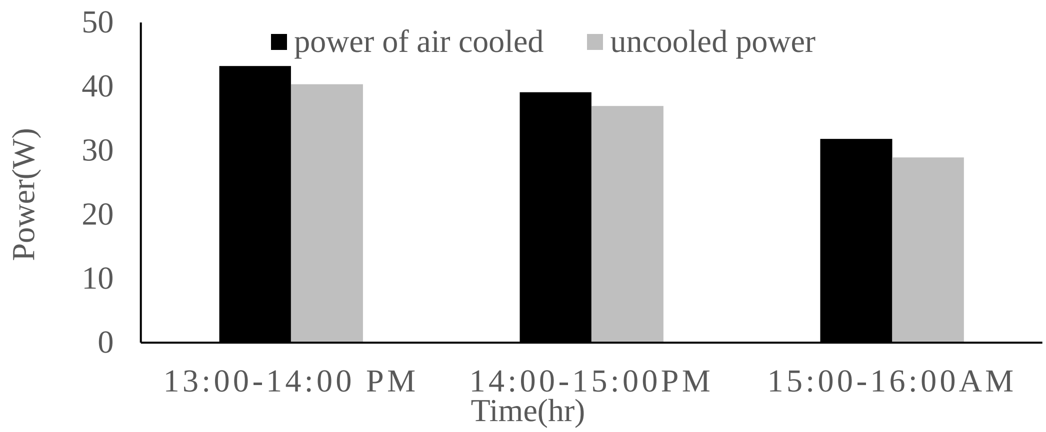

Figure: 5. 80 Graph of the module power of bare PV module and air-cooled versus time.

Figures 5.81 present the electrical efficiency of the photovoltaic module with and with air-cooling and bare PV module on May 20/2021. The maximum air-cooled and dry electrical efficiency was 8.54 and 8 % respectively. The maximum increment in electrical efficiency is due to cooling.

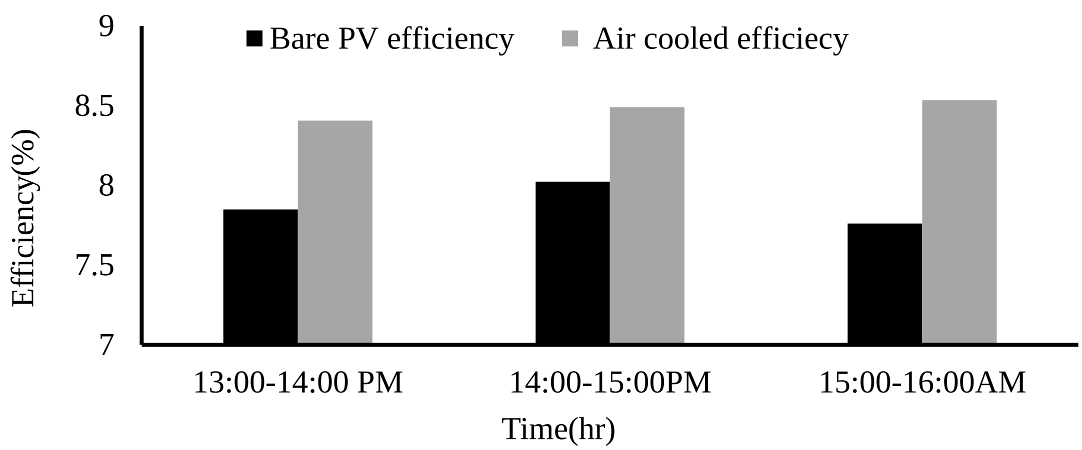

Figure: 5. 81 Graph of the module efficiency of bare and air-cooling versus time

5.6.4 Performance of West Faced Intermittent water Cooled Photovoltaic Module

5.6.4.1 Thermal Performance of West Faced Intermittent water Cooled Photovoltaic Module

The comparison of the module surface temperature with water intermittent and bare PV are illustrated in Figure 5. 82. This experiment was done on May 23, 2021, for west facing. The result of the experiment showed that the maximum difference between cooled and uncooled are 20.73^{o}C. The highest average surface temperature of the PV module without and with cooling are 54.79 and 41.24^{o}C, respectively.

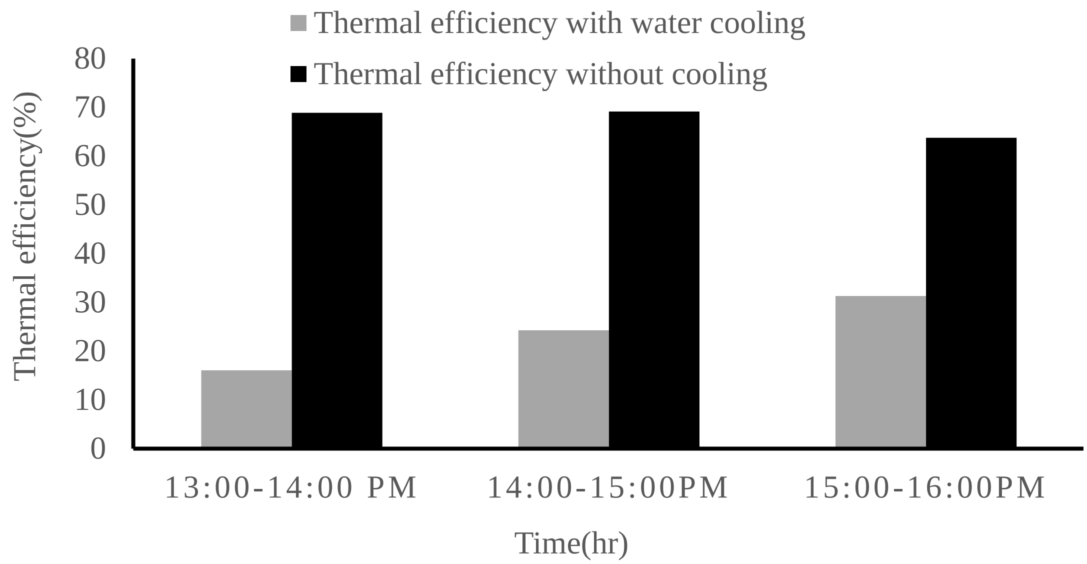

Figure: 5. 82 Thermal efficiency of PV module with and without cooling versus time

5.6.4.2 Electrical Performance of West Faced Intermittent water Cooled Photovoltaic Module

A comparison of current was given in Figure 5.83. The current output of a PV module cooled by intermittent water is higher than that generated by no cooling attached. The maximum current observed to be created by using intermittent water was 3.25 A at 1 PM for the period of the peak ambient temperature. Whereas, in the same situation, only 3.15 A have been produced when no cooling mode was attached.

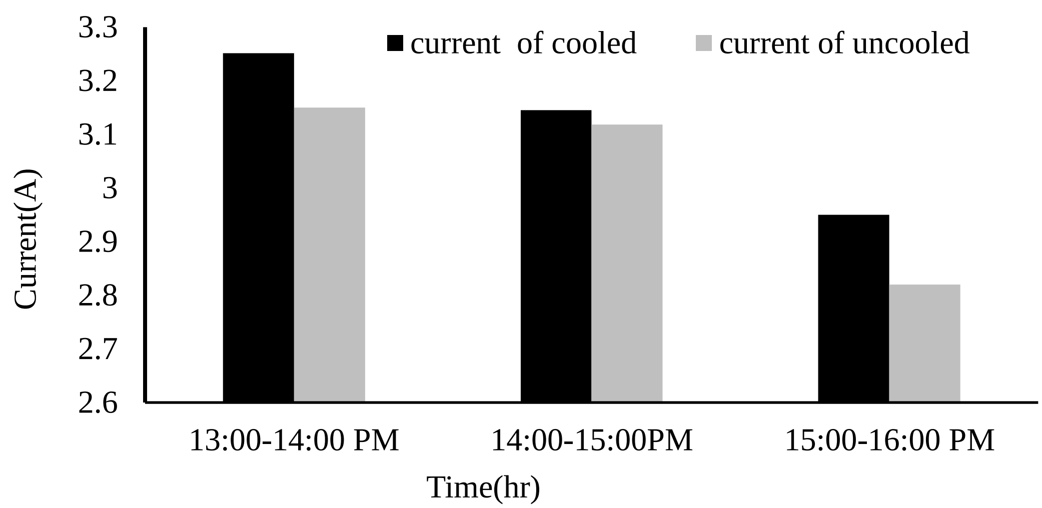

Figure: 5. 83 Cooled and bare PV module current versus time

The comparison of the electric voltage with and without cooling conditions is illustrated in Figure 5.84. At the peak solar intensity and at higher ambient temperature the maximum cooled and uncooled voltage are 19.61 and 18.1 V respectively. The maximum and the minimum increase in voltage are 8.07 and 5%, respectively.

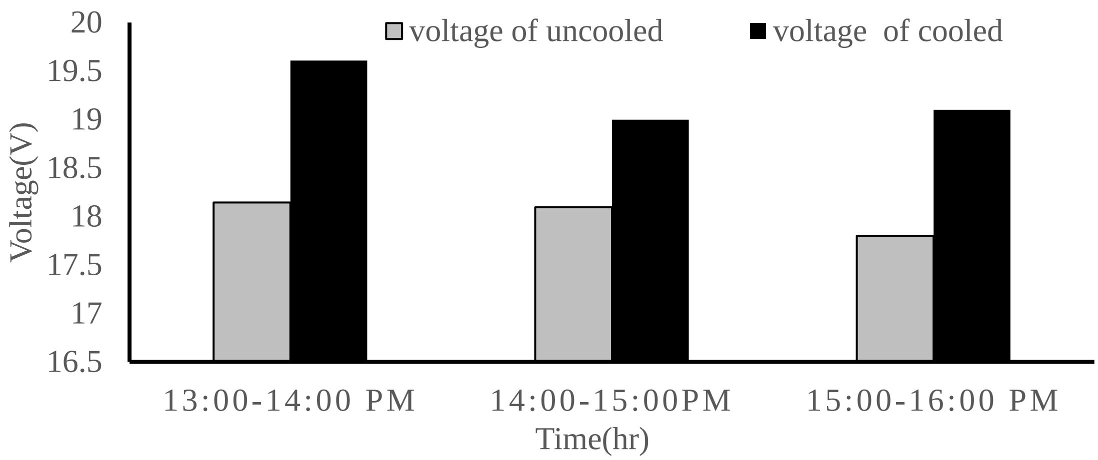

Figure: 5. 84 Variation of the voltage of the bare PV and intermittent water-cooled versus time

Figure: 5.85 shows the power output of the photovoltaic module with and without cooling. As shown in this figure, by applying a cooling system the power output of the photovoltaic module is increased. With intermittent water cooling the maximum power produced was 41.4 W (eq4.1a) was produced at 1 to 2 PM. The maximum increase in output power was 10.35%.

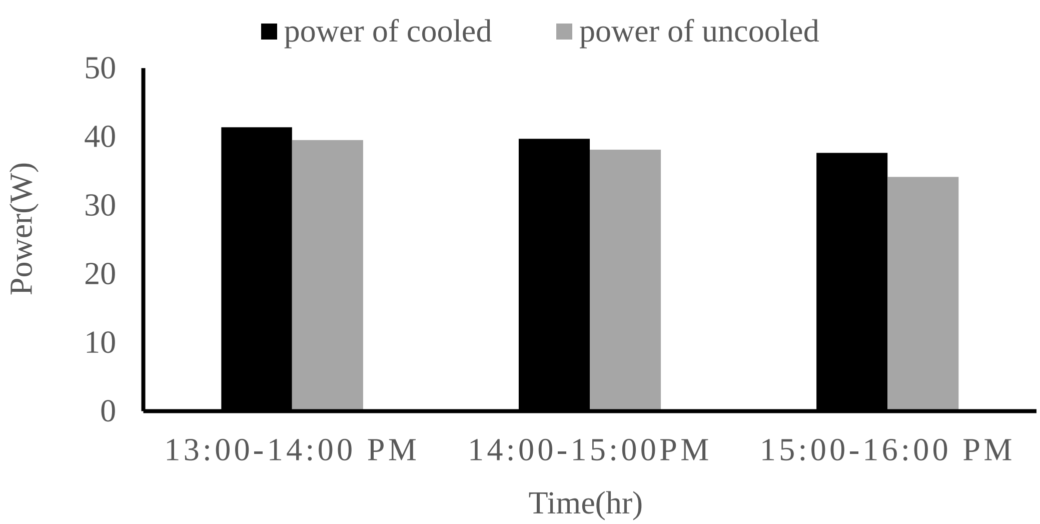

Figure: 5. 85 Power output of the bare PV module and intermittent cooling versus time

CHAPTER SIX
CONCLUSIONS AND RECOMMENDATIONS

6.1. Conclusions

In this study, the experimental electrical and thermal performances of a solar photovoltaic module with and without cooling system are carried out for 8 days starting from 9 AM up to 3 PM usually. The experiments were conducted in the month of May under Adama weather condition. The main objective of this thesis is to evaluate the effect of cooling surface temperature PV module on its thermal and electrical performance by exposing two commercial PV modules one cooled and the other bare in same day. The two commercial PV modules were identical, have 94.5 mm x 55 mm solar collection area, and were inclined at 23.5^{o} from the horizontal. Measuring instruments such as multimeter and thermocouple wires were used to collect thermal and electrical characteristics of the PV modules when exposed to the sun.

Under electrical performance, the voltage and current characteristics were measured every ten minutes to calculate the electrical output power and efficiency. The surface temperature of the PV module was measure at four different points along the length of the PV module with cooling and bare for evaluating the thermal performance and thermal efficiency every ten minute. These experimentation and performance analyses were carried out for East facing, West facing and South facing PV modules. The cooling fluids used were water and air. Four cases of cooling experimentation were conducted: continuously water film cooled verses bare; intermittent water-cooled verses bare; continuous air-cooled verses bare and continuously air cooled verses continuously water-cooled. Then the effect of temperature on the electrical and thermal performances of the photovoltaic modules was investigated. The electrical performance of the photovoltaic module is negatively affected by its operating temperature and it can be affected when the PV module surface temperature being to rise. Hence, the cooling system is necessary to decrease the cell temperature and maintain the electrical performance. The test result showed the maximum average dry PV module cell temperature for East, West, and south facing were 55.43, 58.64 and 50.40℃, respectively. The maximum increase in power output of the PV module due to cooling was 17.01%.The maximum electrical efficiency of the photovoltaic module was 11.11% and it has due to cooled by the front water cooling system. Due to the water-cooling, the maximum increase in electrical efficiency was 23.15%. Therefore, water-cooling is the best techniques from used cooling systems.

Generally, when compared PV continuous water-cooled, intermittent water-cooled and air cooled for East, South and West facing: the maximum average temperature removal was for south facing was 11.09^{o}C when compared with the PV module faced to East and West facing for continuous water cooling. The maximum average increase in electrical efficiency was 16.26% for the PV module faced to south when compared to East and West facing for continuous water-cooling.

6.2. Recommendations

Cooling of PV module offers good opportunity to decrease the surface temperature of the PV module. A cooling system keeps the variation in performance of the PV module; reduces the degradation of PV and keep reduction in open circuit voltage. In addition to this front water cooling system used as cleaning of the PV module and decrease the shadowing of dust on the PV module. Therefore, this thesis strongly recommends that using water for cooling system is the best to avoid the drop in electrical performance of the PV module due to temperature rise.

6.3. Future Works

The results recovered from the analysis have more or less met the objective of the study, which was to decrease surface temperature of the solar PV module to avoid varying in electric performance of the PV module. Therefore, to investigate further the performance enhancement due to cooling of PV system, the following future works are recommended:

- ❖ Experimental evaluation of the solar photovoltaic module with active water cooling system for all months in a year.
- ❖ Numerical investigation of the solar photovoltaic module with and without cooling system
- ❖ Thermal and electrical performances evaluation of solar photovoltaic hybrid cooling system.
- ❖ Numerical analysis of photovoltaic module by using different phase change materials cooling system
- ❖ Numerical and experimental investigation of solar PV module front active water and back finned PCM cooling system.
- ❖ Comparison performance of solar PV panel cooling system by using back fin, PCM and front water-cooling.

SPECIAL ACKNOWLEDGEMENT

This research project is funded by Adama Science and Technology University under the grant number ASTU/SM-R/326/21, Adama, Ethiopia.

REERENCES

Abdelrahman, M., Eliwa, A., & Abdellatif, O. E. (2013). Experimental investigation of different cooling methods for photovoltaic module. *11th International Energy Conversion Engineering Conference*. https://doi.org/10.2514/6.2013-4096

Aldihani, A., Aldossary, A., Mahmoud, S., & Al-Dadaha, R. K. (2014). The effect of cooling on the performance of photovoltaic cells under dusty environmental conditions. *Energy Procedia*, *61*, 2383–2386. https://doi.org/10.1016/j.egypro.2014.12.010

Ale, T. O., & Rotipin, K. J. (2019). Cooling effects on photovoltaic module performance in the tropical region. *Nigerian Journal of Technology*, *38*(3), 702. https://doi.org/10.4314/njt.v38i3.23

Alobaid, M., Hughes, B., O'Connor, D., Calautit, J., & Heyes, A. (2018). Improving thermal and electrical efficiency in photovoltaic thermal systems for sustainable cooling system integration. *Journal of Sustainable Development of Energy, Water and Environment Systems*, *6*(2), 305–322. https://doi.org/10.13044/j.sdewes.d5.0187

Amelia, A. R., Irwan, Y. M., Irwanto, M., Leow, W. Z., Gomesh, N., Safwati, I., & Anuar, M. A. M. (2016). Cooling on Photovoltaic Panel Using Forced Air Convection Induced by DC Fan. *International Journal of Electrical and Computer Engineering (IJECE)*, *6*(2), 526. https://doi.org/10.11591/ijece.v6i2.9118

Amjad, S., Zafar, A., Afzal, S., & Anjum, H. (n.d.). *Impact of Environmental Factors on the Working of Photovoltaic Cells*. 26–31.

Arcuri, N., Reda, F., & De Simone, M. (2014). Energy and thermo-fluid-dynamics evaluations of photovoltaic panels cooled by water and air. *Solar Energy*, *105*, 147–156. https://doi.org/10.1016/j.solener.2014.03.034

Arefin, M. A. (2019). Analysis of an Integrated Photovoltaic Thermal System by Top Surface Natural Circulation of Water. *Frontiers in Energy Research*, *7*(September). https://doi.org/10.3389/fenrg.2019.00097

Arifin, Z., Tjahjana, D. D. D. P., Hadi, S., Rachmanto, R. A., Setyohandoko, G., & Sutanto, B. (2020). Numerical and experimental investigation of air cooling for photovoltaic panels using aluminum heat sinks. *International Journal of Photoenergy*, *2020*. https://doi.org/10.1155/2020/1574274

Bahaidarah, H., Subhan, A., Gandhidasan, P., & Rehman, S. (2013). Performance evaluation of a PV (photovoltaic) module by back surface water cooling for hot climatic conditions. *Energy*, *59*, 445–453.

Baloch, A. A. B., Bahaidarah, H. M. S., Gandhidasan, P., & Al-Sulaiman, F. A. (2015). Experimental and numerical performance analysis of a converging channel heat exchanger for PV cooling. *Energy Conversion and Management*, *103*, 14–27. https://doi.org/10.1016/j.enconman.2015.06.018

Bayrak, F., Oztop, H. F., & Selimefendigil, F. (2020). Experimental study for the application of different cooling techniques in photovoltaic (PV) panels. *Energy Conversion and Management*, *212*(March), 112789. https://doi.org/10.1016/j.enconman.2020.112789

Bhakre, S. S., Sawarkar, P. D., & Kalamkar, V. R. (2021). Performance evaluation of PV panel surfaces exposed to hydraulic cooling – A review. *Solar Energy*, *224*(July), 1193–1209. https://doi.org/10.1016/j.solener.2021.06.083

Ceylan, I., Gürel, A. E., Demircan, H., and Aksu, B. (2014). Cooling of a photovoltaic module with temperature controlled solar collector. *Energy and Buildings*, *72*, 96–101. https://doi.org/10.1016/j.enbuild.2013.12.058

Chandrashekar, S., Sandeep, K., Mulla, J., Bharath, D., & Raghavendra, R. (2020). *SMART COOLING SYSTEM FOR SOLAR PHOTOVOLTAIC MODULE*. *7*(7), 1170–1176.

Dhimish, M., and Silvestre, S. (2019). Estimating the impact of azimuth-angle variations on photovoltaic annual energy production. *Clean Energy*, *3*(1), 47–58. https://doi.org/10.1093/ce/zky022

Dorobanțu, L., Popescu, M. O., Popescu, C. L., & Crăciunescu, A. (2013). Renewable Energy and Power Quality Journal (RE&PQJ) Experimental Assessment of PV Panels Front Water Cooling Strategy. *Renewable Energy and Power Quality Journal*, *1*(11), 1009–1012. https://doi.org/10.24084/repqj11.510

Du, B., Hu, E., & Kolhe, M. (2012). Performance analysis of water cooled concentrated photovoltaic (CPV) system. *Renewable and Sustainable Energy Reviews*, *16*(9), 6732–6736. https://doi.org/10.1016/j.rser.2012.09.007

Duffie, J. A., & Beckman, W. A. (2006). *Solar Engenierring of Thermal Process*.

Duffie, J. A., & Beckman, W. A. (2013). *Solar engineering of thermal processes*. John Wiley & Sons.

Dwivedi, P., Sudhakar, K., Soni, A., Solomin, E., & Kirpichnikova, I. (2020). Advanced cooling techniques of P.V. modules: A state of art. *Case Studies in Thermal Engineering*, *21*(December 2019), 100674. https://doi.org/10.1016/j.csite.2020.100674

El Mays, A., Ammar, R., Hawa, M., Abou Akroush, M., Hachem, F., Khaled, M., & Ramadan, M. (2017). Improving photovoltaic panel using finned plate of aluminum. *Energy Procedia*, *119*, 812–817.

Elbreki, A. M., Sopian, K., Fazlizan, A., & Ibrahim, A. (2020). An innovative technique of passive cooling PV module using lapping fins and planner reflector. *Case Studies in*

Thermal Engineering, *19*(January), 100607. https://doi.org/10.1016/j.csite.2020.100607

Firoozzadeh, M., Shiravi, A. H., & Shafiee, M. (2019). An Experimental Study on Cooling the Photovoltaic Modules by Fins to Improve Power Generation: Economic Assessment. *Iranian Journal of Energy and Environment*, *10*(2), 80–84. https://doi.org/10.5829/ijee.2019.10.02.02

Gana, N. N., Rai, J. K., & Momoh, M. (2014). *Estimation of Global and Diffuse Solar Radiation for Kebbi, North-Western, Nigeria*. *5*(1), 1654–1661.

Govardhanan, M. S., Kumaraguruparan, G., Kameswari, M., Saravanan, R., Vivar, M., & Srithar, K. (2020). Photovoltaic Module with Uniform Water Flow on Top Surface. *International Journal of Photoenergy*, *2020*. https://doi.org/10.1155/2020/8473253

Grubišić-Čabo, F., Nižetić, S., & Marco, T. G. (2016). Photovoltaic panels: A review of the cooling techniques. *Transactions of Famena*, *40*(April 2019), 63–74.

Haroun Shahad Mohammed Hasan Abbood, Z. (2019). Experimental Performance Investigation of Photovoltaic Module and Water Cooled Photovoltaic/Thermal System under Middle of Iraqi Climatic Conditions. *International Journal of Engineering and Technology*, *8*(December), 237–247.

Hasan, A., McCormack, S. J., Huang, M. J., Sarwar, J., & Norton, B. (2015). Increased photovoltaic performance through temperature regulation by phase change materials: Materials comparison in different climates. *Solar Energy*, *115*(May), 264–276. https://doi.org/10.1016/j.solener.2015.02.003

Hasen, Y. (2019). *Investigating the Thermal Performance of a Solar Water Heating System Integrated with Phase Change Material as a Thermal Energy Storage: A Case of Adama Hospital Medical College*. ASTU.

Ibrahim, A. K. (2018). Improving the Solar Panel Efficiency by Using Cooling and Cleaning Techniques. *Journal of University of Babylon, Engineering Sciences*, *26*(1), 7–12.

Iqbal, S., Afzal, S., Mazhar, A. U., Anjum, H., & Diyyan, A. (2016). effect of water cooling on the energy conversion efficiency of PV cell. *American Scientific Research Journal for Engineering, Technology, and Sciences (ASRJETS)*, *20*(1), 122–128.

Johnston, E., Szabo, P. S. B., & Bennett, N. S. (2021). Cooling silicon photovoltaic cells using finned heat sinks and the effect of inclination angle. *Thermal Science and Engineering Progress*, *23*(March). https://doi.org/10.1016/j.tsep.2021.100902

Kadam, N., Singh, R. K., Kumbar, D. S., & Bhimanagouda, S. B. (2018). *Experimental Investigation of Active Cooling System for Photovoltaic Cell*. *V*(Iv), 228–231.

Kalogirou, S. A. (2013). *Solar energy engineering: processes and systems*. Academic Press.

Kaplani, E., & Kaplanis, S. (2014). Thermal modelling and experimental assessment of the dependence of PV module temperature on wind velocity and direction, module orientation and inclination. *Solar Energy*, *107*, 443–460. https://doi.org/10.1016/j.solener.2014.05.037

Khanna, S., Reddy, K. S., & Mallick, T. K. (2018). Optimization of finned solar photovoltaic phase change material (finned pv pcm) system. *International Journal of Thermal Sciences*, *130*(May), 313–322. https://doi.org/10.1016/j.ijthermalsci.2018.04.033

Kiwan, S., Ahmad, H., Alkhalidi, A., Wahib, W. O., & Al-Kouz, W. (2020). Photovoltaic Cooling Utilizing Phase Change Materials. *E3S Web of Conferences*, *160*. https://doi.org/10.1051/e3sconf/202016002004

Mahamudul, H., Rahman, M. M., Metselaar, H. S. C., Mekhilef, S., Shezan, S. A., Sohel, R., Abu Karim, S. Bin, & Badiuzaman, W. N. I. (2016). Temperature Regulation of Photovoltaic Module Using Phase Change Material: A Numerical Analysis and

Experimental Investigation. *International Journal of Photoenergy*, *2016*. https://doi.org/10.1155/2016/5917028

Mehrotra, S., Rawat, P., Debbarma, M., Sudhakar, K., Centre, E., & Pradesh, M. (2014). *Performance of a solar panel.pdf*. *3*(3), 1161–1172.

Milind, N., Antony, M., Francis, F., Francis, J., Varghese, J., & Sajith, U. K. (2017). Enhancing the efficiency of solar panel using cooling systems. *International Journal of Engineering Research and Applications*, *7*(03), 5–7.

Moharram, K. A., Abd-Elhady, M. S., Kandil, H. A., & El-Sherif, H. (2013). Enhancing the performance of photovoltaic panels by water cooling. *Ain Shams Engineering Journal*, *4*(4), 869–877. https://doi.org/10.1016/j.asej.2013.03.005

Nehari, T., Benlakam, M., & Nehari, D. (2016). Effect of the fins length for the passive cooling of the photovoltaic panels. *Periodica Polytechnica Mechanical Engineering*, *60*(2), 89–95. https://doi.org/10.3311/PPme.8571

Nigussie, S. G., & Science, A. (2020). *Performance Investigation of Solar Thermal Local Areke Production System Using Dish Concentrator*.

Nižetić, S., Papadopoulos, A. M., & Giama, E. (2017). Comprehensive analysis and general economic-environmental evaluation of cooling techniques for photovoltaic panels, Part I: Passive cooling techniques. *Energy Conversion and Management*, *149*, 334–354. https://doi.org/10.1016/j.enconman.2017.07.022

Prajapati, S., Fernandez, E., & Saxena, R. (2017). *Experimental Investigations on the Performance of PV Modules with / without Module Cooling*. *9028*, 92–96.

Rahimi, M., Valeh-E-Sheyda, P., Parsamoghadam, M. A., Masahi, M. M., & Alsairafi, A. A. (2014). Design of a self-adjusted jet impingement system for cooling of photovoltaic cells.

Energy Conversion and Management, *83*, 48–57. https://doi.org/10.1016/j.enconman.2014.03.053

Rasham, A. M., Jobair, H. K., & Alkhazzar, A. A. A. (2015). *EXPERIMENTAL AND NUMERICAL INVESTIGATION OF PHOTO-VOLTAIC MODULE PERFORMANCE VIA CONTINUOUS AND INTERMITTENT WATER COOLING TECHNIQUES*. *6*(7), 87–98.

Sajjad, U., Amer, M., Ali, H. M., Dahiya, A., & Abbas, N. (2019). Cost effective cooling of photovoltaic modules to improve efficiency. *Case Studies in Thermal Engineering*, *14*(January), 100420. https://doi.org/10.1016/j.csite.2019.100420

Sato, D., & Yamada, N. (2019). Review of photovoltaic module cooling methods and performance evaluation of the radiative cooling method. *Renewable and Sustainable Energy Reviews*, *104*(January), 151–166. https://doi.org/10.1016/j.rser.2018.12.051

Sedaghat, A., Karami, M. R., & Eslami, M. (2020). Improving Performance of a Photovoltaic Panel by Pin Fins: A Theoretical Analysis. *Iranian Journal of Science and Technology - Transactions of Mechanical Engineering*, *44*(4), 997–1004. https://doi.org/10.1007/s40997-019-00324-w

Stropnik, R., & Stritih, U. (2016). Increasing the efficiency of PV panel with the use of PCM. *Renewable Energy*, *97*, 671–679. https://doi.org/10.1016/j.renene.2016.06.011

Suresh, M., & Shanmadhi, R. (2020). Studies on the performance of 150W solar photovoltaic module with evaporative cooling. *IOP Conference Series: Materials Science and Engineering*, *912*(4). https://doi.org/10.1088/1757-899X/912/4/042016

Tiwari, G. N., & Tiwari, A. (2016). *Handbook of solar energy*. Springer.

Wongwuttanasatian, T., Sarikarin, T., & Suksri, A. (2020). Performance enhancement of a photovoltaic module by passive cooling using phase change material in a finned container heat sink. *Solar Energy*, *195*(October 2019), 47–53. https://doi.org/10.1016/j.solener.2019.11.053

Wu, S., & Xiong, C. (2014). Passive cooling technology for photovoltaic panels for domestic houses. *International Journal of Low-Carbon Technologies*, *9*(2), 118–126. https://doi.org/10.1093/ijlct/ctu013

YEŞİLYURT, M., NASİRİ, M., & OZAKIN, A. (2018). Techniques for Enhancing and Maintaining Electrical Efficiency of Photovoltaic Systems. *International Journal of New Technology and Research*, *4*(4), 263082.

Zubeer, S. A., Mohammed, H. A., & Ilkan, M. (2017). A review of photovoltaic cells cooling techniques. *E3S Web of Conferences*, *22*. https://doi.org/10.1051/e3sconf/20172200205

APPENDIX

APPENDIX A: Thermocouple Calibration

Thermocouples are sensors used to measure temperature by forming a junction between two wires of separate metals. One end of the junction is called the measurement “hot” junction and the other end is called the reference “cold” junction. When there is a temperature variation in the joint, voltage is created and this voltage can be converted into temperature with a thermocouple reference table or data logger. Thermocouples can be calibrated using a reference thermometer in a temperature calibration test by comparing both measurement values of a reference thermometer and other thermometers. The thermocouple used in this study is a K-type four-channel thermocouple and a constant high temperature bath was used for the calibration.

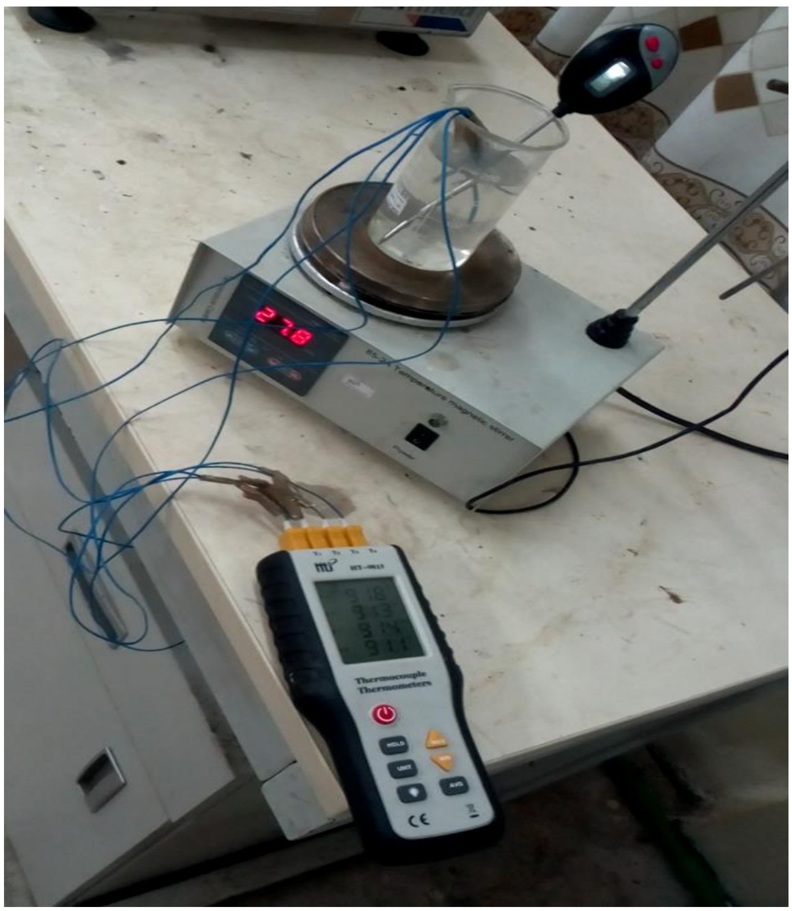

Figure A. 1: Calibration

Table A.1: Data from thermocouples during calibration.

Time	T_1(Digital thermometer)	T_2(K-type thermocouple) (°C)	Uncertainty (% $\frac{(T_1 - T_2) \times 100\%}{T_1}$
	26.6	26.2	1.503759398
	29.1	28.8	1.030927835
	32.4	32.1	0.925925926
	38.9	38.6	0.771208226
	42	41.6	0.952380952
	46	45.7	0.652173913
	49.3	48.9	0.811359026
	52.3	51.8	0.956022945
	55.1	54.6	0.907441016
	59.8	59.3	0.836120401
	61.2	60.8	0.653594771
	64.5	64.1	0.620155039
	69.8	69.3	0.716332378
	72.3	72.1	0.276625173
	76	75.8	0.263157895
	79.5	79	0.628930818
	83.7	83.4	0.358422939
	86.4	86.1	0.347222222
	89.2	88.9	0.33632287
	91.3	91.1	0.21905805
Average uncertainty (%)			0.68835709

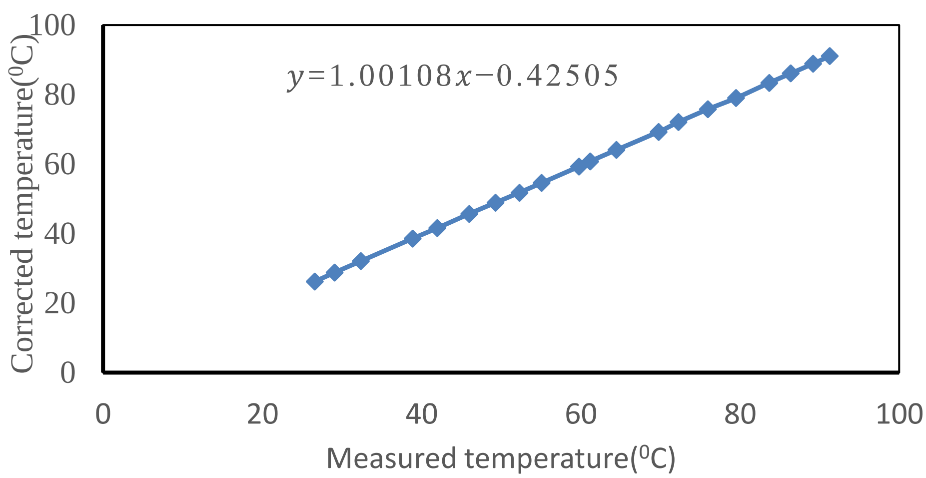

Figure A. 2: Measured temperature versus corrected temperature